

RICE UNIVERSITY

**Sustainable Production of Biofuels:
Plant Optimization and Environmental Impact**

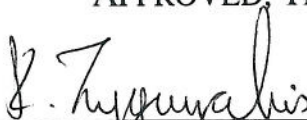
By

Venetia Rigou

A THESIS SUBMITTED
IN PARTIAL FULFILLMENT OF THE
REQUIREMENTS FOR THE DEGREE

Doctor of Philosophy

APPROVED, THESIS COMMITTEE:



Kyriacos Zygorakis, A.J. Hartsook Professor, Chair
Chemical and Biomolecular Engineering



Ramon Gonzalez, Associate Professor
Chemical and Biomolecular Engineering



Kenneth Cox, Professor-in-the-Practice,
Chemical and Biomolecular Engineering



Daniel Cohan, Assistant Professor
Civil and Environmental Engineering

HOUSTON, TEXAS
FEBRUARY 2012

RICE UNIVERSITY

**Sustainable Production of Biofuels:
Plant Optimization and Environmental Impact**

By

Venetia Rigou

A THESIS SUBMITTED
IN PARTIAL FULFILLMENT OF THE
REQUIREMENTS FOR THE DEGREE

Doctor of Philosophy

APPROVED, THESIS COMMITTEE:




Kyriacos Zygorakis, A.J. Hartsook Professor, Chair
Chemical and Biomolecular Engineering



Ramon Gonzalez, Associate Professor
Chemical and Biomolecular Engineering



Kenneth Cox, Professor-in-the-Practice,
Chemical and Biomolecular Engineering



Daniel Cohan, Assistant Professor
Civil and Environmental Engineering

HOUSTON, TEXAS
FEBRUARY 2012

Abstract

Sustainable Production of Biofuels: Plant Optimization and Environmental Impact

by

Venetia Rigou

Many recent studies on the relative costs and benefits of biofuels have raised the need for a detailed and rigorous analysis of the operations of a biorefinery that is focused on optimization. The current thesis concentrates on the design and optimization of plants for producing biodiesel and ethanol from cellulosic biomass. We have performed numerical simulations combined with systematic parametric analyses to investigate the effect of various parameters on the overall material and energy balances of each biorefinery. The efficiency of the simulated processes was investigated by introducing and/or estimating various metrics in order to select the more beneficial directions for process improvements. Particular emphasis has been paid on heat integration and the design of highly efficient combined heat and power (CHP) units that generate the steam and electricity needed for the purification of biofuels and their co-products.

The first part of the thesis is focused on biodiesel production via transesterification of soybean oil with methanol, under alkali-catalyzed conditions. We have analyzed the performance of several reactor configurations in order to improve the conversion of the

reversible transesterification reactions. The effect of the oil to alcohol ratio has also been extensively explored. Furthermore, the energy requirements of the simulated process have been rigorously calculated. Since biodiesel facilities can be used either for small-scale, distributed applications or for large-scale production, we have explored whether it is more energy efficient to burn the glycerol-rich stream in a combined heat and power (CHP) plant, or purify the glycerol and use it a feedstock for producing higher-value chemicals with further biotechnological processes.

The second part of the thesis focuses on the production of cellulosic ethanol. Having developed the process model, a detailed parametric analysis was carried out to determine how the energy balances and overall efficiency of the biorefinery were influenced by changes in (a) the composition of the biomass feedstock, and (b) the conversion levels of the hydrolysis and fermentation stages. Furthermore, the requirements of the utility section of the ethanol plant were calculated. The utility section included a combined heat and power unit where by-product streams of the production process were utilized for energy generation. The parametric analysis indicated that these streams were in most cases an insufficient fuel source for meeting the energy requirements of the plant and thus, additional fuel was required (biomass, coal, or natural gas). The calculations of this section indicated a significant trade-off between ethanol production and external energy inputs, thus casting some doubt on the ultimate effectiveness of efforts to develop genetically modified energy crops (with high carbohydrate content) in order to maximize fuel production.

Acknowledgements

I would like to express my sincerest gratitude to my academic advisor, Professor Kyriacos Zygourakis, for being such a wonderful mentor. His knowledge, constructive criticism, valuable remarks and, above all, encouragement have been invaluable to me. I am truly grateful for his time, energy, and guidance during my research work.

I would also like to thank my thesis committee members: Professor Ramon Gonzalez and Professor Daniel Cohan, for their interest in my research, and their insightful comments; Professor Kenneth Cox for being extremely helpful, and always willing to provide sound advice every time I needed his help.

This project was financially supported by grants from the Rice Shell Center for Sustainability and the Janicek Endowment, whom I gratefully acknowledge.

I would not have the opportunity to pursue graduate studies in the US if it wasn't for my diploma thesis advisor, Professor Andreas Boudouvis. I am truly thankful for his encouragement and advice, generously provided even throughout my graduate studies.

I am also grateful to my friends, for being there for me every time I needed their opinion, support, advice, and great company! Thank you Kosta, Mihali, Vicky, Yanni, Maria, Niko, Spyrantha, Leda, and Ilia! You have been wonderful friends – no matter how many miles come between us!

I would also like to thank my brother, Yanni, for his love, and optimistic attitude. Despite his demanding workload, he was there every time I needed his advice or support.

Last but certainly not least, I am extremely thankful to my parents, Niko and Georgia, for their love and encouragement during all my pursuits. No words can express how appreciative I am for everything they have done for me throughout my life. Thank you mum and dad for guiding, inspiring, supporting and, above all, loving me!

*This thesis is dedicated to my mother and the loving memory of my father:
without their love and encouragement this work would not have been possible.*

Table of Contents

ABSTRACT	II
ACKNOWLEDGEMENTS.....	IV
TABLE OF CONTENTS	VII
LIST OF FIGURES	X
LIST OF TABLES.....	XIV
CHAPTER 1	1
1.1. OVERVIEW.....	1
1.2. RESEARCH MOTIVATION	1
1.3. SPECIFIC OBJECTIVES.....	4
1.4. THESIS STRUCTURE.....	5
CHAPTER 2	7
2.1. PRODUCTION OF BIOFUELS	7
2.2. BIODIESEL PRODUCTION	7
2.2.1. Microemulsions.....	8
2.2.2. Thermal Cracking.....	8
2.2.3. Transesterification.....	8
2.3. CELLULOSIC ETHANOL PRODUCTION.....	10
2.3.1. Pretreatment of the biomass.....	13
2.3.2. Conversion of cellulose to ethanol.....	16
2.3.3. Distillation.....	21

2.4.	ENERGY EFFICIENCY METRICS	22
CHAPTER 3	29	
3.1.	REVIEW OF RELATED STUDIES.....	29
3.2.	KINETICS OF TRANSESTERIFICATION REACTION	29
3.3.	PROCESS OVERVIEW	34
3.4.	BIODIESEL REACTOR DESIGN	36
3.4.1.	Reactor Configurations.....	37
3.4.1.1.	<i>Ideal Batch Reactor</i>	37
3.4.1.2.	<i>Ideal Continuous Reactor</i>	39
3.4.2.	Transesterification.....	41
3.4.3.	Methanol recovery.....	49
3.4.4.	FAME purification	50
3.4.5.	Glycerin utilization.....	52
3.4.5.1.	<i>Glycerin as co-product</i>	52
3.4.5.2.	<i>Glycerin for ethanol production</i>	52
3.4.5.3.	<i>Glycerin for steam and power production</i>	55
3.5.	PROCESS DESIGN	56
3.5.1.	Case I: Transesterification in a single CSTR.....	56
3.5.2.	Case II: Transesterification in a single CSTR; Glycerin purification	64
3.5.3.	Case III: Transesterification in two CSTRs.....	65
3.5.4.	Case IV: Transesterification in two CSTRs; Glycerin fermentation.....	67
3.5.5.	Case V: Transesterification in two CSTRs; Glycerin for steam and power production.....	68

CHAPTER 4	70
4.1. PROCESS OVERVIEW: CELLULOSIC ETHANOL PRODUCTION	70
4.2. DESIGN BASIS	72
4.3. MATERIAL AND ENERGY BALANCES.....	74
4.4. SENSITIVITY ANALYSIS – MONTE CARLO ANALYSIS	84
4.5. FEEDSTOCK COMPOSITION	89
4.5.1. Case I: Increased Carbohydrate Content	89
4.5.2. Case II: Increased Lignin Content.....	92
4.5.3. Case III: Corn stover (realistic scenario) & herbaceous crops.....	97
4.6. EFFECT OF FUEL USED IN THE AUXILIARY CHP SECTION	114
4.7. EFFECT OF CONVERSION DURING ENZYMATIC HYDROLYSIS.....	120
4.8. EFFECT OF FERMENTATION CONVERSION.....	123
4.9. EFFECT OF HEAT INTEGRATION	127
CHAPTER 5	129
CONCLUDING REMARKS AND FUTURE DIRECTIONS.....	129
REFERENCES	134
APPENDIX A	151
APPENDIX B.....	159
APPENDIX C	168

List of Figures

Figure 1: Biomass yields for low-input, high-diversity (LIHD) native grassland perennials	2
Figure 2: Schematic representation of biomass conversion to ethanol	11
Figure 3: Biomass conversion to cellulosic ethanol.....	13
Figure 4: Schematic representation of the separate hydrolysis and fermentation technique (SHF)	19
Figure 5: Schematic representation of simultaneous saccharification and co-fermentation (SSCF) of pentoses and hexoses	20
Figure 6: Schematic representation of the direct microbial conversion	21
Figure 7: Schematic representation of the energy flows during biofuel production.....	23
Figure 8: Energy balance for corn ethanol.....	24
Figure 9: Energy balance for biodiesel.....	24
Figure 10: Schematic representation of a batch reactor.....	38
Figure 11: Plug flow reactor	39
Figure 12: Continuous-flow stirred tank reactor	41
Figure 13: Methyl ester conversion of triglycerides for different alcohol to oil ratio.....	44
Figure 14: The metabolic pathways for the production of ethanol from glycerol, for <i>Escherichia coli</i>	54
Figure 15: Transesterification in a single CSTR.....	57
Figure 16: Neutralization and methanol recovery	58
Figure 17: Washing and FAME purification	59
Figure 18: Combined heat and power unit, producing power and steam	59

Figure 19: Transesterification in two CSTRs	65
Figure 20: Cellulosic ethanol production from corn stover (saccharification and fermentation)	72
Figure 21: Pretreatment section & enzymatic hydrolysis of the biomass	75
Figure 22: Fermentation section of bioethanol production.....	76
Figure 23: Ethanol purification section (distillation & dehydration)	77
Figure 24: Utility section integrated to the biorefinery	78
Figure 25: Auxiliary CHP unit, operating with natural gas	79
Figure 26: Deviation from nominal value (%) for various process parameters.....	87
Figure 27: Histogram for the distribution of ethanol production data, and the cumulative probability	88
Figure 28: Ethanol production with respect to carbohydrate content of the biomass (Case I).....	91
Figure 29: Natural gas demand with respect to carbohydrate content of the biomass (Case I).....	91
Figure 30: Biorefinery net energy value with respect to carbohydrate content of biomass (Case I).....	92
Figure 31: Net energy ratio with respect to carbohydrate content of biomass (Case I)	92
Figure 32: Ethanol production with respect to lignin content of the biomass (Case II)....	94
Figure 33: Natural gas demand with respect to lignin content of the biomass (Case II)...	94
Figure 34: Biorefinery net energy value with respect to lignin content of biomass (Case II)	95
Figure 35: Net energy ratio with respect to lignin content of biomass (Case II).....	95

Figure 36: Ethanol production with respect to carbohydrate content for corn stover.....	96
Figure 37: Natural gas demand with respect to carbohydrate content for corn stover.....	96
Figure 38: Biorefinery net energy value with respect to carbohydrate content for corn stover.....	97
Figure 39: Net energy ratio with respect to carbohydrate content for corn stover.....	97
Figure 40: Ethanol production with respect to carbohydrate content of the biomass (Case III-a).....	100
Figure 41: Ethanol production with respect to carbohydrate content of the biomass (Case III-c).....	105
Figure 42: Biorefinery net energy value with respect to ethanol production (Case III-c).	106
Figure 43: Ethanol production with respect to carbohydrate content for all herbaceous crops.....	112
Figure 44: Biorefinery net energy values with respect to ethanol production for all herbaceous crops	112
Figure 45: Total CO ₂ emissions values with respect to ethanol production for all herbaceous crops	113
Figure 46: Effect of fuel input at CHP auxiliary unit on the total CO ₂ emissions (corn stover)	119
Figure 47: Effect of fuel input at CHP auxiliary unit on the total CO ₂ emissions (switchgrass)	119
Figure 48: Ethanol production with respect to cellulose conversion during hydrolysis .	121
Figure 49: Natural gas demand with respect to cellulose conversion during hydrolysis	122

Figure 50: Biorefinery net energy value with respect to cellulose conversion during hydrolysis	122
Figure 51: Net energy ratio with respect to cellulose conversion during saccharification	123
Figure 52: Ethanol production with respect to fermentation conversion, for constant biomass input	125
Figure 53: Natural gas demand with respect to fermentation conversion, for constant biomass input	125
Figure 54: Biorefinery net energy value with respect to fermentation conversion, for constant biomass input.....	126
Figure 55: Net energy ratio with respect to fermentation conversion, for constant biomass input	126
Figure 56: Natural gas requirements with respect to carbohydrate content of the biomass, for biorefinery operation with and without heat integration.....	127
Figure 57: Biorefinery net energy value with respect to carbohydrate content of the biomass, for biorefinery operation with and without heat integration	127
Figure 58: Net energy ratios with respect to carbohydrate content of the biomass, for biorefinery operation with and without heat integration	128

List of Tables

Table 1: Comparison of the options for cellular hydrolysis	17
Table 2: Raw materials and operating conditions for transesterification reaction.....	32
Table 3: Reaction rate constants for transesterification.....	43
Table 4: Methyl ester conversions for various systems.....	45
Table 5: Effect of residence time on methyl ester conversion.....	45
Table 6: Steady-state concentration of the components at the exit of each reactor	46
Table 7: Conversion of triglycerides to methyl esters (%).....	47
Table 8: Steady-state concentration of methyl esters at the exit of each reactor	47
Table 9: Conversion of triglycerides to methyl esters (%).....	48
Table 10: Steady-state concentration of the components at the exit of each reactor	49
Table 11: Boiling point of the components entering the distillation column (ROH removal)	50
Table 12: Material input and energy demand during biodiesel production (base-case)....	60
Table 13: Mass balance for the base-case scenario (kg/hr)	61
Table 14: Steam and power balance for the biorefinery (GJ/hr) (base-case)	61
Table 15: Metrics estimation, w/ and w/o co-product credit (co-product: glycerin) (base-case)	62
Table 16: Effect of MeOH to oil ratio in the energy demand during biodiesel production	62
Table 17: Effect of MeOH to oil ratio in the energy balance for the biorefinery	63
Table 18: Effect of MeOH to oil ratio in metrics estimation, w/o co-product credit (glycerin).....	63

Table 19: Effect of MeOH to oil ratio in metrics estimation, w/ co-product credit (glycerin).....	63
Table 20: Material input and energy demand during biodiesel production (Case II)	64
Table 21: Steam and power balance for the biorefinery (GJ/hr) (Case II)	64
Table 22: Metrics estimation, w/ and w/o co-product credit (co-product: glycerin) (Case II)	64
Table 23: Mass balance for Case III (kg/hr)	66
Table 24: Material input and energy demand during biodiesel production (Case III)	66
Table 25: Steam and power balance for the biorefinery (GJ/hr) (Case III)	66
Table 26: Metrics estimation, w/ and w/o co-product credit (co-product: glycerin) (Case III)	66
Table 27: Material input and energy demand during biodiesel production (Case IV)	67
Table 28: Steam and power balance for the biorefinery (GJ/hr) (Case IV)	67
Table 29: Metrics estimation, w/ and w/o co-product credit (co-product: ethanol) (Case IV)	68
Table 30: Material input and energy demand during biodiesel production (Case V)	68
Table 31: Steam and power balance for the biorefinery (GJ/hr) (Case V)	69
Table 32: Metrics estimation (Case V)	69
Table 33: Corn stover composition and properties	73
Table 34: Process parameters	73
Table 35: Mass balance for the base-case scenario (MT/hr)	79
Table 36: Biomass content and energy demand during ethanol production (base-case)...	80
Table 37: Steam and power balance for the biorefinery (GJ/hr) (base-case)	81

Table 38: Metrics estimation (base-case)	81
Table 39: Steam and power requirements per sector (base-case)	81
Table 40: CO ₂ emissions per sector (MT/hr) (base-case).....	82
Table 41: Net energy summary (incl. co-products), adapted from literature.....	83
Table 42: Input parameters for the sensitivity analysis	85
Table 43: Estimation of the variation coefficient.....	86
Table 44: Statistics for ethanol production	88
Table 45: Corn stover w/ increased carbohydrate scenario, w/ heat integration (Case I) .	90
Table 46: Metrics estimation (Case I)	90
Table 47: Corn stover w/ increased lignin scenario, w/ heat integration (Case II).....	93
Table 48: Metrics estimation (Case II)	93
Table 49: Energy content of biomass feedstock.....	98
Table 50: Corn stover used as feedstock, w/ integration (Case III-a)	99
Table 51: Metrics estimation (Case III-a).....	99
Table 52: Steam requirements per sector (MT/hr) (Case III-a)	100
Table 53: CO ₂ emissions per sector (MT/hr) (Case III-a)	101
Table 54: Switchgrass used as feedstock, w/ heat integration (Case III-b)	102
Table 55: Metrics estimation (Case III-b).....	102
Table 56: Steam requirements per sector (MT/hr) (Case III-b)	103
Table 57: CO ₂ emissions per sector (MT/hr) (Case III-b)	103
Table 58: Big bluestem used as feedstock, w/ heat integration (Case III-c).....	104
Table 59: Metrics estimation (Case III-c).....	104
Table 60: Steam requirements per sector (MT/hr) (Case III-c)	106

Table 61: CO ₂ emissions per sector (MT/hr) (Case III-c)	107
Table 62: Sericea Lespedeza used as feedstock, w/ heat integration (Case III-d)	108
Table 63: Metrics estimation (Case III-d).....	109
Table 64: Steam requirements per sector (MT/hr) (Case III-d)	110
Table 65: CO ₂ emissions per sector (MT/hr) (Case III-d)	111
Table 66: Comparison between different varieties of feedstock (*) for ethanol production	113
Table 67: Comparison between different varieties of feedstock for ethanol production (II)	114
Table 68: Wyodak-Anderson coal – elemental analysis (wt. %)	115
Table 69: Wyodak-Anderson coal – proximate analysis (wt. %)	115
Table 70: Corn stover used as feedstock, w/ integration (Case IV-a)	116
Table 71: Metrics estimation (Case IV-a).....	116
Table 72: CO ₂ emissions per sector (MT/hr) (Case IV-a)	117
Table 73: Switchgrass used as feedstock, w/ heat integration (Case IV-b)	117
Table 74: Metrics estimation (Case IV-b)	118
Table 75: CO ₂ emissions per sector (MT/hr) (Case IV-b).....	118
Table 76: Effect of cellulose conversion during hydrolysis on ethanol production.....	120
Table 77: Effect of cellulose conversion during hydrolysis at metrics estimation	121
Table 78: Effect of the fermentation conversion at ethanol production	124
Table 79: Effect of the fermentation conversion at metrics estimation.....	124

Chapter 1

1.1. Overview

Concerns about global warming as well as about the availability and security of petroleum supplies have led the U.S. and other industrialized nations to seek alternative energy sources. Chapter 1 presents the motivation and specific objectives of this research project, which focuses on biofuel production processes for biodiesel and cellulosic ethanol.

1.2. Research Motivation

The transition to alternative transportation fuels from renewable sources has been the subject of hotly contested debates about the net energy values, the economics and the environmental impact of biofuels. At first, the utilization of biomass to produce liquid transportation fuels appeared as an attractive option. For example, several studies reported that the United States could sustainably produce enough biomass to substitute one-third or more of the motor gasoline used in 2005 by ethanol derived from corn and cellulosic materials (Shay, 1993; Worldwatch Institute: Earthscan, 2007; Ma and Hanna, 1999). Biodiesel produced from soybean, rapeseed or palm oil was also offered as a possible substitute of a significant fraction of the petrodiesel consumed in the U.S. every year. At the same time, the biomass-derived transportation fuels would significantly reduce the carbon dioxide emissions associated with the increasing use of gasoline and petrodiesel. Thus, biofuels were touted as the green technological solution that promised

both a sustainable source of liquid fuels and significant reductions of carbon dioxide emissions from the transportation sector.

Many of the available studies, however, used either unrealistic biomass yields or less-than-rigorous approaches for estimating the energy inputs for the biorefinery phase (see, for example, Farrell *et al.*, 2006, Hill *et al.*, 2006, Agarwal, 2007). While some studies claimed that biomass yields between 12.5 and 25 dry tons per hectare could be obtained from monocultures of energy crops like switchgrass, other studies indicated that biomass yields (from marginal lands in particular) would be significantly lower as shown in Figure 1 (Tilman *et al.*, 2006; Fargione *et al.*, 2008).

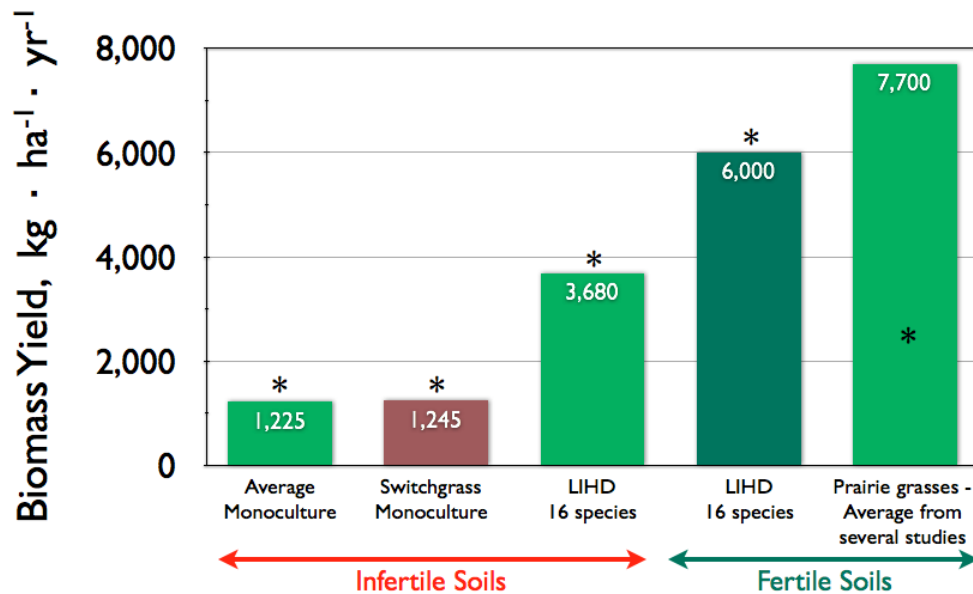


Figure 1: Biomass yields for low-input, high-diversity (LIHD) native grassland perennials. Data from (Tilman *et al.* 2006; Fargione *et al.* 2008)

More important, however, was the lack of rigorous analysis of the energy needs of biorefineries. Often, estimates of energy needs were based on simplified calculations or extrapolations from similar processes (Pimentel and Patzek, 2005; Farrell *et al.*, 2006).

These limitations cast some doubt on the validity of studies predicting that biofuels (particularly cellulosic ethanol) can be produced with large positive energy balances and whose adoption will result in significant environmental benefit. These studies have raised the need for an analysis of the operations of a biorefinery that is far more detailed and focused on optimization.

The overarching goal of this thesis is to introduce a modeling and computational framework that will allow for rigorously testing the validity of earlier studies. To achieve this goal, we have developed and used computational tools for the optimal design of chemical reactors and other processing units used for the production of cellulosic ethanol and biodiesel. We paid particular emphasis on heat integration and the design of highly efficient combined heat and power (CHP) units that will generate the steam and electricity needed for the production and purification of biofuels and their co-products.

Having developed the model, we analyzed the energy needs of cellulosic ethanol and biodiesel plants that use a variety of feedstocks. This allowed us to accurately quantify the effect of feedstock composition on biofuel yields, calculate the amount of extra fossil fuel that must be used to meet the steam and power needs that cannot be satisfied by burning the unreacted biomass, and provide accurate estimates of the net energy values

for the overall plant. In the case of cellulosic ethanol, our calculations can help us decide whether the proposed efforts to develop genetically modified plants with less lignin and more cellulose (Lynd *et al.*, 2008; Rubin, 2008; Somerville *et al.*, 2010; Fu *et al.*, 2011; Fu *et al.*, 2011) will improve the energy efficiency of the overall process. We also analyzed the energy efficiency of biodiesel plants that burn the produced glycerin and unreacted alcohol to meet the energy demands of the biorefinery or to generate and sell electricity (co-product).

1.3. Specific Objectives

As previously mentioned, the main objective of this work is the development of a comprehensive simulation framework for the optimal design of biofuel production facilities using a system-based approach that considers all the critical components of a biorefinery. Specifically, we will address the following questions:

- a. Which reactor configuration should be used to optimize the operation of each facility?
- b. Which is the optimal sequence of separation processes that should be used in each case? How will this analysis be affected if a decision is made to utilize a byproduct stream for energy generation instead of purifying it in order to sell it?
- c. How much can the energy efficiency of our biorefinery be improved by heat integration?
- d. How can we best utilize various biomass fractions and/or byproducts for energy generation? What is the specific configuration of power plant that must be used for

- each application and how important is the role of these units in determining the overall energy efficiency of the biorefinery?
- e. What is the net energy value of the produced biofuels and how does it vary with biomass yields and compositions?
 - f. What is the effect of biofuels production in the carbon dioxide emissions, and how significant is the environmental benefit?

1.4. Thesis Structure

The subsequent chapters of this thesis are structured in the following way:

- **Chapter 2** reviews previously published work concerning biofuel production. Existing technologies for the production of biodiesel and bioethanol are assessed. Based on that review, we propose alternatives to rigorously simulate and explore critical parts of these processes. The final section of this chapter introduces the metrics that will be used to evaluate the energy efficiency of the biorefineries.
- **Chapter 3** begins with a detailed description of the steps involved in biodiesel production and reviews the literature on transesterification kinetics. Next, we investigate the optimal design of biodiesel reactors using the methanolysis of soybean oil with alkali catalysts as our base case. We then develop a model for the entire biodiesel plant and perform a rigorous analysis of its energy needs. We finally consider alternative utilization of reaction co-product stream (mainly glycerin) to meet the energy requirements of the biorefinery.

- **Chapter 4** considers the production of cellulosic ethanol from corn stover and other biomass feedstocks. After developing the simulation model, we assess the effect of critical parameters (like feedstock compositions, conversions etc.) on the performance of the biofinery through a systematic parametric analysis. We also explore the effect of heat integration in the energy efficiency of the facility.
- **Chapter 5** summarizes the key findings of the thesis and proposes directions for future investigations.

Chapter 2

2.1. Production of Biofuels

This chapter provides an overview of existing methods for biofuels production. The first part presents the main methods for biodiesel production: microemulsions, pyrolysis, and transesterification. The second part of this chapter briefly presents existing technologies for the production of cellulosic ethanol, namely the separate hydrolysis and fermentation (SHF), the simultaneous saccharification and fermentation (SSF), the simultaneous saccharification and co-fermentation of hexoses and pentoses (SSCF), and the direct microbial conversion (DMC). The third and final part introduces the metrics that we will use to evaluate the energy efficiency of biofuel production plants.

2.2. Biodiesel Production

Methods for biodiesel production that have been used over time include direct use of vegetable oils, microemulsions, pyrolysis, and transesterification (Ma and Hanna, 1999). Direct use of vegetable oils has certain advantages, because they are renewable and readily available. However, the high viscosity and low volatility of vegetable oils prohibit their direct utilization as diesel fuel. Even though they could be used for a short period of time, they cause problems in the long run, like thickening and gelling of the oil in low temperatures, and carbon deposits on the engine. Additionally, their extensive use would result in oil deterioration and incomplete combustion, which would ultimately damage the engine.

2.2.1. Microemulsions

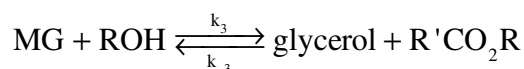
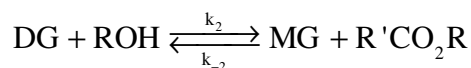
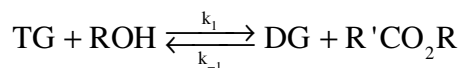
The use of microemulsions was introduced to deal with the high viscosity issue. The solvents used were primarily methanol, and ethanol. Results indicated this process led to a good quality of alternative fuel. However, several drawbacks have been associated with this technology: increase in the viscosity of the vegetable oil (after long-term use), formation of carbon deposits, or incomplete combustion (Ma and Hanna, 1999).

2.2.2. Thermal Cracking

Thermal cracking of vegetable oils to produce biofuels is an approach that had been used since WWI (Ma and Hanna, 1999]. The principal goal was to synthesize petroleum. Catalytic cracking of vegetable oils had been studied in the 90's also (Billaud *et al.*, 1995; Pioch *et al.*, 1993). This process resulted in fuels of better quality, yet the cost was quite high for a medium-scale production.

2.2.3. Transesterification

Transesterification is the most widely used approach for the production of biodiesel. It is basically the reaction of a fat or oil with a low-molecular-weight alcohol to produce esters and glycerol. Generally, it is considered to be a reaction that requires three reversible reaction steps: triglycerides react with an alcohol and are successively converted into diglycerides, monoglycerides, and glycerol, successively. The reaction scheme can be represented by the following set of reactions:



where TG, DG, and MG, denote the triglycerides, diglycerides, and monoglycerides, respectively. Methanol, ethanol, propanol, and butanol are the alcohols used more frequently, with methanol as the most preferable choice due to its low cost and physical properties (Ma and Hanna, 1999).

Acid and alkali catalysts can be used to speed up the reaction. Alternatively, high conversion of triglycerides can be achieved when using alkaline earth metal catalysts, like calcium (Ca) or strontium (Sr). In this case, however, glycerin recovery is more difficult, and treatment of alkaline wastewater treatment is also required. During the past few years, another approach has been introduced, characterized by the utilization of enzymes. Lipases have been reported to be effective in both aqueous and non-aqueous systems (Wang *et al.*, 2006; Lu *et al.*, 2010). In this case, transesterification takes place under low to moderate temperatures and atmospheric pressure, resulting in higher purity of the product. Yet, the cost to produce these enzymes is significantly higher than the corresponding expense for an inorganic catalyst.

The majority of biodiesel producers are using sodium hydroxide (NaOH) in their facilities. Potassium hydroxide (KOH) is an alternative attractive option. It has been

reported that its removal produces potassium phosphate that can be used as a fertilizer (Isigigur *et al.*, 1994).

When transesterification takes place under alkali- or acidic conditions and in moderate temperatures ($\sim 60^{\circ}\text{C}$), a 6:1 alcohol (MeOH) to oil ratio is required to achieve satisfactory ester yields. When supercritical methanol is used, the alcohol to oil ratio is significantly greater (42:1). The reaction in this case takes place at $\sim 350^{\circ}\text{C}$, and esters can be generated from both free fatty acids and triglycerides, thus resulting in higher yields of biodiesel (Kusdiana and Saka, 2001).

2.3. Cellulosic Ethanol Production

Cellulosic ethanol is a biofuel produced from cellulosic biomass, which comprises the polymeric compounds that form plant biomass. The three main components of cellulosic biomass are cellulose, hemicellulose, and lignin. Because of its recalcitrance to enzymatic deconstruction, lignin is primarily used for generating energy for the ethanol biorefinery operations.

Cellulose is a homopolysaccharide of glucose ($(\text{C}_6\text{H}_{10}\text{O}_5)_n$) and constitutes 40-60% of the cellulosic biomass. It is the structural component of the primary cell wall of green plants. Its basic compound is cellobiose, which is produced by two glucose molecules, which are linked together with $\beta(1,4)$ bonds (Berg, 2007).

Hemicellulose comprises 10-25% of the total cellulosic biomass. It is a branched heteropolysaccharide, consisting of 5-carbon (xylose, arabinose) and 6-carbon molecules (glucose, mannose, and galactose). Hemicellulose is easier to hydrolyze and has a lower tolerance in thermal treatment or mechanical stress than cellulose, due to its branched nature, lack of crystallinity (percentage of the volume of the material that is crystallized), and lower degree of polymerization. The degree of polymerization (DP) is the number of repeating units in the polymer molecule (Wyman, 1996).

Lignin makes up 10-25% of cellulosic biomass. It is difficult to estimate the degree of polymerization of lignin, since it essentially fills the space in the cell walls between their cellulose, hemicellulose, and pectin. Pectin is a set of polysaccharides (at least 65% galacturonic acid units) contained in the cell walls of plants, which contributes to plant growth. The functional groups associated with lignin include phenolic and alcoholic hydroxyl groups, aldehyde and methoxy-groups. Due to this formation, lignin can be converted into higher value products like organic acids, phenols, and vanillin.

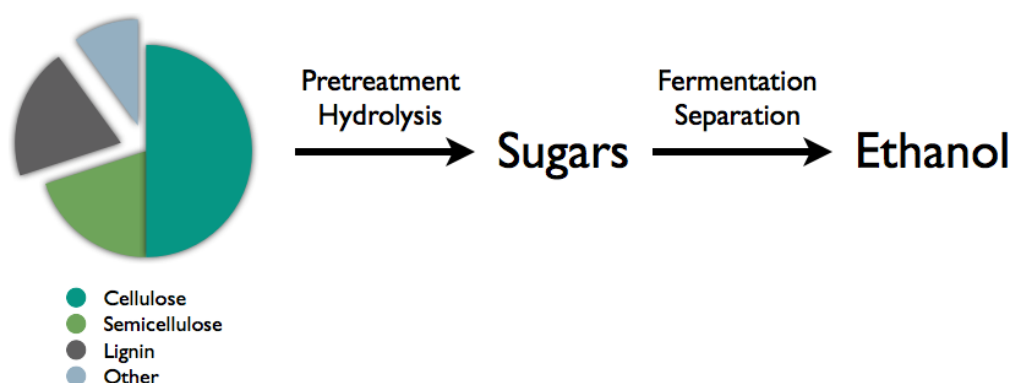


Figure 2: Schematic representation of biomass conversion to ethanol

Potential biomass feedstocks include energy crops, agricultural residues, and forestry waste (Speight, 2008). Several studies, dated back in the 70's, introduced the concept of utilizing an alternative renewable energy resource, such as biomass. The first studies were targeted in the production of biofuels from vegetable oil, starch, sugar, or animal fat. The basic feedstock for the production of these first generation biofuels is grains, like corn or wheat, and seeds, which are converted to vegetable oil, used for biodiesel production.

The second generation of biofuels incorporates a more viable approach to renewable energy production. Those biofuels are derived from non-food crops. Thus, the effect in both the food supplies and economy is lessened compared to first generation biofuels. Fast-growing trees, like willows or eucalypts, hedge plants, hybrid poplars, or a variety of grasses, with switchgrass as the most commonly proposed alternative, comprise the body of the dedicated energy crops that may be utilized for bioethanol production.

Since the ethanol yield is determined by the cellulose/hemicellulose content of the biomass, the choice of the feedstock will depend on the availability, cost, and environmental impact of the biomass. For example, greenhouse gas (GHG) emissions from the production of corn ethanol are significantly greater than the corresponding values when using switchgrass. However, the ethanol yield per acre is lower in the second case (Tilman *et al.*, 2006). What we should also take into consideration is the growing debate of "food vs. fuel", that is to what extent agricultural crops that could be used as food supplies should be employed for biofuel production.

A variety of physical, chemical, and enzymatic processes have been developed for the production of cellulosic ethanol. The basic (generic) scheme for this conversion is depicted in Figure 3.

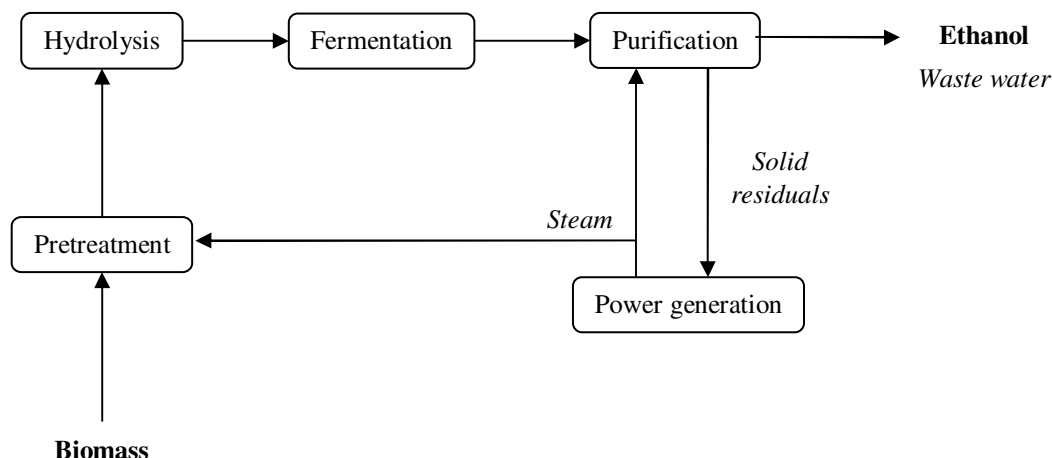


Figure 3: Biomass conversion to cellulosic ethanol

As represented above, the basic steps for the ethanol production include pretreatment of the biomass, hydrolysis of cellulose and hemicellulose, fermentation of the 5- and 6-carbon molecules, and purification of the final products.

2.3.1. Pretreatment of the biomass

This step is required to deconstruct the cellulosic biomass into its components. This involves mostly breaking down the crystalline formation and removing the lignin, which is very difficult to hydrolyze. The first step of pretreatment usually includes a size reduction technique, or comminution: increasing the surface area of the raw material results in a more efficient hydrolysis.

In general, the available pretreatment techniques can be classified as physical, chemical, and biological. Physical techniques include irradiation, steam explosion, and hydrothermolysis. Irradiation techniques can be subcategorized in electron beam irradiation (Horton *et al.*, 1980; Khan *et al.*, 1987), microwave heating (Ooshima *et al.*, 1984), and other irradiation techniques (Hill *et al.*, 2006). The drawbacks of these methods, related to their high cost and ineffectiveness, prohibit their application as industrial pretreatment techniques.

Steam explosion is the sole methodology that requires no detoxification steps. This technique involves the breakdown of the plant's structure by saturating the pores of the biomass with steam, followed by rapid decompression. The plant is separated in fibers and thus, it is hydrolyzed more easily. It has also been reported that steaming of biomass for several minutes releases the acetylated hemicellulose in the form of acetic acid (autohydrolysis). However, this process hinders the yield of hemicellulosic sugars due to partial hydrolysis and pyrolytic decomposition (Wyman, 1996).

Hydrothermolysis is another technique that has not been applied to large-scale. Biomass is cooked in water of high temperature. Existing reports support the assertion that despite the high xylose yields, hydrothermolysis is not suitable for large-scale operations. This process can also be referred to as aqueous fractionation, uncatalyzed solvolysis, or aquasolv process (Wyman, 1996).

Chemical pretreatment involves the presence of a chemical agent. That chemical compound can be acid or alkaline, ammonia, sulfur dioxide (SO₂), or carbon dioxide (CO₂). Acid pretreatments include pretreatment using dilute solutions of sulfuric acid (H₂SO₄), hydrochloric acid (HCl), nitric acid (HNO₃), and phosphoric acid (H₃PO₄). Taking into account the cost of the corresponding acids, the most attractive option is using H₂SO₄ (Ropars *et al.*, 1992) or SO₂ (Barbosa *et al.*, 1992).

In alkaline pretreatment, sodium hydroxide and sodium hydroxide with peroxide are the most common solutions utilized for the breakdown of the lignocellulosic biomass. This technique has been found to be more efficient for herbaceous and agricultural crops than wood residues (Wyman, 1996).

An alternative pretreatment process, ammonia fiber explosion (AFEX), utilizes liquid ammonia under pressure. Biomass is treated with concentrated ammonia under high pressures (more than 12 atm) at room temperature, or under pressure at high temperatures (up to 100°C). Decompression follows, and the ammonia evaporates and is recovered. The resulting biomass is much easier to be hydrolyzed. It has also been reported that ammonia fiber explosion is giving better yields than most of the other pretreatment methods (Sheehan *et al.*, 1998). Despite the good performance of the technique in agricultural residues though, poor yields have been reported in the case of wood and forestry residues.

In addition to the aforementioned techniques, the removal of lignin can take place following a biological pretreatment with lignin-modifying enzymes (LMEs). It has been reported that this technique has the advantage of lower energy input. However, the oxidation that takes place using those fungal enzymes takes a significant amount of cultivation time, compared to the other techniques. Another drawback is that there is a danger that cellulose and hemicellulose may be solubilized or consumed (Wyman, 1996).

2.3.2. Conversion of cellulose to ethanol

A variety of techniques can be applied after the pretreatment step to convert cellulose to ethanol. Separate hydrolysis and fermentation (SHF) is the most common process that can be implemented in large-scale. This process takes place in two sequential steps. Cellulose is first hydrolyzed, and the glucose produced is then fermented to ethanol.

During the first step (hydrolysis), the chains of sugar molecules are broken down and sugars are obtained. Hydrolysis can be categorized in chemical and enzymatic hydrolysis.

Chemical hydrolysis includes the acid treatment of the cellulose. It can take place either using a dilute acid at high temperatures, or a concentrated acid at moderate temperature and atmospheric pressure. In the latter case, higher yields of sugars have been observed (Hamelinck *et al.*, 2005; Kumar *et al.*, 2009). Concentrated acid can be recovered and recycled, a practice that is usually followed to reduce the capital cost of the hydrolysis.

Whilst no pretreatment step is required when performing acid hydrolysis (apart from size reduction), enzymatic hydrolysis requires a preceding separation of cellulose, hemicellulose, and lignin. Enzymatic hydrolysis utilizes cellulase enzymes under mild conditions to break down cellulose to beta-glucose. Those enzymes are produced mainly by bacteria, fungi, and protozoa. It has also been found that herbivores can produce those enzymes in their stomach. Ideally, the enzymes used should simultaneously exhibit the following properties: i) synthesis of an active cellulase enzyme system at high levels, ii) fermentation and growth on sugars arising from both cellulose and hemicellulose, and iii) production of ethanol at high selectivity and high concentration (Lynd, 1996). Table 1 summarizes and compares the characteristics of different hydrolysis techniques (Hamelinck *et al.*, 2005).

Table 1: Comparison of the options for cellular hydrolysis

	Consumables	Temperature	Reaction time	Glucose yield	Availability
Dilute acid hydrolysis	<1% H ₂ SO ₄	215°C	3 min	50-70%	Now
Concentrated acid hydrolysis	30-70% H ₂ SO ₄	40°C	2-6 hr	90%	Now
Enzymatic hydrolysis	Cellulase	70°C	1.5 days	75 → 95%	Now → 2020

Following hydrolysis, fermentation constitutes the final step for converting cellulosic biomass to ethanol. Fermentation is a set of reactions where the pentoses generated from hemicellulose hydrolysis, and the hexoses from cellulose hydrolysis, are converted to ethanol. Usually, the fermentation is performed by yeast or bacteria, which feed on the sugars. The conversions of xylose and glucose to ethanol and carbon dioxide are:



Performing hydrolysis and fermentation sequentially, allows each reaction to take place at its optimum temperature, resulting in superior product yields. However, the released sugars inhibit cellulase and beta-glucosidase during hydrolysis. That decreases the ethanol concentration and ultimately, makes its recovery more energy consuming, adding to the total cost of the fermentation.

Apart from the aforementioned process where fermentation takes place after hydrolysis, other methodologies can be also implemented. In simultaneous saccharification and fermentation (SSF), the two separate steps of hydrolysis and fermentation are combined, resulting in higher product yield. Coupling the steps increases the hydrolysis rate because the sugars produced inhibit the cellulase activity. Additional advantages related to the SSF process are the lower enzyme requirements, and the shorter process time (Hamelinck *et al.*, 2005).. In terms of equipment, SSF is economically more advantageous because a single reactor is used instead of two separate units, which decreases the capital cost of the process. This advantage though is just one side of the coin: having one reactor, the problem of determining an optimum temperature for both hydrolysis and fermentation is not easy. In the SHF, hydrolysis takes place at around 45°C-50°C, while the sugars produced are fermented at around 30°C. Another drawback that has been reported is related to the inhibition of the enzymes in the reactor by ethanol (Sun and Cheng, 2002).

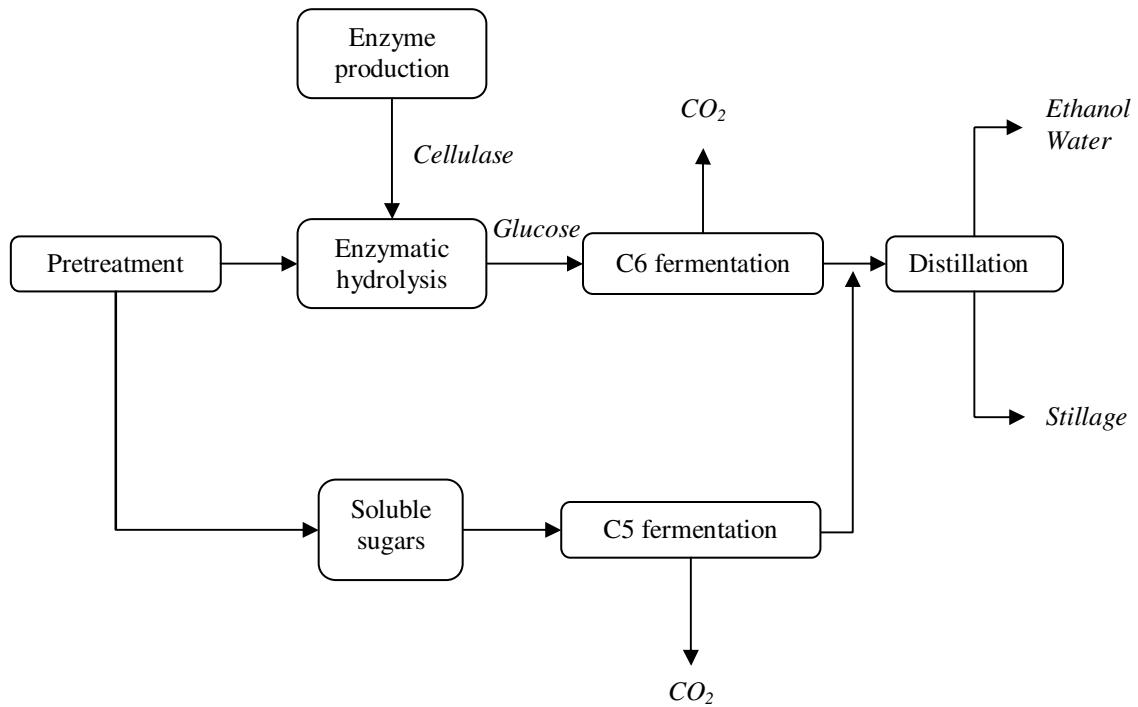


Figure 4: Schematic representation of the separate hydrolysis and fermentation technique (SHF)

An alternative to the SSF process that can be implemented is the simultaneous saccharification and co-fermentation of hexoses and pentoses (SSCF), i.e. the co-fermentation of glucose and xylose. Figure 5 is a schematic representation of this process (Hamelinck *et al.*, 2005).

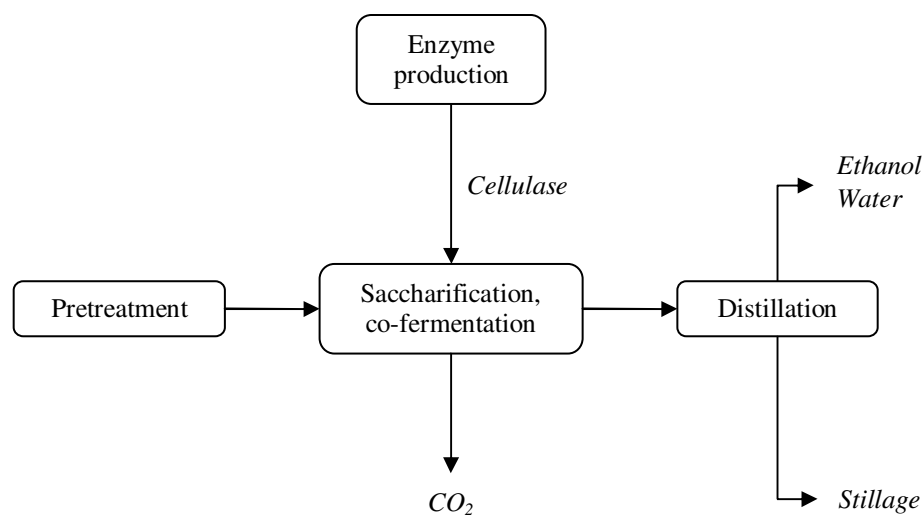


Figure 5: Schematic representation of simultaneous saccharification and co-fermentation (SSCF) of pentoses and hexoses

Several studies report that SSCF process is inefficient in terms of the product yield (Wyman, 1996). However, promising results have been reported in the literature, where genetically engineered microorganisms have managed to co-ferment cellulose and xylose to ethanol (Barbosa *et al.*, 1992; Padukone *et al.*, 1995; Wayman and Parekh, 1998; Wayman *et al.*, 1987). In these cases, the yield of the reaction has been found to be quite high, reaching almost complete xylose conversion, and approximately 80% conversion for ethanol (Wyman, 1996).

Last but not least, direct microbial conversion (DMC), also known as consolidated bioprocessing (CBP), constitutes another alternative for the conversion of cellulose to ethanol. This process essentially combines cellulase production, cellulose hydrolysis, and glucose fermentation, in a single step. The integration is quite beneficial, as the process requires a minimal number of reactors compared to the previous technologies, and the

cost of chemicals required is reduced. However, product inhibition is a frequent phenomenon, and so is the production of undesirable co-products, such as acetic and lactic acids (Wyman, 1996; Brown, 2003). As a result, the product yields observed are relatively lower compared to the ones obtained when implementing SHF, or SSF.

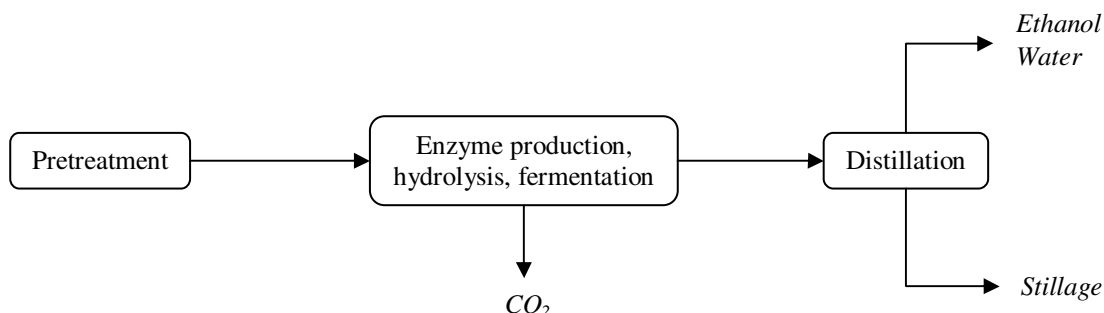


Figure 6: Schematic representation of the direct microbial conversion

The use of either glucose or xylose has been reported in the literature (Wyman, 1996; Lin and Tanaka, 2006). The results have indicated that some microorganisms prefer to utilize glucose over xylose, others the opposite, or both simultaneously. For those using xylose though, the process incorporates certain drawbacks, such as providing low ethanol yields or resulting in ethanol inhibition (Lin and Tanaka, 2006). Consequently, in the long run, this increases the operational cost for the ethanol production.

2.3.3. Distillation

This step is performed to separate the ethanol from the water and the soluble products of the fermentation. The ethanol concentration in the fermentation broth usually varies between 5% and 12% (wt) (Vane, 2008; Galbe and Zacchi, 2002; Lamsal *et al.*, 2011). The feed of the distillation column determines the energy demand for ethanol recovery:

increased ethanol concentration in the distillation feed, results in lower energy requirements. Reported values for the amount of energy required to recover ethanol are from 5 to 20 MJ-fuel/kg ethanol (Galbe and Zacchi, 2002).

Distilling the solution we have retrieved from fermentation sometimes results in ethanol of lower purity (Brown, 2003). In that case, a second distillation is required to recover ethanol of higher purity. The ethanol-rich stream from the second distillation however, is at or near the water-ethanol azeotrope (Brown, 2003). Therefore, an additional dehydration step is required so that the remaining water can be removed with the help of molecular sieves.

2.4. Energy Efficiency Metrics

Much of the public debate about fuels focuses on the net energy of biodiesel and cellulosic ethanol. However, several net energy metrics have been used in the literature. For instance, net energy may be defined as the “energy content of ethanol minus fossil energy used to produce ethanol,” or it may be defined as “the energy in ethanol and co-products less the energy in the inputs”.

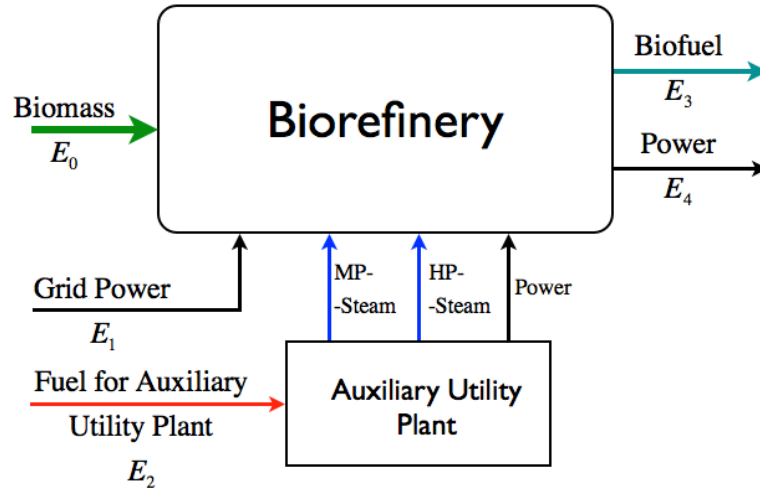


Figure 7: Schematic representation of the energy flows during biofuel production

A common metric used to measure the sustainability of biofuels is its net energy ratio (NER). This ratio is defined as:

$$\text{NER} = \frac{\left[\begin{array}{c} \text{Energy content} \\ \text{of biofuel} \end{array} \right] + \left[\begin{array}{c} \text{Energy content} \\ \text{of co-product} \end{array} \right]}{\left[\begin{array}{c} \text{Energy used in} \\ \text{agricultural phase} \end{array} \right] + \left[\begin{array}{c} \text{Energy in fuel used for} \\ \text{the auxiliary utility plant} \end{array} \right]}$$

The following figure depicts the net energy ratio for corn ethanol from data collected from the literature. As displayed, NER is above 1.0 when co-product credit is taken into account. The only value below unity has been given by Patzek (Patzek, 2004). Figure 9 represents the corresponding energy balance for biodiesel.

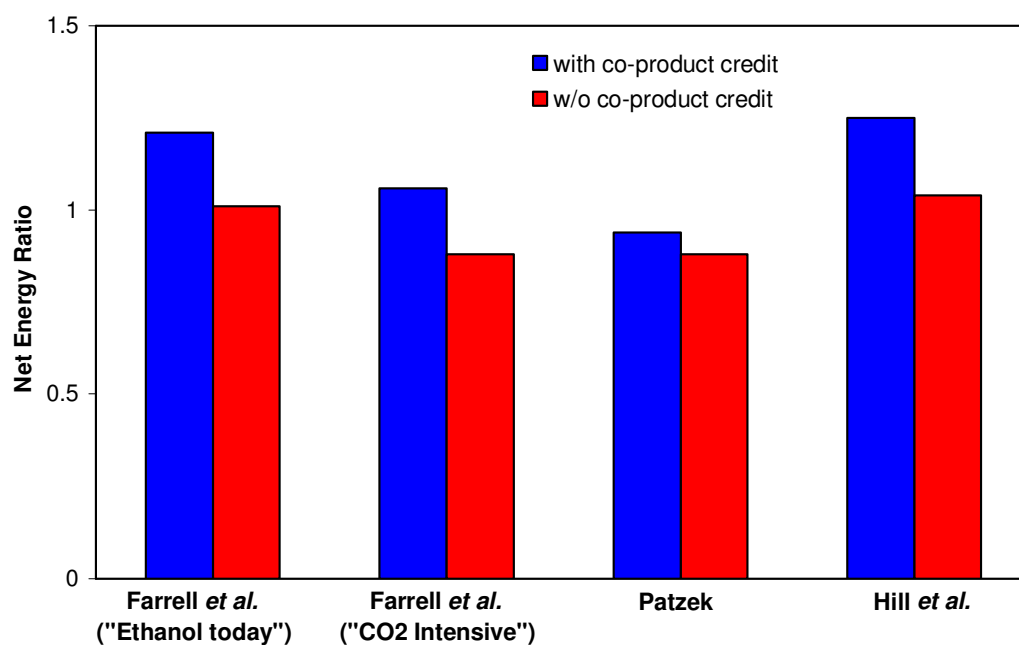


Figure 8: Energy balance for corn ethanol
(Data collected from Hill *et al.*, 2006; Patzek, 2004; Farrell *et al.*, 2006)

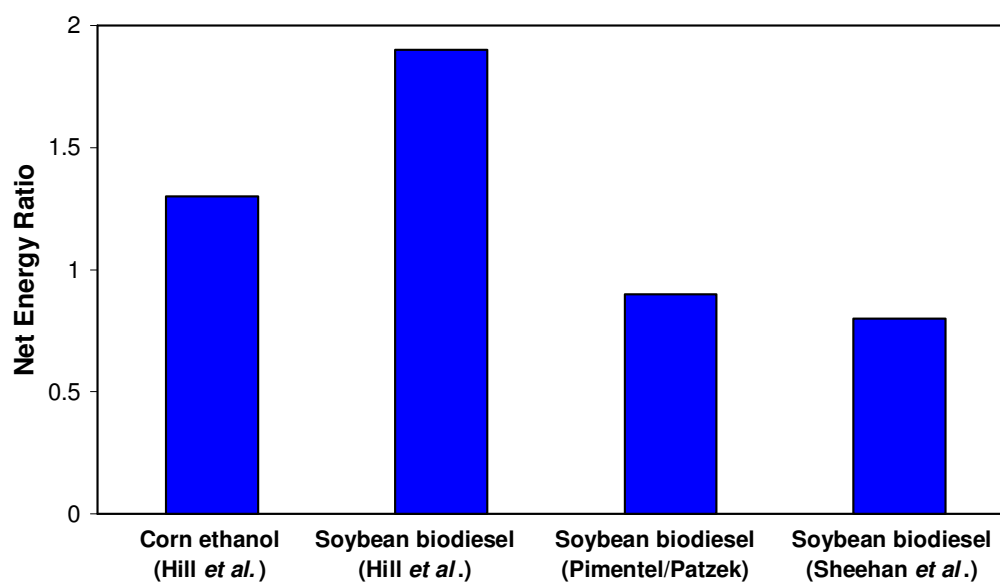


Figure 9: Energy balance for biodiesel
(Data collected from Hill *et al.*, 2006; Pimentel and Patzek, 2005; Sheehan *et al.*, 1998)

Our research project aims in providing an evaluation/estimation of the energy requirements for biofuel production, for both biodiesel and cellulosic ethanol. Therefore, the definition for Net Energy Ratio shown above results in:

$$NER^* = \frac{\left[\begin{array}{c} \text{Energy content} \\ \text{of biofuel} \end{array} \right] + \left[\begin{array}{c} \text{Energy content} \\ \text{of co-product} \end{array} \right]}{\left[\begin{array}{c} \text{Energy in fuel used for} \\ \text{the auxiliary utility plant} \end{array} \right]}$$

or, using the notation of Figure 7:

$$NER^* = \frac{E_3 + E_4}{E_2} \quad (\text{if } E_4 > 0 \text{ and } E_1 = 0)$$

Alternatively (if we have to buy power from the grid):

$$NER^* = \frac{E_3}{E_1 + E_2} \quad (\text{if } E_1 > 0 \text{ and } E_4 = 0)$$

It should be noted that the fuel used for the utility plant can be either a fossil fuel (natural gas or coal) or it can be **additional** biomass that is burned to meet the energy needs of the biorefinery. However, we will not include in this fuel any components of the biomass that are burned in the utility plant of the main biorefinery. Also, the energy for extracting and transporting the raw material or the final product has not been incorporated/taken into account in the model.

Additional metrics that will be used for our analysis will be:

- **The net energy value (NEV)** defined as:

$$NEV = \left[\begin{array}{c} \text{Energy content} \\ \text{of biofuel} \end{array} \right] + \left[\begin{array}{c} \text{Energy content} \\ \text{of co-product} \end{array} \right] - \left[\begin{array}{c} \text{Energy used in} \\ \text{agricultural phase} \end{array} \right] - \left[\begin{array}{c} \text{Energy in fuel used for} \\ \text{the auxiliary utility plant} \end{array} \right]$$

Since we are only interested in biorefinery operations:

$$NEV^* = \left[\begin{array}{c} \text{Energy content} \\ \text{of biofuel} \end{array} \right] + \left[\begin{array}{c} \text{Energy content} \\ \text{of co-product} \end{array} \right] - \left[\begin{array}{c} \text{Energy in fuel used for} \\ \text{the auxiliary utility plant} \end{array} \right]$$

Using the notation of Figure 7:

$$NEV^* = E_3 + E_4 - E_2 \quad (\text{if } E_4 > 0 \text{ and } E_1 = 0)$$

or (if we have to buy power from the grid):

$$NEV^* = E_3 - E_2 - E_1 \quad (\text{if } E_1 > 0 \text{ and } E_4 = 0)$$

Net energy value will be expressed in (MJ/L_{biofuel}), and for the calculations we will take into account only the biorefinery phase of the production process.

- **The overall efficiency of the biorefinery** defined as:

$$\eta = \frac{[\text{Energy content of products}]}{[\text{Energy content of input}]}$$

Based on Figure 7:

$$\eta = \frac{E_3 + E_4}{E_0 + E_2} \quad (\text{if } E_4 > 0 \text{ and } E_1 = 0)$$

or

$$\eta = \frac{E_3}{E_0 + E_1 + E_2} \quad (\text{if } E_1 > 0 \text{ and } E_4 = 0)$$

As energy content of the products we have considered that of biofuel and electricity produced, whereas the input energy content will include biomass, natural gas (or some other fuel source), and electricity consumed. The overall efficiency will be expressed as (%).

For the case of cellulosic ethanol production, two more metrics will be estimated:

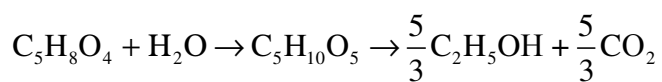
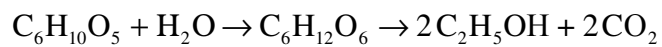
- **The conversion of biomass to biofuel (x)** defined as:

$$x = \frac{[Amount\ of\ biofuel\ produced]}{[Maximum\ theoretical\ amount\ of\ biofuel\ that\ can\ be\ produced\ from\ this\ feedstock]}$$

The maximum theoretical amount of ethanol produced from a certain feedstock, has been calculated analytically, based on the elemental composition of the biomass, and the reactions that take place during the conversion to ethanol. More specifically, the reactions we have assumed to occur during hydrolysis and fermentation are:



or, for simplicity reasons, use the overall reactions:



- **Carbon efficiency (*c.e.*)** defined as :

$$c.e. = \frac{[\textit{Carbon in biofuel produced}]}{[\textit{Carbon in biomass carbohydrate}]}$$

The amount of carbon is expressed as (% w.t.).

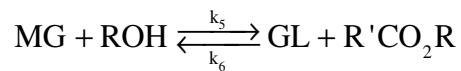
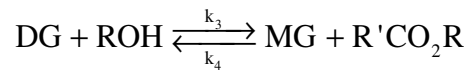
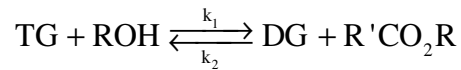
Chapter 3

3.1. Review of related studies

Transesterification of vegetable oils is the most widely used method for biodiesel production. To our knowledge, this study is the first reported attempt to rigorously analyze the steady-state and transient operation of chemical reactors used for the production of biodiesel in order to optimize their operation. Furthermore, the energy balance of biodiesel production plants has been carefully analyzed to determine the relative energy demands of their various sections. Finally, we have investigated possible approaches to improve the efficiency of biodiesel plants by utilizing reaction by-products to meet the energy demands of the biodiesel plant.

3.2. Kinetics of transesterification reaction

Transesterification involves the reaction of vegetable oils (triglycerides) with an alcohol to produce esters (biodiesel) and glycerol. The conversion of triglycerides to esters proceeds according to the following set of reversible reactions:



where TG, DG, MG, and GL denote the triglycerides, diglycerides, monoglycerides, and glycerol respectively, and k_1 , k_2 , k_3 , k_4 , k_5 , and k_6 are the kinetic constants of the

reactions. Several kinetic expressions have been proposed for the reaction rates r_1 through r_6 . The most commonly used expressions involve first order kinetics for the forward and reverse reactions (Noureddini and Zhu, 1997)

$$r_1 = k_1[\text{TG}][\text{ROH}] \quad (1.1)$$

$$r_2 = k_2[\text{DG}][\text{R}'\text{CO}_2\text{R}] \quad (1.2)$$

$$r_3 = k_3[\text{DG}][\text{ROH}] \quad (1.3)$$

$$r_4 = k_4[\text{MG}][\text{R}'\text{CO}_2\text{R}] \quad (1.4)$$

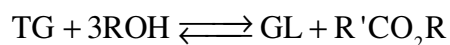
$$r_5 = k_5[\text{MG}][\text{ROH}] \quad (1.5)$$

$$r_6 = k_6[\text{GL}][\text{R}'\text{CO}_2\text{R}] \quad (1.6)$$

Bambase and coworkers used the same reaction scheme to model the methanolysis reactions for the conversion of sunflower oil to methyl esters (Bambase *et al.*, 2007). They assumed second-order kinetics and reported a good fit of their experimental data by the second-order reaction rates. The conversions calculated by these rate expressions are very comparable to the ones obtained using the Noureddini and Zhu kinetics (Noureddini and Zhu, 1997; Bambase *et al.* 2007).

Darnoko and Cheryan have studied the transesterification of palm oil with methanol, under alkali catalysts. The conversion of triglycerides (TG), diglycerides (DG), and monoglycerides (MG) appeared to be second order up to 30 min of reaction time, followed by first-order or zero-order kinetics (Darnoko and Cheryan, 2000). Kamee and coworkers studied the kinetics of base-catalyzed transesterification of *Pongamia* oil

(Karmee *et al.*, 2006). The kinetics of non-catalytic transesterification reactions were also studied by several investigators using, for example, soybean oil and methanol at higher temperatures (Diasakou *et al.*, 1998) and rapeseed (canola) oil and supercritical methanol (Kusdiana and Saka, 2001; Saka and Kusdiana, 2001). In the last study, the reaction scheme has been simplified to a single-step, reversible reaction:



The kinetics proposed was of first order, and the kinetic constant was determined for various operating conditions, resulting in acceptable agreement between simulations and experimental results.

Vicente and coworkers studied the kinetics of sunflower oil transesterification using a 6:1 methanol to oil ratio and potassium hydroxide (KOH) (Vicente *et al.*, 2005). They also assumed that the reactions for the conversion of tri- to diglycerides and of di- to monoglycerides were reversible. The third reaction that leads to the production of glycerol, however, was considered as irreversible.

Foon and coworkers (Foon *et al.*, 2004) studied the kinetics of palm oil transesterification at 60 °C using excess methanol (10:1 methanol to oil molar ratio) and NaOH or NaOCH₃ as catalysts. They assumed that transesterification is a second-order, irreversible reaction. However, doubts have been raised about the validity of their results since they claim to have achieved conversions higher than 99%. We have also chosen to disregard the study published by Kapilakarn and Peugtong for the transesterification

of palm oil with methanol (Kapilakarn and Peugtong, 2007). They reported that reaction was carried out at 60°C without a catalyst.

The table below summarizes the published work regarding the transesterification reaction. We can see that the most common scheme involves methanolysis (MeOH to oil ratio 6:1), alkali conditions and temperatures around 60°C.

Table 2: Raw materials and operating conditions for transesterification reaction

Published Work	Oil	Alcohol	ROH:Oil	Catalyst	Temperature
Freedman <i>et al.</i>(1986)	Soybean	MeOH	6:1		
		BuOH	30:1	H ₂ SO ₄ (1%)	77°C
		BuOH	30:1	NaOBu (1%)	60°C
		BuOH	30:1	NaOBu (0.5%)	60°C
Nourreddini & Zhu (1997)	Soybean	MeOH	6:1	NaOH (1%)	50°C
Ávila <i>et al.</i> (2008)	African palm	EtOH	6:1	KOH (1.3%)	30°C
					40°C
					50°C
					60°C
Vicente <i>et al.</i> (2005)	Sunflower	MeOH	6:1	KOH (0.5%) KOH (1%) KOH (1.5%)	(25-) 65°C
Darnoko & Cheryan (2000)	Palm	MeOH	6 :1	KOH (1%)	50-65 °C
Zhang <i>et al.</i> (2005) (simulations)	Soybean		6:1	NaOH (1%)	60°C
	Waste cooking		6:1	NaOH (1%)	70°C
	Waste cooking	MeOH	50:1	H ₂ SO ₄ (1.3%)	80°C
	Waste cooking		50:1	H ₂ SO ₄ (1.3%)	80°C
	(C ₆ H ₁₄ extraction)				
	Waste cooking		245:1	H ₂ SO ₄ (1.3%)	80°C
Sheehan <i>et al.</i> (1998) (Simulations –NREL)	Soybean	MeOH			60°C
Haas <i>et al.</i> (2006) (simulations)	Soybean	MeOH	6 :1	NaOCH ₃	60°C

Table 2 (cont): Raw materials and operating conditions for transesterification reaction

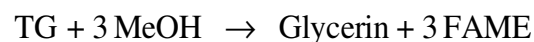
Published Work	Oil	Alcohol	ROH:Oil	Catalyst	Temperature
			6 :1		
Diassakou <i>et al.</i> (1998)	Soybean	MeOH	12 :1	No catalyst	220-235°C
			21 :1		
Bikou <i>et al.</i> (1999)	Cotton seed	EtOH			
Kusdiana & Saka (2001)	Rapeseed	MeOH	42:1		200-500°C
Komers <i>et al.</i> (2002)					
Turner (2005) (thesis based on Komers' paper)	Rapeseed	MeOH	Effect of saponification was included in the simulations		
Kapilakarn & Peugtong (2007)	Palm	MeOH	6:1	No catalyst	60°C
He <i>et al.</i> (2007)	Soybean	MeOH	42:1	No catalyst	210-280°C
Bambase <i>et al.</i> (2007)	Sunflower	MeOH	6:1 - 20:1	NaOH	25-60°C
Foon <i>et al.</i> (2004)	Palm	MeOH	10:1	NaOH or NaOCH ₃	60°C
Harding <i>et al.</i> (2007) (simulations based on Zhang's paper)	Rapeseed	MeOH	6:1	NaOH (1%)	60°C
		MeOH	3:1	Immob. Enzyme	25°C
		MeOH	6:1	NaOH (1%)	60°C
		EtOH	6:1	NaOH (1%)	60°C
		EtOH	3:1	Immob. Enzyme	25°C
Jansri <i>et al.</i> (2011)	Palm	MeOH	6:1	NaOH	55-65°C

All simulations performed for this study will assume the use of soybean oil, methanol, NaOCH₃ catalyst and the kinetic expressions described by equations (1.1) through (1.6) above. The temperature of transesterification is set to 60°C. Based on these conditions, the conversion of triglycerides to fatty acid methyl esters has been rigorously estimated, as described in Section 3.1 of the current chapter.

3.3. Process Overview

A computational framework for the biodiesel production process has been developed using MATLAB and SuperPro Designer. Our process includes the following stages:

1. Transesterification. A reaction between methanol and soybean oil is carried out in a continuous stirred tank reactor. The reaction takes place with a 6:1 methanol to oil ratio, using NaOCH_3 as catalyst, at 60°C . The streams with the reactants are mixed and heated prior to their entering the reactor. Triglycerides are converted to biodiesel (or FAME that stands for Fatty Acid Methyl Esters) according to the overall reaction scheme:

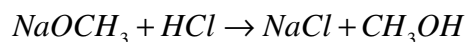


The conversion level of the reaction was rigorously calculated using MATLAB, as described in Section 4.1 of the current chapter.

Exiting the transesterification reactor, the stream containing the remaining oil, methanol, glycerin, FAME, enters a separation unit, where the FAME-rich phase is separated from the glycerin-rich one. Different scenarios were explored, as described in Section 4.1, to determine the optimum reactor configuration for transesterification: a reactor unit followed by a separator, two reactors followed by a separator, and a scheme involving two reactor/separator units. Moreover, the alternative of using three or more reactors was investigated.

2. Neutralization. Exiting the transesterification/separation section, part of the catalyst remains in both the glycerin- and the methyl ester-rich phases. In order to neutralize

NaOCH₃, dilute HCl is added to the streams, assuming 100% conversion. Neutralization of the catalyst is described by:



The exit stream, which is rich in glycerin, is led through a distillation column in order to recover the methanol and recycle it back to the transesterification reactor(s). The oil-rich stream is washed, and enters the methyl ester purification stage.

3. FAME purification. After the neutralization, the stream rich in methyl esters is washed and led through a centrifuge. Glycerin and methanol are removed and led to the glycerin processing section. The rest of the materials are heated and sent to a flash unit from where we recover the final product.

4. Glycerin processing. Glycerin recovery takes place through distillation: the glycerin-rich streams exiting the transesterification and the neutralization sections are led through a distillation column. The excess methanol is recovered and recycled to the transesterification reactor(s). A second distillation column is used to remove the excess water, which is recycled and used for the washing step of the biofuel production process. The final co-product is of approximately 80% purity. Depending on our ultimate objective however, different scenarios have been explored, involving either further purification of glycerin, or its utilization for a) ethanol production or b) steam and power generation in a combined heat and power unit integrated in biodiesel production process.

3.4. Biodiesel Reactor Design

Given the many choices of feedstock or catalysts and the reversible kinetic expressions of the reaction sequence for transesterification, it is reasonable to ask which reactor configuration will provide the optimal solution in each case. This is a classical reaction engineering problem that has not been addressed for biodiesel production until now.

Using transient material and energy balances, we will study the dynamics of the transesterification reaction sequence place in:

- a) a batch reactor,
- b) a single continuous stirred tank reactor (CSTR), and
- c) a cascade of CSTRs. A cascade with several CSTRs can be used to approximate a continuous flow reactor. Transesterification requires rigorous mixing to ensure that we have enough interfacial area for mass transport between the immiscible oil and alcohol phases. Such rigorous mixing cannot be easily achieved with a continuous reactor configuration and, thus, a cascade of CSTRs may offer an attractive alternative.

Even though there are many sophisticated models in the literature concerning reactor design, to our knowledge there was no systematic study that analyzed the performance of various reactor configurations for biodiesel production. Therefore, our goal was to obtain information concerning the amount of desired products (fatty acid methyl ester and glycerin) obtained from each configuration, and to determine which one is the most

preferable. This will form the basis for designing a sophisticated unit for biodiesel production.

3.4.1. Reactor Configurations

The base-case scenarios examined included ideal, isothermal reactors. For component j , the general formulation of the mass balance (molar) is:

$$\text{Accumulation} = \text{Input} - \text{Output} + \text{Production} - \text{Consumption}$$

$$\frac{d}{dt} \int_{V_R} C_j dV = F_0 C_{j_0} - F_1 C_{j_1} + \int_{V_R} R_j dV \quad (1.7)$$

where:

C_j : concentration of component j ,

F : volumetric flowrate,

R_j : reaction rate for component j ,

V_R : system volume,

and 0 and 1 denote the conditions at the inlet and outlet of the reactor.

3.4.1.1. Ideal Batch Reactor

A simplistic schematic of a batch reactor is depicted in Figure 10. Reactants A and B are charged, mixed, and transesterification takes place under isothermal conditions. We assume that mixing and heat transfer are ideal, thus resulting in uniform conditions within

the reactor (no concentration gradients). The volume of the tank is selected as the system volume.

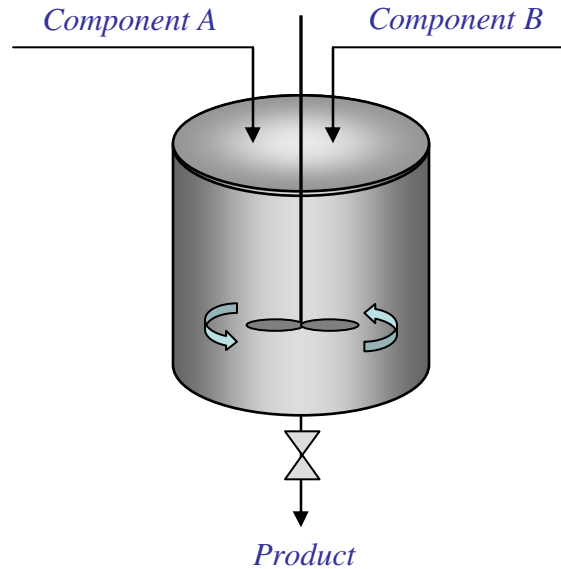


Figure 10: Schematic representation of a batch reactor

Since there is no inflow or outflow in this type of reactor, i.e. $F_0 = F_1 = 0$, the balance for component j is reduced in:

$$\frac{d}{dt} \int_{V_R} C_j dV = \int_{V_R} R_j dV \quad (1.8)$$

Assuming that the rate law is a known function, and the system volume remains constant, we obtain the reactor design equation for an ideal batch reactor:

$$\frac{dC_j}{dt} = R_j \quad (1.9)$$

with $C_j(t = 0) = C_{j_0}$.

3.4.1.2. Ideal Continuous Reactor

There are two main categories of continuous reactors: the plug flow reactors (PFRs) and the perfectly mixed, continuous flow stirred tank reactors (CSTRs). A schematic representation of a plug flow reactor is depicted in Figure 11.

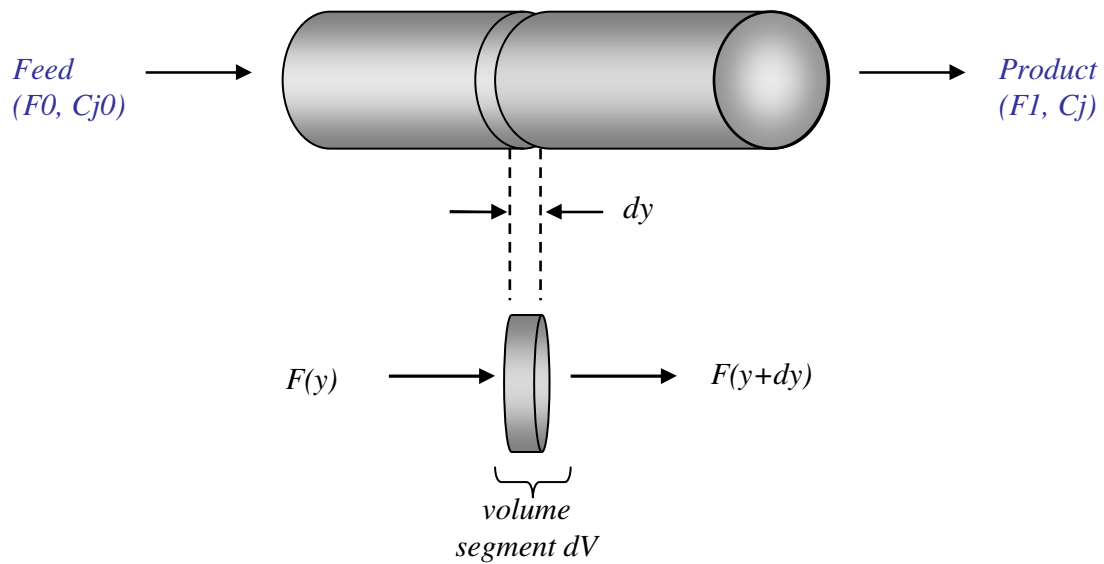


Figure 11: Plug flow reactor

In a plug flow reactor, the fluid is considered to be perfectly mixed along the radial direction. In order to develop the balances, steady-state condition is assumed, and thus the accumulation term is zero, resulting in:

$$F_j(y) - F_j(y + dy) + R_j dV = 0 \quad (1.10)$$

The volume segment can be expressed as $dV = A dy$, where A is the unit area of the reactor (assumed constant). Therefore, the equation above becomes:

$$F_j(y) - F_j(y + dy) + R_j A dy = 0 \quad (1.11)$$

or

$$\frac{F_j(y+dy) - F_j(y)}{dy} = R_j A \quad (1.12)$$

Taking the limit as dy goes to zero, we get:

$$\lim_{dy \rightarrow 0} \frac{F_j(y+dy) - F_j(y)}{dy} = R_j A \quad (1.13)$$

and using the definition for the derivative, we obtain the governing equation for the plug flow reactor:

$$\frac{dF_j}{dy} = R_j A \quad (1.14)$$

This can be also expressed in terms of unit volume as:

$$\frac{dF_j}{dV} = R_j \quad (1.15)$$

Due to the geometrical characteristics of these reactors, and the frequently observed turbulent flows, temperature control is hard and thus, undesired thermal gradients may occur.

Those issues can be handled by using a continuous-flow stirred tank reactor (CSTR), like the one presented in Figure 12. The material balance for the CSTR can be expressed by:

$$\frac{d}{dt} \int_{V_R} C_j dV = F_0 C_{j_0} - F_1 C_{j_1} + \int_{V_R} R_j dV \quad (1.16)$$

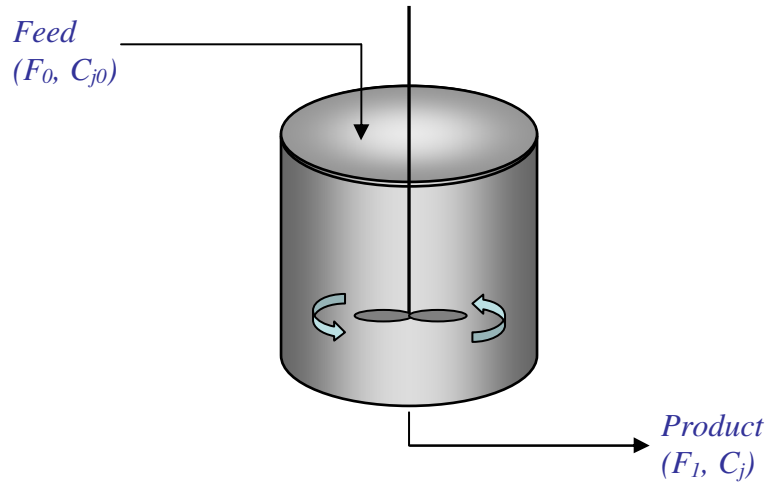


Figure 12: Continuous-flow stirred tank reactor

Assuming constant reactor volume, the equation above becomes:

$$\frac{d(C_j V_R)}{dt} = F_0 C_{j_0} - F_1 C_{j_1} + R_j V_R \quad (1.17)$$

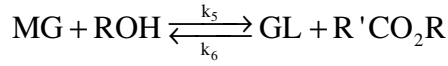
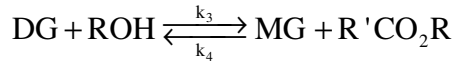
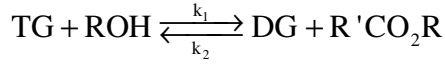
If the density of the mixture is also constant, then:

$$\frac{dC_j}{dt} = \frac{F_0}{V_R} (C_{j_0} - C_{j_1}) + R_j \quad (1.18)$$

where $\tau = \frac{V_R}{F_0}$ the residence time for the reactor.

3.4.2. Transesterification

As mentioned previously, the reaction scheme for transesterification can be represented by the following set of reactions:



where TG, DG, MG, and GL denote the triglycerides, diglycerides, monoglycerides, and glycerol respectively.

In the case of a **continuous stirred tank reactor** (CSTR) the change in the concentration of the components over time can be expressed by the following system of ODEs:

$$\frac{d[\text{TG}]}{dt} = \frac{F}{V_R} ([\text{TG}]_0 - [\text{TG}]) - r_1 + r_2 \quad (1.19)$$

$$\frac{d[\text{DG}]}{dt} = \frac{F}{V_R} ([\text{DG}]_0 - [\text{DG}]) + r_1 - r_2 - r_3 + r_4 \quad (1.20)$$

$$\frac{d[\text{MG}]}{dt} = \frac{F}{V_R} ([\text{MG}]_0 - [\text{MG}]) + r_3 - r_4 - r_5 + r_6 \quad (1.21)$$

$$\frac{d[\text{GL}]}{dt} = \frac{F}{V_R} ([\text{GL}]_0 - [\text{GL}]) + r_5 - r_6 \quad (1.22)$$

$$\frac{d[\text{R}'\text{CO}_2\text{R}]}{dt} = \frac{F}{V_R} ([\text{R}'\text{CO}_2\text{R}]_0 - [\text{R}'\text{CO}_2\text{R}]) + r_1 - r_2 + r_3 - r_4 + r_5 - r_6 \quad (1.23)$$

$$\frac{d[\text{ROH}]}{dt} = \frac{F}{V_R} ([\text{ROH}]_0 - [\text{ROH}]) - r_1 + r_2 - r_3 + r_4 - r_5 + r_6 \quad (1.24)$$

where the corresponding rate laws for each component, $r_1 - r_6$, are expressed by equations (1.1) - (1.6), with k_1, k_2, k_3, k_4, k_5 , and k_6 the kinetic constants for the reactions, as presented in Table 3 (obtained from Nouredдини and Zhu, 1997). Subscript 0 indicates the concentration of the reactants at $t=0$. Here, $[DG]_0 = [MG]_0 = [GL]_0 = [R'CO_2R]_0 = 0$.

Table 3: Reaction rate constants for transesterification

Rate constant	Value
k_1	0.050
k_2	0.110
k_3	0.215
k_4	1.228
k_5	0.242
k_6	0.007

For the **steady-state** operation of the CSTR, the system described by equations (1.19) – (1.14) is reduced to a linear system of algebraic equations:

$$\frac{F}{V_R}([TG]_0 - [TG]) - r_1 + r_2 = 0 \quad (1.25)$$

$$\frac{F}{V_R}([DG]_0 - [DG]) + r_1 - r_2 - r_3 + r_4 = 0 \quad (1.26)$$

$$\frac{F}{V_R}([MG]_0 - [MG]) + r_3 - r_4 - r_5 + r_6 = 0 \quad (1.27)$$

$$\frac{F}{V_R}([GL]_0 - [GL]) + r_5 - r_6 = 0 \quad (1.28)$$

$$\frac{F}{V_R}([R'CO_2R]_0 - [R'CO_2R]) + r_1 - r_2 + r_3 - r_4 + r_5 - r_6 = 0 \quad (1.29)$$

$$\frac{F}{V_R}([ROH]_0 - [ROH]) - r_1 + r_2 - r_3 + r_4 - r_5 + r_6 = 0 \quad (1.30)$$

Since the flow rate and the reactor volume are the adjustable design variables, the algebraic system is well determined with the components' concentrations as the only unknowns.

The effect of alcohol to oil ratio in the methyl ester conversion has been captured by Figure 13. The reaction temperature has been assumed constant (60°C).

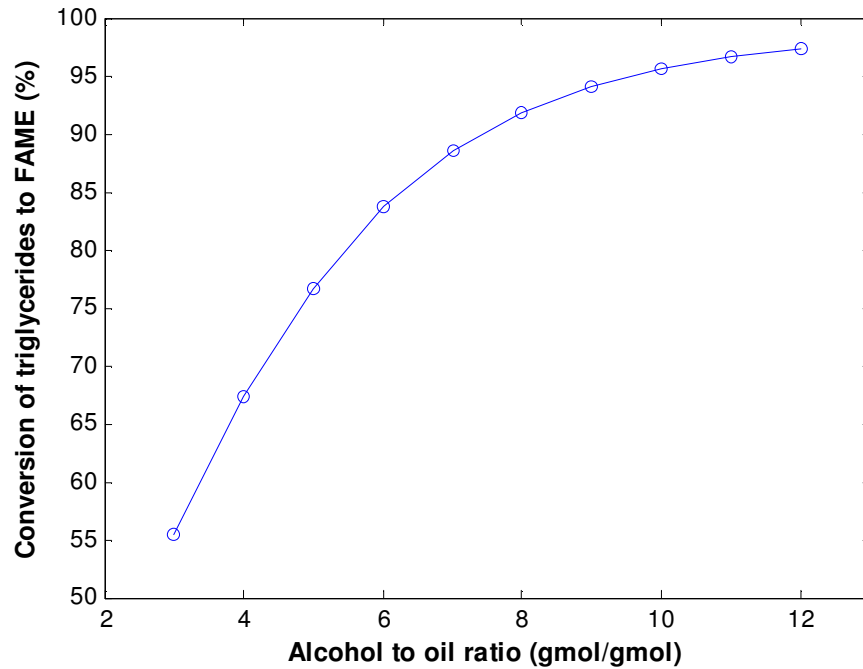


Figure 13: Methyl ester conversion of triglycerides for different alcohol to oil ratio

For a 6:1 methanol to oil ratio, the conversion level is approximately 84%. This outcome is in accordance with yields reported in literature, as shown in Table 4 below.

Table 4: Methyl ester conversions for various systems

	Catalyst	Conversion
Our study (based on Nouredini & Zhu)	NaOH	0.84
Freedman <i>et al.</i>	1% H ₂ SO ₄	0.86
Freedman <i>et al.</i>	0.5% NaOBu	0.85
Ávila <i>et al.</i>	KOH	0.81
Bambase <i>et al.</i> *	0.5% NaOCH ₃	0.94
Bambase <i>et al.</i> *	1% NaOCH ₃	0.84

* The conversion levels represent the final yield for methyl esters (incl. soap formation): increased catalyst concentration was reported to result in excess soap formation, hindering methyl ester recovery.

Furthermore, the effect of the residence time on the conversion of triglycerides appears in Table 5. The methanol to oil ratio is 6:1, and we have assumed initial concentrations 1 mol/L and 6 mol/L for oil and alcohol, respectively.

Table 5: Effect of residence time on methyl ester conversion

	Residence time		
	60 min	120 min	180 min
Methyl ester conversion (%)	73.62	78.10	79.84

The simulation of biodiesel production will take place with significantly larger amounts of reactants. In that case, in order to achieve maximum conversion (~84%), the residence time will be 1hr.

The addition of more than one CSTR, having the same flow rate and reactor volume, results in an increased production of the fatty acid methyl ester (FAME). The mass

balances, when having a series of CSTRs, at steady-state, can be formulated by the following mathematical equations (i denotes the number of the reactor):

$$\frac{F_i}{V_{R_i}}([TG]_i - [TG]_{i+1}) - r_{1,i} + r_{2,i} = 0 \quad (1.31)$$

$$\frac{F_i}{V_{R_i}}([DG]_i - [DG]_{i+1}) + r_{1,i} - r_{2,i} - r_{3,i} + r_{4,i} = 0 \quad (1.32)$$

$$\frac{F_i}{V_{R_i}}([MG]_i - [MG]_{i+1}) + r_{3,i} - r_{4,i} - r_{5,i} + r_{6,i} = 0 \quad (1.33)$$

$$\frac{F_i}{V_{R_i}}([GL]_i - [GL]_{i+1}) + r_{5,i} - r_{6,i} = 0 \quad (1.34)$$

$$\frac{F_i}{V_{R_i}}([R'CO_2R]_i - [R'CO_2R]_{i+1}) + r_{1,i} - r_{2,i} + r_{3,i} - r_{4,i} + r_{5,i} - r_{6,i} = 0 \quad (1.35)$$

$$\frac{F_i}{V_{R_i}}([ROH]_i - [ROH]_{i+1}) - r_{1,i} + r_{2,i} - r_{3,i} + r_{4,i} - r_{5,i} + r_{6,i} = 0 \quad (1.36)$$

The results for the steady-state concentration of each species for a residence time of 1 hr are shown in Table 6. The total conversion of triglycerides to FAME is summarized in Table 7.

Table 6: Steady-state concentration of the components at the exit of each reactor

Component	1 st reactor	2 nd reactor	3 rd reactor	4 th reactor	5 th reactor
TG	0.193	0.1206	0.1598	0.1101	0.1099
DG	0.095	0.0738	0.0929	0.0693	0.0692
MG	0.024	0.0179	0.0231	0.0168	0.0168
ROH	3.791	3.5272	3.6884	3.4857	3.4850
FAME	2.209	2.4728	2.3116	2.5143	2.5150
GL	0.689	0.7877	0.7242	0.8038	0.8041

Table 7: Conversion of triglycerides to methyl esters (%)

1 st reactor	2 nd reactor	3 rd reactor	4 th reactor	5 th reactor
73.62	82.43	83.64	83.81	83.83

As shown in the tables above, increasing the number of reactors raises the concentration of the desired final product. However, the increases in the final FAME concentration becomes smaller and smaller as more CSTRs are added: starting from an approximately 35% increase when we go from one to two reactors, it drops to a 2% increase when we go from four and five reactors. In this case, all reactors have the same volume ($V_{R_1} = V_{R_2} = V_{R_3} = V_{R_4} = V_{R_5} = 1000 \text{ L}$).

An alternative scenario explored is to compare the conversion of triglycerides using one CSTR of volume 1000 liters to the total conversion obtained using a cascade of CSTRs whose **total** volume equals again 1000 liters. In the first case we have a reactor with $V=1000 \text{ L}$, in the second two reactors of 500 L each, and so on. As the number of CSTRs increases, this cascade will approach the performance of a continuous plug flow reactor (PFR). The results are summarized in Tables 8 and 9. The flow rate has been assumed to remain the same as before.

Table 8: Steady-state concentration of methyl esters at the exit of each reactor

# of reactors	1 st reactor	2 nd reactor	3 rd reactor	4 th reactor	5 th reactor
1	2.2087	--	--	--	--
2	2.0050	2.3949	--	--	--
3	1.8514	2.3113	2.4492	--	--
4	1.7278	2.2303	2.4058	2.4722	--
5	1.6243	2.1541	2.3592	2.4460	2.4842

Table 9: Conversion of triglycerides to methyl esters (%)

# of reactors	Total conversion (%)
1	73.62
2	79.83
3	81.64
4	82.41
5	82.81

The findings above indicate that using cascades of CSTRs with constant total volume will raise the yield of transesterification (scenario 1). The relative benefit from adding one more reactor however, decreases as we add more CSTRs. This is particularly apparent for lower flow rates: starting from approximately 6% (difference between one and two reactors), it reaches 0.2% (difference between four and five reactors).

The case of a semi-batch reactor where additional methanol is added to the reacting liquid at a constant flow rate was also explored. However, the results we obtained indicated that this configuration has no apparent benefit compared to the aforementioned designs.

An additional scenario we investigated includes the addition of a settling tank following the reactor where transesterification takes place. This separator unit contains an oil phase (oil and methyl ester), and an aqueous phase (glycerin and part of the methanol). Literature data concerning the relative solubilities of the component are not many (Zhou, 2006; França *et al.*, 2009; Mesquita *et al.*, 2011). Based on these studies, we assumed that the inlet entering the second reactor included almost the entire amount of

triglycerides, diglycerides, monoglycerides, and FAME, 60% of methanol, and 6% of the glycerin exiting the first reactor. The results obtained are presented in Table 10.

Table 10: Steady-state concentration of the components at the exit of each reactor

Component	1 st reactor	2 nd reactor
TG	0.193	0.1516
DG	0.095	0.0560
MG	0.024	0.0079
ROH	3.791	2.0583
FAME	2.209	2.4230
GL	0.689	0.1372

The total conversion achieved from this configuration was ~81%, slightly lower than the case where no separator was used. Therefore, the aforementioned design would not be beneficial if we wanted to achieve higher biofuel yields. However, when a small amount of additional ethanol enters the second reactor, the aforementioned configuration is improved, resulting in conversions up to 85% (for the given flow rates and reactor volumes). For that reason, this appeared to be the optimal configuration for our system.

3.4.3. Methanol recovery

Having designed and optimized the reactor(s) where transesterification takes place, we further considered the outlet stream of the reactor. This exiting stream contains a large amount of methanol, as methanol is always used in significant excess to drive the reaction equilibrium to the right. Alcohol is the most expensive of raw materials and therefore, recycling the excess amount can improve the economics of the process.

The unit used for alcohol removal is a distillation column. The stream that enters the column is at the operating conditions of the transesterification reactor (60°C and atmospheric pressure). For simplicity, our initial calculations have not considered the intermediate products and we have assumed that triglycerides are converted to glycerin and fatty acid methyl esters only.

For the column design, we have assumed that there is no pressure drop along the column, and that it operates under atmospheric pressure. The boiling points of the materials that enter the distillation column appear in Table 11. To obtain an initial estimate of the operation of the column, we have performed a steady-state simulation using the RADFRAC unit in ASPEN (distillation), and UNIQUAC model, since we will have more than one liquid phases.

Table 11: Boiling point of the components entering the distillation column (ROH removal)

Component	Boiling Point (°C)
Methanol	65
Glycerin	290
Biodiesel	344
Oil	847

3.4.4. FAME purification

After transesterification, a washing step will take place, to remove glycerin and some of the remaining alcohol. Slightly acidic water will be used, which will neutralize any remaining traces of the catalyst (Demirbas and Kara, 2006; Van Gerpen, 2005). After the washing, the materials are separated using a centrifuge (Predojevic, 2008).

One of the streams exiting the washing column is rich in fatty acid methyl esters. This stream will also contain amounts of water, methanol, and perhaps oil. Our objective is to separate biodiesel from the rest, acquiring our product with high purity.

The primary step is to determine what kind of separator we may use. A separator tank for example, could potentially work; yet, in reality it would be extremely difficult to obtain a product of high purity. Thereby, utilizing distillation seems as the most appealing option for our system. Heating the stream to over 100°C, before entering the unit, will remove the components with lower boiling point, i.e. methanol and water, without inhibiting the quality of biodiesel. The remaining oil and methyl ester (FAME) will enter the distillation unit.

FAME purification will be designed taking into consideration the boiling points of the components that need to be separated. The reported methodologies for the purification of methyl esters so far, include some cases of distillation or the use of a vacuum dryer (Zhang *et al.*, 2004; Sheehan *et al.*, 1998). In the first study, the results are somewhat questionable, primarily due to errors in the reported material balances.

Vacuum distillation is an alternative to be explored, due to the high boiling points of the key components. An additional advantage is that this methodology will reduce the number of stages needed, resulting in obtaining our highly pure product. Furthermore, it is expected that using vacuum will reduce the capital cost of the unit (smaller size compared to a traditional unit), yet increasing the operating cost for the process.

3.4.5. Glycerin utilization

Three potential scenarios for glycerin utilization are investigated:

- a) Glycerin purification to sell as a co-product.
- b) Glycerin used to produce high-value chemicals.
- c) Glycerin used for steam and power production.

A detailed description of each case is presented in the following sections.

3.4.5.1. *Glycerin as co-product*

Having glycerin purified allows the production of high-value chemicals, improving the economics of the overall process. The base-case scenario includes glycerin production of approximately 81% purity. In the alternative, we assume that the produced glycerin is used to produce high-value chemicals and/or fuels, ethanol to be exact.

How is glycerin purification going take place: the glycerin-rich stream exiting the water-washing column contains traces of the catalyst (a neutralization step will take place for the removal of the catalyst), water, and traces of alcohol. Water and glycerin however, are miscible in all proportions, and thus their separation can be performed via either evaporation or distillation. In our study, we have determined to use a distillation column.

3.4.5.2. *Glycerin for ethanol production*

Glycerin can be converted into higher value products by either biological or chemical transformations. Chemical transformations have been reported to be less favorable

primarily because of the low product specificity (Yazdani *et al.*, 2010). An additional drawback, as discussed previously, is related to the high energy demand of glycerin's purification step. On the other hand, the biological techniques not only have higher product specificity, but they also require milder operating conditions. Thus, they have the potential of being more energy efficient.

It has recently been reported that *E. coli* has been engineered to produce, L- and D-lactate, succinate, and 1,2-propanediol from glycerin (Gonzalez *et al.*, 2008; Murarka *et al.*, 2008). Another desired product of glycerol's fermentation is ethanol, which could be further utilized in the biorefinery. Figure 14 depicts the metabolic pathways for ethanol production. The enzymes catalyzing each metabolic step and their corresponding genes (in bracket) are shown.

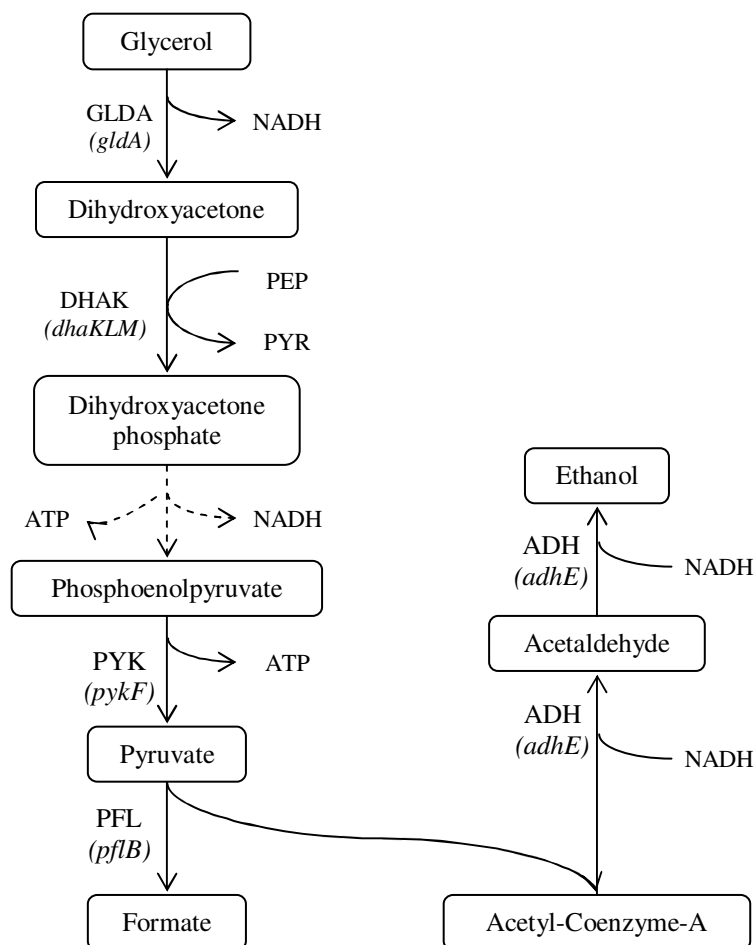


Figure 14: The metabolic pathways for the production of ethanol from glycerol, for *Escherichia coli*. The enzymes appearing in the figure: GLDA - glycerol dehydrogenase; DHAK - dihydroxyacetone kinase; PYK - pyruvate kinase; PFL - pyruvate formate lyase; ADH - alcohol dehydrogenase

Experimental data concerning the conversions to each product are available from the work of Gonzalez *et al.* (Gonzalez *et al.*, 2008) and consequently, we may accurately estimate the composition of the fermentation broth. For simplicity however, and considering that the desired final product is ethanol, we have assumed that the conversion that takes place is a single-step reaction, with ethanol and H_2 yields as high as 0.96 mol per mol glycerol, as reported by Gonzalez *et al.* (Gonzalez *et al.*, 2008).

The amounts of the co-products in the fermentation broth have been assumed to be negligible. In a more realistic scenario however, a further separation should be considered, so that they would become commercially available. The separation could take place using, for example, distillation, ion exchange chromatography (Ataei and Vasheghani-Farahani, 2007), high performance liquid chromatography (HPLC), membrane filtration (Kang and Chang, 2005), electrodialysis and precipitation (Hábová *et al.*, 2004; Kim and Moon, 2001; Cheryan and Parekh, 1995), solvent extraction (Harington and Hossain, 2008), or selective sorption-desorption (Pitt *et al.*, 1983). However, no data concerning our system could be obtained, therefore this section was not further explored.

3.4.5.3. Glycerin for steam and power production

Glycerin purification is one of the most energy intensive steps in biodiesel production process. Therefore, we have explored the option of eliminating the glycerin purification step, and using that product stream (potentially together with the unreacted alcohol) for energy generation in a compact CHP plant. To our knowledge, this is the first reported attempt to: i) determine whether utilizing the co-product for energy production within the facility will cover the energy requirements of the overall production process, and subsequently ii) perform a rigorous heat integration in our system, that will potentially prove to be of major economic and environmental benefit.

3.5. Process Design

SuperPro Designer was used to simulate biodiesel production process. The material balance for each scenario has been estimated. Additionally, the energy requirements of the proposed designs have been calculated in order to assess the overall efficiency of the biorefinery.

3.5.1. Case I: Transesterification in a single CSTR

Oil and methanol are pre-heated to 60°C, and enter the CSTR reactor. The methanol to oil ratio is 6:1. We have assumed that transesterification is a single-step reaction, and the residence time of the components in the reactor is 1 hr. The conversion of triglycerides to fatty acid methyl esters (FAME), based on the results of the previous section, has been set to be ~84%.

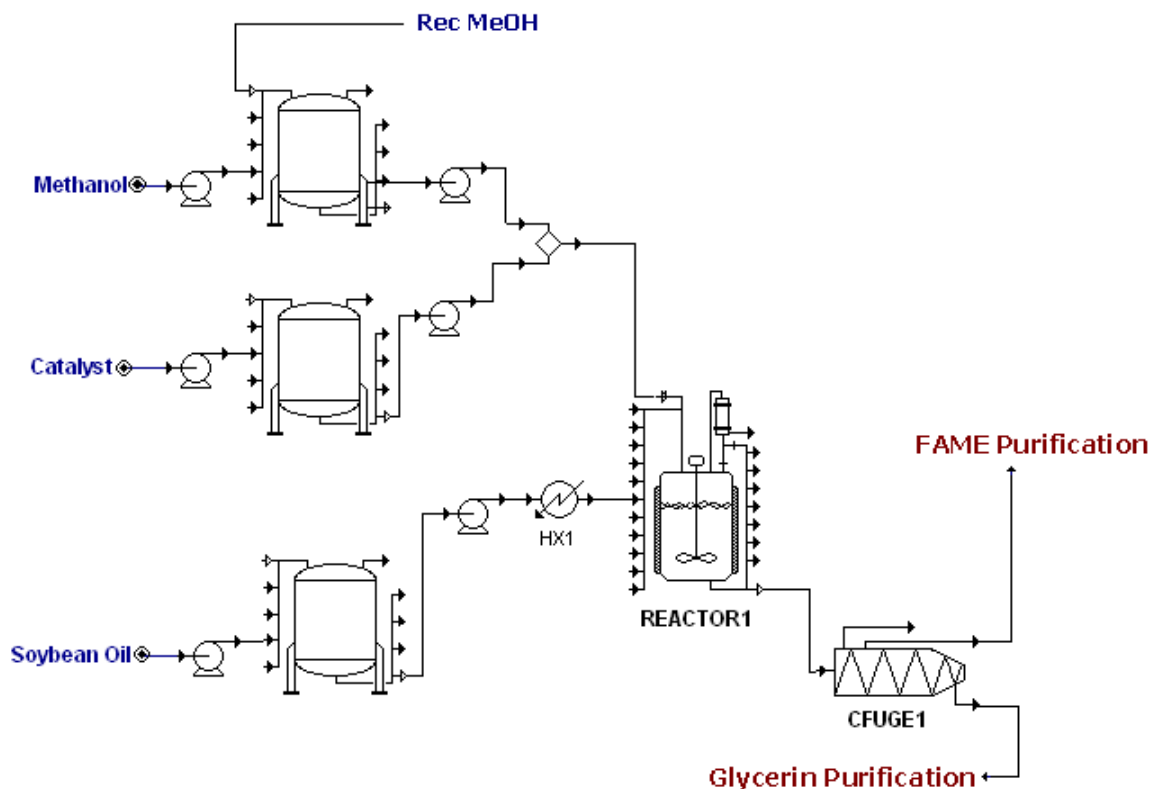


Figure 15: Transesterification in a single CSTR

The outlet stream is led through a settling tank, and cooled. Methanol and glycerin are separated from the oil phase, and the stream containing the unconverted oil, FAME, and part of glycerin and methanol, is led to a neutralization tank, where catalyst neutralization and solids removal take place. The stream containing FAME (~78%), oil (~14%), and some methanol and water, is led to the FAME purification section, to retrieve biodiesel of higher purity; the rest of the materials are led to the section where methanol recovery and glycerin purification will take place. Methanol recovery and FAME purification sections have been initially simulated using the shortcut distillation unit in HYSYS.

For methanol recovery, a distillation column with 15 trays will be used. The inlet stream will enter the column at the first stage. Based on the results from the shortcut

column simulated in HYSYS, the minimum reflux ratio is 1.93, when the column operates in atmospheric pressure. The distillate contains 99.4% methanol, and some water, and it is recycled to the transesterification reactor. No cooling/heating is required, as the stream's temperature is at $\sim 64^{\circ}\text{C}$.

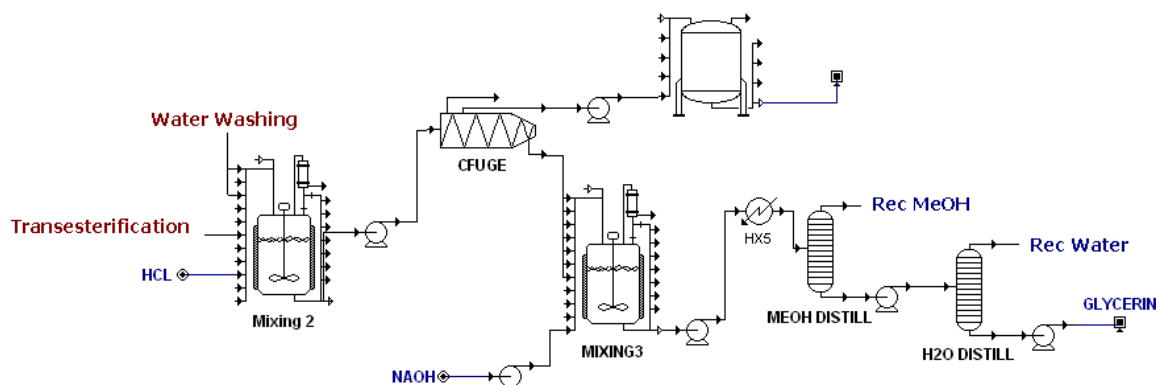


Figure 16: Neutralization and methanol recovery

The bottoms stream has more than 90% water, and glycerin, therefore evaporation or distillation should follow. The additional distillation column will remove the excess water (which can be recycled or treated as waste), and the stream retrieved from the bottom will have 80% glycerin. This column has been designed with 10 theoretical stages, and a reflux ratio of 0.13. It will operate in atmospheric pressure, and high-pressure steam will be consumed for the operation of the reboiler.

Concerning FAME purification, two methodologies have been proposed in the literature: the first, by Zhang *et al.* (Zhang *et al.*, 2003) included a distillation column, while the second, explored by Sheehan *et al.* (Sheehan *et al.*, 1998) suggesting leading the product through a vacuum dryer, after a washing step has taken place. Given that the second methodology proved to be less energy intensive, we determined to include that

one as the final purification step. The details of the material balance have been included in Appendix A; biodiesel is produced with 97% purity.

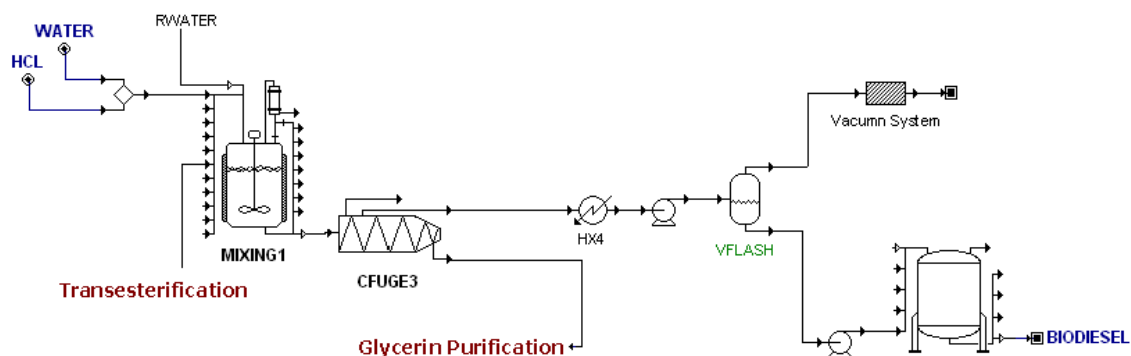


Figure 17: Washing and FAME purification

The material input and energy demand for the facility are shown in Table 12. The overall material balance is presented in Table 13. The results indicate that approximately 2 MT/hr of high-pressure steam and 2.5 MT/hr of medium-pressure steam are additionally required. Our design includes a combined heat and power (CHP) unit that will generate the required steam using natural gas as fuel source.

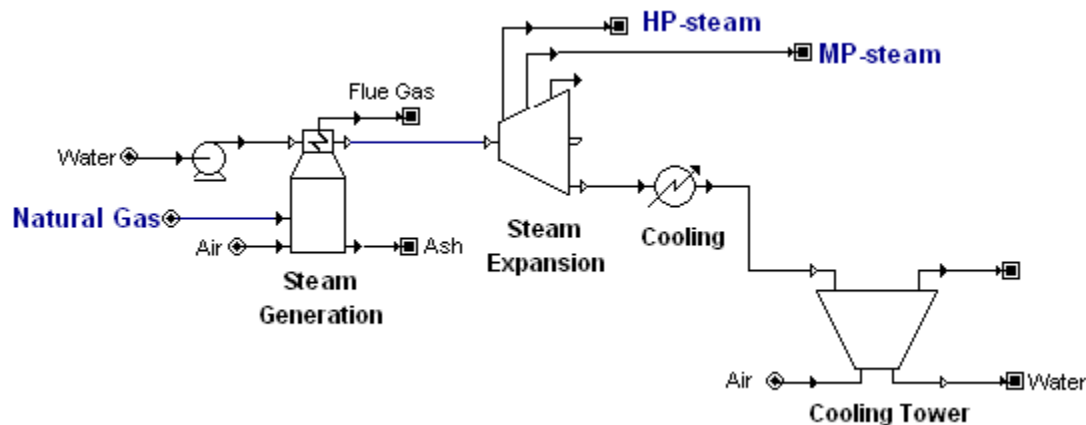


Figure 18: Combined heat and power unit, producing power and steam

The CHP unit consists of a boiler and a turbogenerator. Fuel combustion takes place with 5% excess oxygen. The flue gas exit temperature has been set to 200°C. The overall heat losses of the boiler are 5%. The exit steam enters the multi-stage turbine: its design parameters are the amount and pressure of the steam produced. MP-steam is produced (50% of the feed) at 5 bar, and 16% of the feed is converted to HP-steam (10 bar). We have also assumed that the power produced is 90% of the total shaft power. The condensate is cooled at 25°C using a cooling tower (assuming it will be discarded to the environment).

Natural gas enters the boiler and is burned in order to produce the amount of steam necessary for the operation of the biorefinery. As shown in Table 12, 0.77 MT/hr of natural gas are required to cover the energy demand. The steam and power balance after the operation of the CHP unit are presented in Table 14. The values in the parentheses indicate a positive value for the energy balance.

Table 12: Material input and energy demand during biodiesel production (base-case)

MeOH (MT/hr)	Oil (MT/hr)	Biodiesel Production (MT/hr)	Glycerin Production (MT/hr)	HP-steam Demand (MT/hr)	MP-steam Demand (MT/hr)	Natural Gas Demand (MT/hr)
0.41	4.25	3.58	0.37	-1.99	-2.51	0.76

Table 13: Mass balance for the base-case scenario (kg/hr)

Component	Inlet	Outlet	Outlet - Inlet
Methanol	411.15	31.79	- 379.36
Soybean Oil	4,250.16	685.98	- 3,564.18
NaOCH ₃	13.27	0.43	- 12.838
Biodiesel	0.00	3,580.37	3,580.37
Glycerin	0.00	370.69	370.69
HCl	10.60	0.29	- 10.31
Sodium Chloride	0.00	16.52	16.52
Sodium Hydroxide	1.80	0.00	- 1.80
Water	185.76	186.58	0.81
TOTAL	4872.74	4,872.64	- 0.10

Table 14: Steam and power balance for the biorefinery (GJ/hr) (base-case)

HP-steam	MP-steam	Power
--	(7.59)	(0.67)

Table 15 summarizes the outcome for the metrics estimation. As mentioned in Chapter 2, we are only interested in the biorefinery phase of the production process. The metrics used for our analysis are:

- **The net energy value (NEV)** defined as:

$$NEV^* = \left[\begin{array}{c} \text{Energy content} \\ \text{of biofuel} \end{array} \right] + \left[\begin{array}{c} \text{Energy content} \\ \text{of co-product} \end{array} \right] - \left[\begin{array}{c} \text{Energy in fuel used for} \\ \text{the auxiliary utility plant} \end{array} \right]$$

- **The net energy ratio (NER)** defined as:

$$NER^* = \frac{\left[\begin{array}{c} \text{Energy content} \\ \text{of biofuel} \end{array} \right] + \left[\begin{array}{c} \text{Energy content} \\ \text{of co-product} \end{array} \right]}{\left[\begin{array}{c} \text{Energy in fuel used for} \\ \text{the auxiliary utility plant} \end{array} \right]}$$

- The overall efficiency of the biorefinery defined as:

$$\eta = \frac{[Energy\ content\ of\ products]}{[Energy\ content\ of\ input]}$$

It should be noted that the fuel used for the utility plant was natural gas. No additional power was bought from the grid.

Table 15: Metrics estimation, w/ and w/o co-product credit (co-product: glycerin) (base-case)

	Biorefinery Net Energy Value (MJ/L _{fuel})	Net Energy Ratio	Overall Efficiency
w/ co-product credit	25.89	3.90	0.674
w/o co-product credit	24.42	3.73	0.666

Furthermore, the effect of the alcohol to oil ratio was explored, based on the analysis of Section 3.1.1. The results are presented in Tables 16 to 19. Note that the purity of the final product varies from 85% (when MeOH:oil = 3:1) to ~98% (when MeOH:oil = 8:1).

Table 16: Effect of MeOH to oil ratio in the energy demand during biodiesel production

Ratio	Biodiesel Production (MT/hr)	Glycerin Production (MT/hr)	HP-steam Demand (MT/hr)	MP-steam Demand (MT/hr)	Power Demand (GJ/hr)	Natural Gas Demand (MT/hr)
3:1	2.36	0.24	-1.23	-2.20	0.49	0.47
4:1	2.88	0.30	-1.45	-2.31	0.45	0.56
5:1	3.28	0.34	-1.59	-2.29	0.42	0.61
6:1	3.58	0.37	-1.99	-2.51	0.40	0.76
7:1	3.78	0.39	-2.32	-2.61	0.39	0.89
8:1	3.92	0.41	-2.65	-2.71	0.38	1.02

Table 17: Effect of MeOH to oil ratio in the energy balance for the biorefinery

Ratio	HP-steam (GJ/hr)	MP-steam (GJ/hr)	Power (GJ/hr)
3:1	--	(3.35)	(0.75)
4:1	--	(4.54)	(1.00)
5:1	--	(5.44)	(1.17)
6:1	--	(7.59)	(1.60)
7:1	--	(9.45)	(1.94)
8:1	--	(11.38)	(2.28)

Table 18: Effect of MeOH to oil ratio in metrics estimation, w/o co-product credit (glycerin)

Ratio	Biorefinery Net Energy Value (MJ/L _{fuel})	Net Energy Ratio	Overall Efficiency
3:1	25.12	4.01	0.48
4:1	25.41	4.14	0.57
5:1	25.74	4.31	0.64
6:1	24.65	3.76	0.67
7:1	23.80	3.42	0.69
8:1	22.85	3.10	0.69

Table 19: Effect of MeOH to oil ratio in metrics estimation, w/ co-product credit (glycerin)

Ratio	Biorefinery Net Energy Value (MJ/L _{fuel})	Net Energy Ratio	Overall Efficiency
3:1	26.59	4.18	0.49
4:1	26.87	4.32	0.58
5:1	27.20	4.50	0.65
6:1	26.12	3.92	0.68
7:1	25.27	3.57	0.69
8:1	24.31	3.24	0.70

3.5.2. Case II: Transesterification in a single CSTR; Glycerin purification

The process design is similar to the one presented in Section 3.2.1., only in this case we aim to produce glycerol of higher purity. Therefore, the settings in the final distillation column (appearing as H2O DISTILL of Figure 14) are altered (11 theoretical stages, and ~90% glycerin in the final product). These alterations however, result in significantly higher MP-steam requirements, as shown in Table 20.

Table 20: Material input and energy demand during biodiesel production (Case II)

MeOH (MT/hr)	Oil (MT/hr)	Biodiesel Production (MT/hr)	Glycerin Production (MT/hr)	HP-steam Demand (MT/hr)	MP-steam Demand (MT/hr)	Natural Gas Demand (MT/hr)
0.41	4.25	3.58	0.37	-1.98	-4.18	0.76

Table 21: Steam and power balance for the biorefinery (GJ/hr) (Case II)

HP-steam	MP-steam	Power
--	(4.09)	(1.58)

Table 22: Metrics estimation, w/ and w/o co-product credit (co-product: glycerin) (Case II)

	Biorefinery Net Energy Value (MJ/L _{fuel})	Net Energy Ratio	Overall Efficiency
w/ co-product credit	26.18	3.95	0.68
w/o co-product credit	24.71	3.79	0.67

As shown in the tables above, glycerin purification from 80% to 90%, despite the higher energy requirements, has only a minor effect (less than 3%) in biorefinery's net energy value and the net energy ratio.

3.5.3. Case III: Transesterification in two CSTRs

In this design, transesterification takes place in a configuration consisting of two CSTRs, each one followed by a centrifuge (Figure 19). Additional alcohol is added to the second reactor, as the preliminary results in previous sections proved that this configuration resulted in increased biofuel yields.

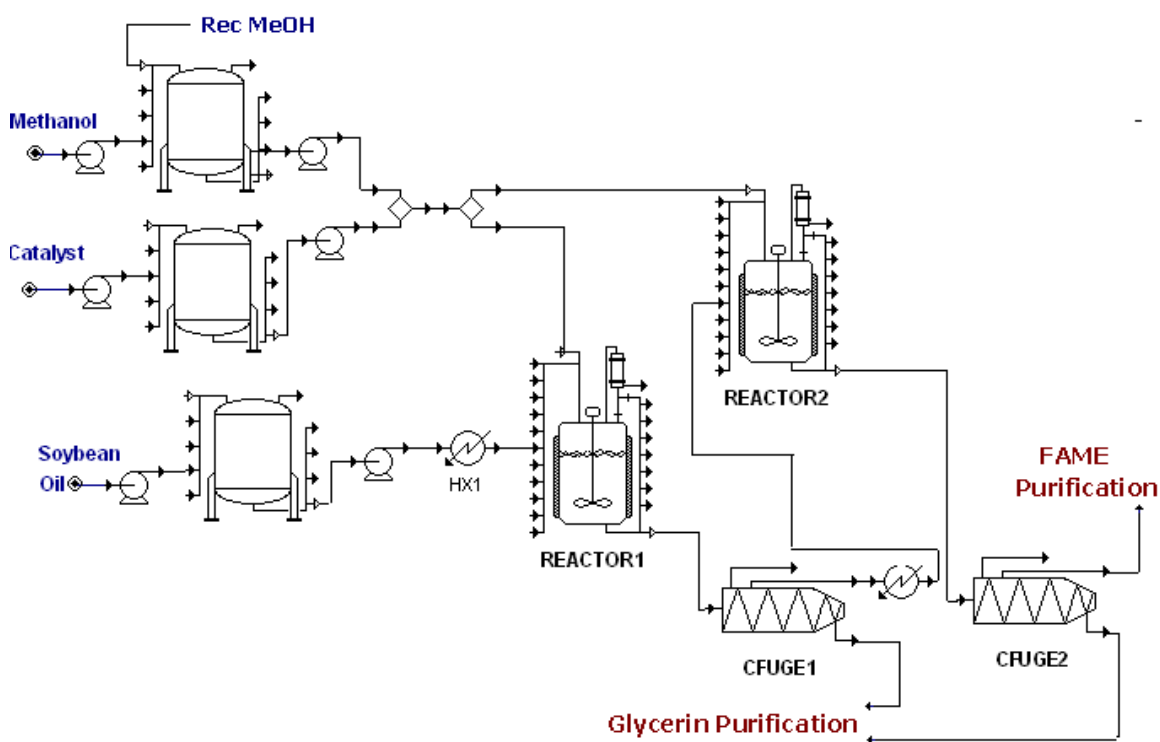


Figure 19: Transesterification in two CSTRs

The results of the process have been summarized in Table 24 - Table 26. A more detailed report has been included in Appendix B.

Table 23: Mass balance for biodiesel production (Case III) (kg/hr)

Component	Inlet	Outlet	Outlet - Inlet
Biodiesel	0.00	4,062.25	4,062.25
Glycerin	0.00	420.58	420.58
HCl	10.60	0.10	- 10.50
Methanol	453.44	22.15	- 431.29
NaOCH ₃	13.27	0.14	- 13.12
Sodium Chloride	0.00	16.83	16.83
Sodium Hydroxide	1.80	0.00	- 1.802
Soybean Oil	4,250.16	206.27	- 4,043.89
Water	185.76	186.58	0.81
TOTAL	4915.03	4914.90	- 0.13

Table 24: Material input and energy demand during biodiesel production (Case III)

MeOH (MT/hr)	Oil (MT/hr)	Biodiesel Production (MT/hr)	Glycerin Production (MT/hr)	HP-steam Demand (MT/hr)	MP-steam Demand (MT/hr)	Natural Gas Demand (MT/hr)
0.45	4.25	4.06	0.42	-2.15	-2.72	0.82

Table 25: Steam and power balance for the biorefinery (GJ/hr) (Case III)

HP-steam	MP-steam	Power
--	(8.16)	(1.80)

Table 26: Metrics estimation, w/ and w/o co-product credit (co-product: glycerin) (Case III)

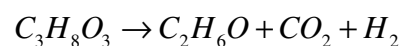
	Biorefinery Net Energy Value (MJ/L _{fuel})	Net Energy Ratio	Overall Efficiency
w/ co-product credit	26.56	4.13	0.755
w/o co-product credit	25.09	3.95	0.748

Compared to the base-case scenario, the outcome of the tables above indicates that using a second reactor results in minor increase of biodiesel. This increase is

accompanied with higher values for the metrics estimated as well, no higher than 6% though.

3.5.4. Case IV: Transesterification in two CSTRs; Glycerin fermentation

This scenario is an additional step to Case III. Glycerin produced through the process described above, is led through the fermentation tank, where we have assumed it is converted to ethanol via a single-step reaction:



We have assumed that the conversion of glycerin to ethanol is 96% (Gonzalez *et al.*, 2008). To our knowledge, this is the first reported attempt to use a co-product of biodiesel production for ethanol production. Excess steam is required to cover the needs of the biodiesel production facility. Therefore, the CHP unit will operate and, ultimately, approximately 0.8 MT/hr of natural gas are required to cover the energy demand of the main process. The key results of the simulation are depicted in Table 27 - Table 29.

Table 27: Material input and energy demand during biodiesel production (Case IV)

MeOH (MT/hr)	Oil (MT/hr)	Biodiesel Production (MT/hr)	Ethanol Production (MT/hr)	HP-steam Demand (MT/hr)	MP-steam Demand (MT/hr)	Natural Gas Demand (MT/hr)
0.45	4.25	4.06	0.18	-2.15	-2.72	0.82

Table 28: Steam and power balance for the biorefinery (GJ/hr) (Case IV)

HP-steam	MP-steam	Power
--	(8.17)	(1.57)

Table 29: Metrics estimation, w/ and w/o co-product credit (co-product: ethanol) (Case IV)

	Biorefinery Net Energy Value (MJ/L _{fuel})	Net Energy Ratio	Overall Efficiency
w/ co-product credit	25.64	4.01	0.749
w/o co-product credit	25.03	3.94	0.746

Converting glycerin to ethanol results in an increase of the net energy ratio (approximately 3%) compared to Case III. In terms of the environmental impact of the process however, CO₂ emissions in this case are higher compared to the amount of carbon dioxide emitted during the previous process (2.44 MT/hr vs. 2.26 MT/hr).

3.5.5. Case V: Transesterification in two CSTRs; Glycerin for steam and power production

In the final scheme, we have explored the potential of utilizing glycerin for steam and power production, to meet the energy requirements (partially or entirely) of the biorefinery.

The glycerin-rich stream is used as fuel for a boiler that will produce required steam to drive a turbine. The specifications for both the boiler and the turbine are similar to the ones described in Section 3.2.1. The efficiency of the turbine is 85%. The results for the material input and the energy balance for the biorefinery appear in Table 30 - Table 32.

Table 30: Material input and energy demand during biodiesel production (Case V)

MeOH (MT/hr)	Oil (MT/hr)	Biodiesel Production (MT/hr)	HP-steam Demand (MT/hr)	MP-steam Demand (MT/hr)	Natural Gas Demand (MT/hr)
0.45	4.25	4.06	-0.32	-0.68	0.12

Table 31: Steam and power balance for the biorefinery (GJ/hr) (Case V)

HP-steam	MP-steam	Power
--	(0.66)	(0.01)

Table 32: Metrics estimation (Case V)

Biorefinery Net Energy Value (MJ/L _{fuel})	Net Energy Ratio	Overall Efficiency
31.95	26.28	0.88

As indicated by the results obtained, burning the co-products of the process leads to a significant increase in the overall efficiency of biodiesel production. A minimal amount of natural gas is required as additional fuel in order to cover the energy requirements of the process. Therefore, compared to the previous cases, the net energy value and the net energy ratio are significantly increased. Moreover, the CO₂ emissions have been estimated to be approximately half of the previous cases (~1.00 MT/hr). Based on this outcome, we may infer that using glycerin for steam and power generation during biodiesel production is the most energy efficient alternative for our system.

Chapter 4

The theme of this chapter is ethanol production from biomass feedstock, via sequential hydrolysis and fermentation. The process design proposed is flexible, and offers the ability to explore the effect of several parameters, including feedstock composition, on the energy efficiency of the biorefinery, and ethanol production. Emphasis has been placed on the operation of the utilities section of the plant, where a combined heat and power (CHP) unit has been designed, and its operation was integrated to the biorefinery. The key contributions of this work come from the results of a parametric study that determines how ethanol yields and net energy values are affected with changes in the % composition of biomass and various operating parameters, like the conversion levels during the hydrolysis and fermentation stages.

4.1. Process Overview: Cellulosic Ethanol Production

We simulated the operation of a cellulosic ethanol plant using SuperPro Designer and MATLAB. The proposed ethanol plant includes the following sections:

i) Pretreatment (thermal hydrolysis). The process of biofuel production begins with the pretreatment of the feedstock. Size reduction is essential to increase the surface area of the raw material so that the biomass may be hydrolyzed more efficiently and with lower energy requirements. A pre-hydrolysis step follows. Using hot water pretreatment, the conversion of hemicellulose to 5-carbon sugars is achieved with ~80% yield. The reported conversion of cellulose to glucose is around 8% (Humbird *et al.*, 2011).

ii) Enzymatic hydrolysis. Enzymatic hydrolysis takes place at elevated temperature, especially if increased enzyme activity is desired. The overall yield of the reaction is expected to depend on the type of reactor used. Most commonly, conversions around 90% are achieved for cellulose (Humbird *et al.*, 2011).

iii) Fermentation. The 5-carbon and 6-carbon sugars are converted to ethanol. For the base-case-scenario, we have assumed that the conversion level of the 5-carbon (xylose) and 6- carbon (glucose) sugars to ethanol are ~80% and ~90%, respectively (Aden *et al.*, 2002; Humbird *et al.*, 2011).

iv) Distillation. The final stage of the process design includes distillation, where the dissolved CO₂ and H₂O removal takes place, and ethanol is obtained. Lignin and any other insoluble solids are sent for dewatering and combustion.

v) Utility Section. We have integrated the ethanol production facility with a combined heat and power section. The lignin and other solids collected in the previous stages are fed as fuel to a boiler and turbogenerator that produce steam and electricity for the ethanol plant. An auxiliary unit, again consisting of a boiler and turbogenerator, is also used to meet plant requirements for steam or power that go beyond what the main unit can generate.

A proposed overall process scheme for the production of ethanol from cellulosic biomass (like corn stover or switchgrass) appears in Figure 20.

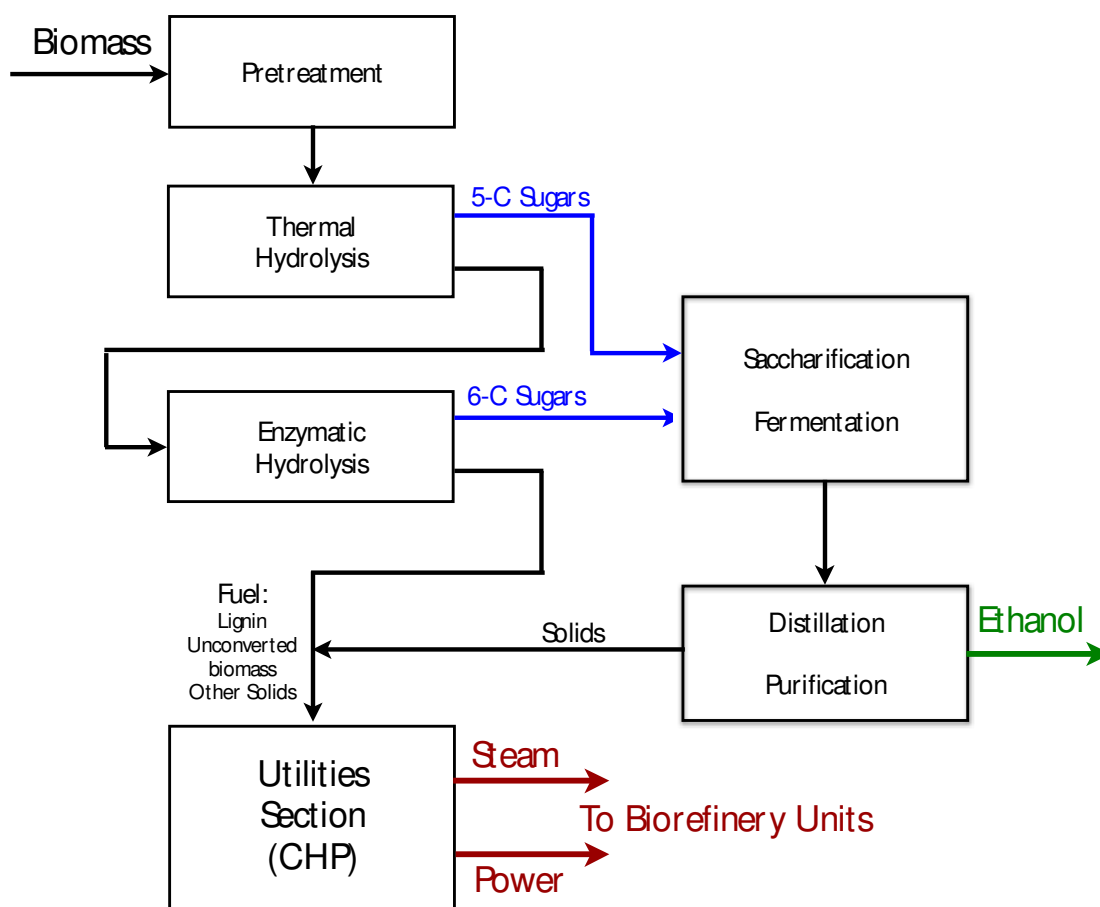


Figure 20: Cellulosic ethanol production from corn stover (saccharification and fermentation)

4.2. Design Basis

The biorefinery has been assumed to have a capacity of 2000 MT/day of dry biomass. The value was chosen so that we could have a common reference with published studies (Aden *et al.*, 2002; Humbird *et al.*, 2011) and compare the results. Corn stover was chosen as feedstock for the base-case scenario, and its composition is shown in Table 33.

Table 33: Corn stover composition and properties

Component	Formula	MW (g/gmol)	Quantity (%)
Cellulose	$C_6H_{10}O_5$	162.14	37.73
Hemicellulose	$C_5H_8O_4$	132.12	26.00
Lignin	$C_8H_8O_3$	152.15	19.24
Ash			3.79
Other Solids	$C_8H_8O_3$	152.15	13.24

The moisture content of the biomass has been assumed to be 50%. Table 34 presents the process parameters for the operation of the biorefinery.

Table 34: Process parameters

Feedstock		
Amount (MT/hr)	166.66	
Moisture Content	50%	
Conversions		
	Pretreatment	Enzymatic Hydrolysis
Cellulose to Glucose	10%	90%
Hemicellulose to Xylose	70%	50%
Fermentation		
Glucose to Ethanol	95%	
Xylose to Ethanol	95%	

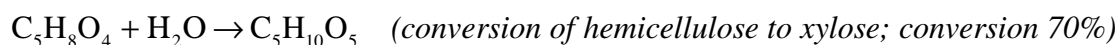
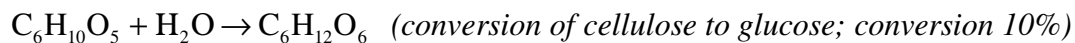
Table 34 (cont'd): Process parameters

CHP Unit	
Boiler efficiency	80%
Heat losses	5%
Turbine efficiency	85%
Total Generator Output (MW)	11.23
HP-steam	16%
MP-steam	50%

4.3. Material and Energy Balances

Corn stover, composed of cellulose, hemicellulose, lignin, ash, and other solids, enters the feed handling area of the biorefinery. The pretreatment section of the facility, depicted in Figure 21, includes a size-reduction stage, with washing and grinding of the biomass, and removal of the fine particles. The slurry is conveyed to a tank where prehydrolysis takes place, at high temperature (approximately 180°C) (Humbird *et al.*, 2011).

During the prehydrolysis stage, some of the cellulose and most of hemicellulose are converted to glucose and xylose, respectively (Kwiatkowski *et al.*, 2006; Humbird *et al.*, 2011). We have assumed that none of the lignin or the rest of the solids are solubilized during that step. The reactions that take place:



The mixture enters a flash tank, where some of the water is vaporized. The liquefied materials are cooled, and after removing some of the solids, the stream is led to the tank where saccharification will take place (Figure 20). The vapor exiting the flash unit could be used for covering the heating duty of another section of the biorefinery, however, for simplicity reasons we decided not to consider that stream during heat integration.

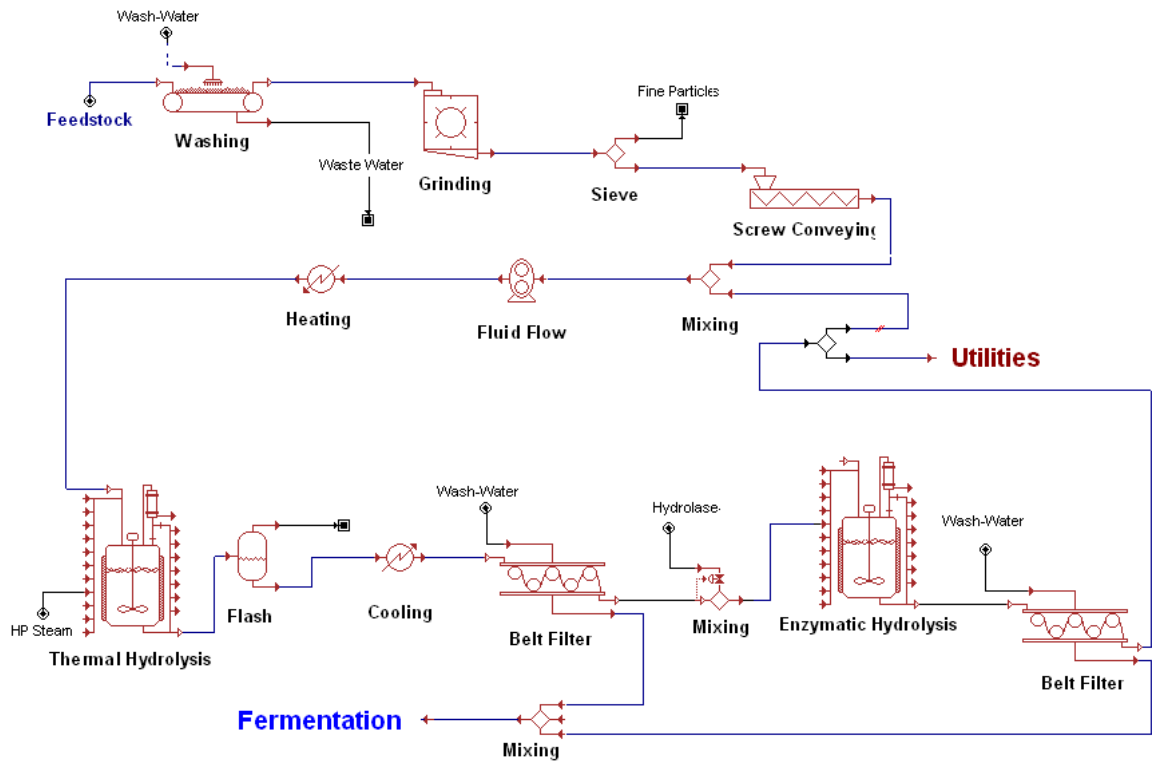
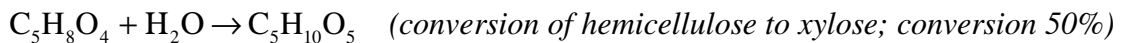
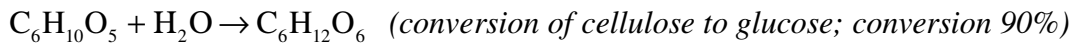


Figure 21: Pretreatment section & enzymatic hydrolysis of the biomass

Saccharification occurs after the material enters the hydrolysis tank. Hydrolase is the enzyme added to catalyze the reactions that take place (Kwiatkowski *et al.*, 2006; Humbird *et al.*, 2011):



The stream exiting the hydrolysis tank is led to a liquid-solid separator: the insoluble materials are led to the utility section of the biorefinery, where they will be used for steam and power generation. The rest of the slurry is led to the fermentation section (Figure 21).

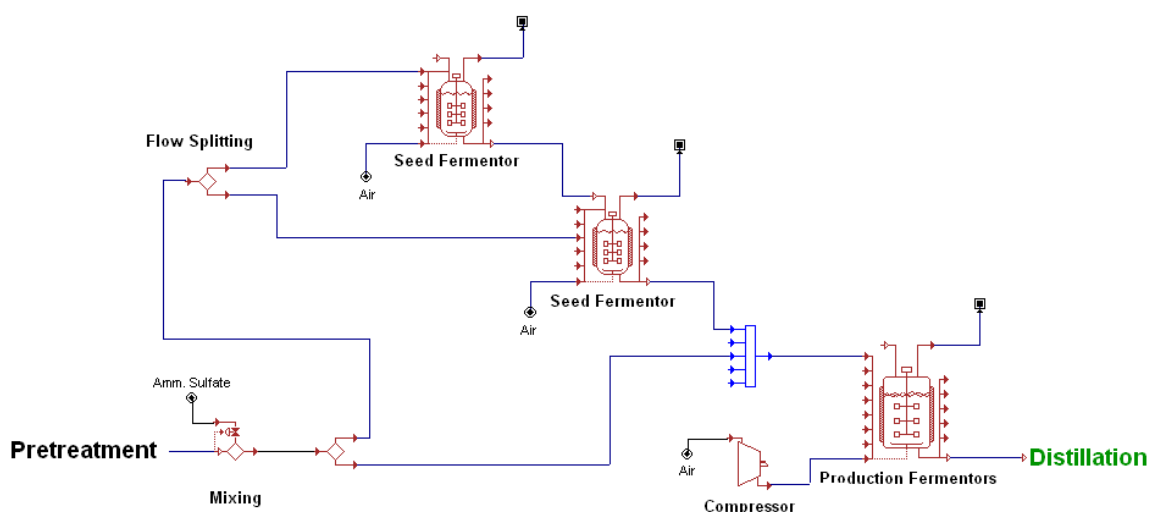
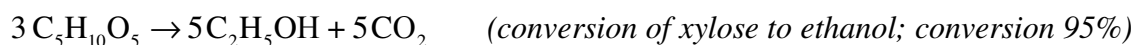
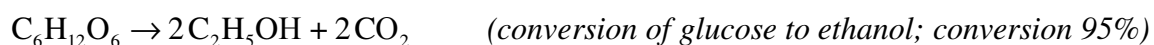


Figure 22: Fermentation section of bioethanol production

During fermentation, glucose and xylose are converted to ethanol under aerobic conditions, according to the reaction scheme:



Saccharomyces cerevisiae is added into the fermentation tank for the conversion of the carbohydrates to ethanol and carbon dioxide. The temperature of the fermenter has been set to approximately 40°C, in order to achieve optimal growth of the microorganism (Humbird *et al.*, 2011). One of the key assumptions at this point is that the only active pathway is the conversions of the sugars to ethanol; other potential fermentation

products, for instance succinic or acetic acid, have not been considered (reported conversions $< 1\%$).

The exit stream containing ethanol, water, and small amounts of the unconverted materials, is heated using a heat exchanger, and enters the purification section (Figure 20). Two distillation columns are required to achieve optimal separation of ethanol and water. The first one removes most of the water and the soluble solids (led to the utilities section), while the second distillation is used to obtain ethanol of higher purity. Exiting the column, the stream is led to a dehydration tank, and from there, we obtain the final product.

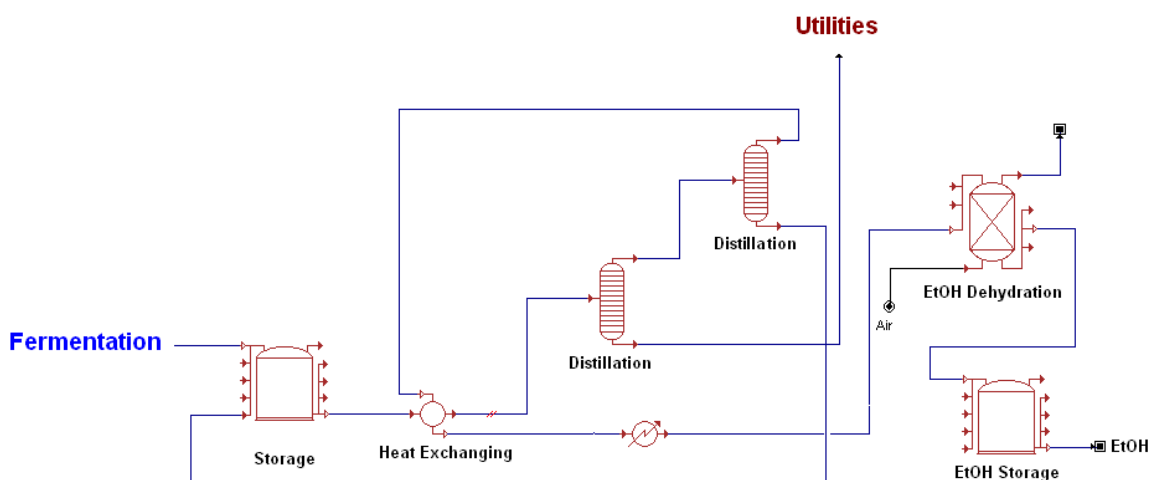


Figure 23: Ethanol purification section (distillation & dehydration)

As mentioned above, all the solids are collected and fed to the utility section. This part of the biorefinery consists of a boiler and a turbo-generator, and its sole purpose is to produce steam and power to cover all or part of the biorefinery energy requirements. The material stream enters the boiler, which (based on heuristics) has been assumed to have 80% efficiency. The exit stream is led through a 2-stage steam turbine, because our goal

is to produce both high- and medium-pressure steam to cover the requirements of the biorefinery (HP-steam: 10 bar, MP-steam: 5 bar). The condensate produced is led through a cooling tower, and the excess water produced is discarded to the environment.

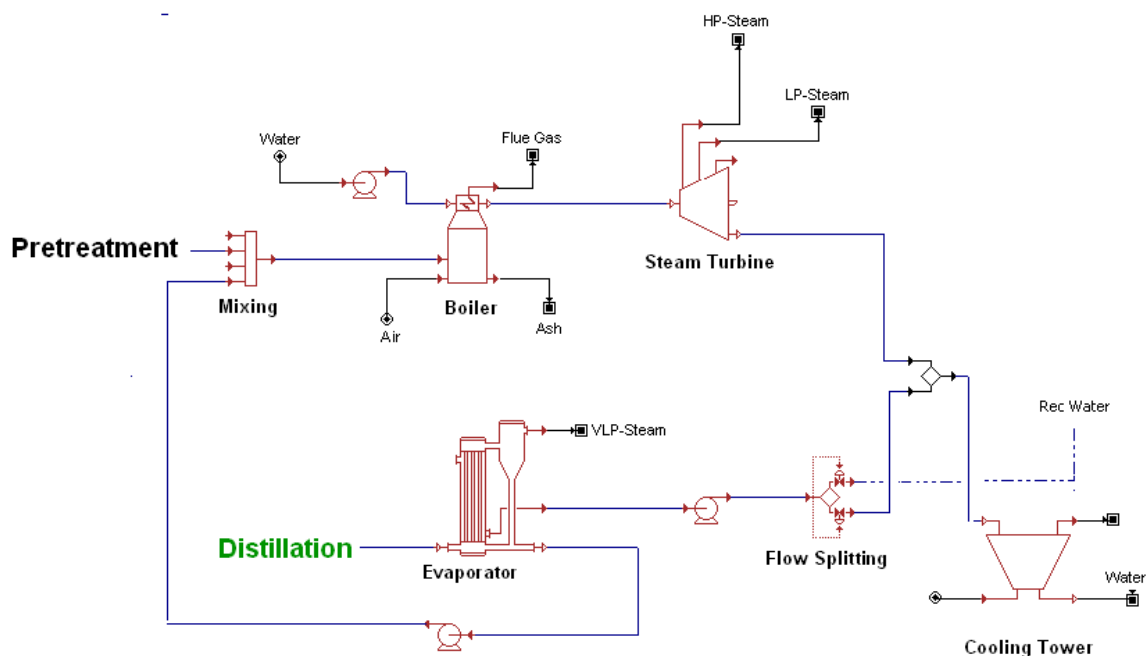


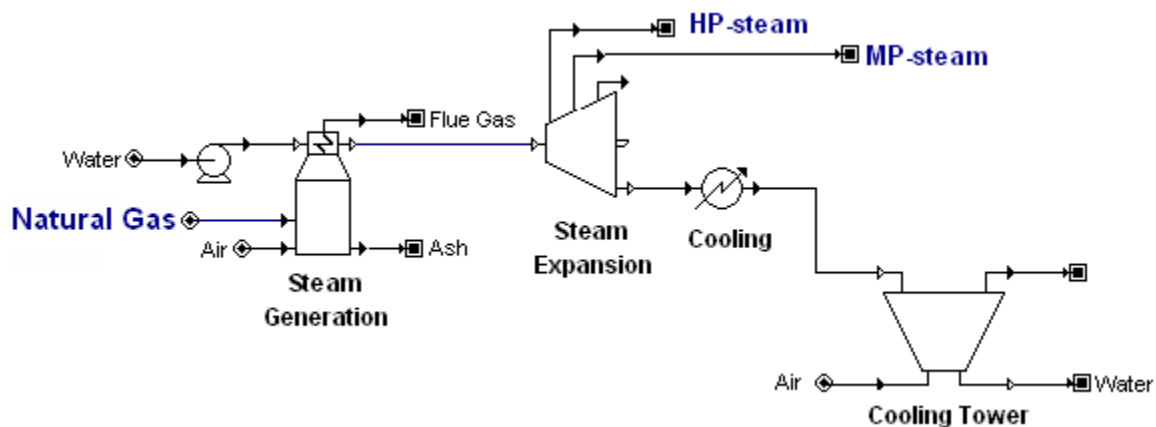
Figure 24: Utility section integrated to the biorefinery

The mass balance for the base-case scenario has been included in Table 35. The unconverted amounts of biomass characterized as "outlet" in this table are losses from the process during the pretreatment stage. A detailed report of the results from the simulation has been included in Appendix C.

Table 35: Mass balance for the base-case scenario (MT/hr)

Component	Inlet	Outlet	Outlet - Inlet
Cellulose	31.44	1.57	- 29.87
Hemicellulose	21.67	1.08	- 20.58
Lignin	16.03	0.80	- 15.23
Ash	3.16	3.15	- 0.00
Other Solids	11.03	0.55	- 10.48
Ethyl Alcohol	0.00	19.97	19.97
Water	419.99	437.03	17.04
Hydrolase	0.28	0.00	- 0.28
Oxygen	390.70	323.73	- 66.97
Nitrogen	1286.97	1286.97	0.00
Carbon dioxide	0.00	106.38	106.38
TOTAL	2181.27	2181.23	- 0.03

If lignin and the solids are used in the utility section, the steam requirements of the overall ethanol production cannot be covered (Table 36: MP-steam demand: ~14 MT/hr). The additional energy demands of the biorefinery will be covered using the auxiliary CHP unit (Figure 25), which will operate with natural gas.

**Figure 25: Auxiliary CHP unit, operating with natural gas**

The minimum amount of natural gas required in this case will be 1.71 MT/hr, as shown in Table 36.

Table 36: Biomass content and energy demand during ethanol production (base-case)

Carbohydrate Content (%)	Lignin Content (%)	Ethanol Production (MT/hr)	HP-steam Demand (MT/hr)	MP-steam Demand (MT/hr)	Natural Gas Demand (MT/hr)
63.73	19.24	19.82	(6.00)	-13.96	1.71

The energy balance for the facility, taking into account the operation of the auxiliary CHP unit has been summarized in Table 37. The surplus of the produced electricity (~5.5 MWh) can be sold to the grid. Table 38 includes the metrics estimation for bioethanol production, taking into account the operation of the auxiliary CHP unit. As mentioned in the previous sections, the energy metrics estimated were:

- **The net energy value (NEV) defined as:**

$$NEV^* = \left[\begin{array}{c} \text{Energy content} \\ \text{of biofuel} \end{array} \right] + \left[\begin{array}{c} \text{Energy content} \\ \text{of co-product} \end{array} \right] - \left[\begin{array}{c} \text{Energy in fuel used for} \\ \text{the auxiliary utility plant} \end{array} \right]$$

- **The net energy ratio (NER) defined as:**

$$NER^* = \frac{\left[\begin{array}{c} \text{Energy content} \\ \text{of biofuel} \end{array} \right] + \left[\begin{array}{c} \text{Energy content} \\ \text{of co-product} \end{array} \right]}{\left[\begin{array}{c} \text{Energy in fuel used for} \\ \text{the auxiliary utility plant} \end{array} \right]}$$

- **The overall efficiency of the biorefinery defined as:**

$$\eta = \frac{[Energy\ content\ of\ products]}{[Energy\ content\ of\ input]}$$

The fuel used for the utility plant in this case was natural gas. No additional power was bought from the grid.

Table 37: Steam and power balance for the biorefinery (GJ/hr) (base-case)

HP-steam	MP-steam	Power
(18.14)	$(9.3 \cdot 10^{-3})$	(20.26)

Table 38: Metrics estimation (base-case)

Biorefinery Net Energy Value (MJ/L _{fuel})	Net Energy Ratio	Overall Efficiency
18.75	6.76	0.34

As displayed in Table 36, additional steam is required for the operation of the biorefinery. The pretreatment of the biomass is the requires a significantly higher amount of electricity compared to the other sections of the biorefinery, while product recovery and energy co-generation are the most energy intensive stages in terms of steam consumption (Table 39). Carbon dioxide emissions have also been estimated, to gain an insight into the environmental impact of the biofuel production process (Table 40).

Table 39: Steam and power requirements per sector (base-case)

	Pretreatment Section	Purification Section	Utilities Section
Steam (MT/hr)	19.91	60.98	45.56
Power (MW)	5.58	1.09	0.17

Table 40: CO₂ emissions per sector ^(*) (MT/hr) (base-case)

Fermentation Section	Utilities Section	Auxiliary CHP Section
27.48	78.90	4.71

^(*) The amounts of CO₂ do not take into account any co-product credit.

Table 41 compares our results to those of published studies (Farrell *et al.*, 2006; Pimentel and Patzek, 2005; Wang, 2001). For consistent comparison, neither the energy input during the agricultural phase nor the energy consumed during feedstock transportation to the biorefinery have been considered for the numbers presented in this table. Also, the energy value of ethanol is based on lower heating value (LHV).

The NEV computed from this study is lower than the NEV values provided by Farrell and coworkers (2006) and Wang (2001). It is, however, significantly higher than the NEV computed by Patzek and Pimentel who did not use the lignin and other solids as fuel for meeting at least a part of the energy needs of the plant.

Table 41: Net energy summary (incl. co-products), adapted from literature

Energy Value (MJ/L _{fuel})	Current study	Farrell ("Cellulosic")	Pimentel	Wang
Total input	3.25 ^(a)	1.08 ^(b)	27.04 ^(c)	0.06 ^(b)
Ethanol	21.20	21.20	21.20	21.20
Co-products	0.80	4.79	0.00	4.79
Total output	22.00	26.00	21.20	25.99
Biorefinery NEV	18.75	23.47	-5.80	25.93

^(a) This value takes into account only the natural gas demand for the operation of the biorefinery. The rest of the energy requirements have been subtracted from the co-product credit.

^(b) There is an additional energy input (26.3 MJ/L), which comes from biomass and thus, it is accounted as recycled biomass energy.

^(c) Electricity is purchased, not generated from lignin; steam is produced from purchased natural gas.

In the current study, the excess amount of electricity has been considered as co-products. The rest of the authors included in Table 41 have included other material outputs (e.g. products from pretreatment). Furthermore, the biorefinery in our process design has heat integration, which eventually increases the NEV by more than 10%. The effect of heat integration in the production process shall be investigated in a subsequent section of this thesis. Furthermore, it should be mentioned that when lignin was not used for heat and power generation, the natural gas demand increased significantly (~11.5 MT/hr, or 21.8 MJ/L_{fuel}), resulting in a much lower net energy value for the biorefinery (0.71 MJ/L_{fuel}).

4.4. Sensitivity Analysis – Monte Carlo Analysis

A Monte Carlo analysis was performed to assess the effect of several process parameters on the overall ethanol production. The variables we looked into for the sensitivity analysis were:

- a. Biomass composition: cellulose, hemicellulose, and lignin content (%)
- b. Total amount of feedstock (MT/hr)
- c. Moisture content of the feedstock(%)
- d. Conversion of cellulose during enzymatic hydrolysis (%)
- e. Conversion of glucose (or xylose) during fermentation (%)

The ranges of the variables are shown in Table 42. The mean (μ) has been assumed to be equal to the nominal value, and the standard deviation (σ) was calculated using Matlab, assuming 90%, 95% and 99% confidence intervals, according to equation:

$$\Phi_{\mu,\sigma^2}(X_H) - \Phi_{\mu,\sigma^2}(X_L) = 0.90 \quad (1.37)$$

(for a 90% confidence interval; analogous calculation for the other values), where $\Phi_{\mu,\sigma^2}(X)$ is the Gaussian cumulative distribution function. Φ , can be computed as an integral of the probability density function:

$$\Phi(x) = \frac{1}{\sqrt{2\pi}} \int_{-\infty}^x e^{-t^2/2} dt \quad (1.38)$$

or, in terms of the error function (erf):

$$\Phi(x) = \frac{1}{2} \left[1 + \operatorname{erf} \left(\frac{x - \mu}{\sqrt{2\sigma^2}} \right) \right] \quad (1.39)$$

X_H and X_L are the upper and lower limits of the data range, respectively.

Table 42: Input parameters for the sensitivity analysis

Input Parameters	Nominal Value	Minimum	Maximum
Feedstock			
Total amount (MT/hr)	166.66	120	200
Moisture content (%)	50	45	70
Composition			
Cellulose (%)	31.44	25.15	44.02
Hemicellulose (%)	21.67	17.34	30.34
Lignin (%)	16.03	12.82	22.45
Conversion			
Hydrolysis (%)	90	85	99
Fermentation (%)	95	90	99

In order to compare the effect of each variable, we need to have a dimensionless number. Therefore, we estimate the variation coefficient (cv):

$$cv = \frac{\sigma}{|\mu|} \quad (1.40)$$

The results are given in Table 43 that follows. Alternatively, we could use the relative standard deviation (RSD), which is the absolute value of the coefficient of variation.

Table 43: Estimation of the variation coefficient

	Mean	St. dev. ($\alpha=0.10$)	cv	St. dev. ($\alpha=0.05$)	cv	St. dev. ($\alpha=0.01$)	cv
Feedstock							
Total amount (MT/hr)	166.66	23.39	0.14	19.31	0.12	14.21	0.09
Moisture content (%)	50	3.90	0.08	3.04	0.06	2.15	0.04
Composition							
Cellulose (%)	31.44	4.53	0.14	3.71	0.12	2.70	0.09
Hemicellulose (%)	21.67	3.31	0.15	2.63	0.12	1.86	0.09
Lignin (%)	16.03	2.46	0.15	1.95	0.12	1.38	0.09
Conversion							
Hydrolysis (%)	90	3.76	0.04	3.01	0.03	2.15	0.02
Fermentation (%)	95	2.69	0.03	2.24	0.02	1.68	0.02

The results presented in Table 43 indicate that among our key variables, the biomass entering the biorefinery, in terms of both amount and composition, is more dispersed than the rest. In other words, that is the parameter with the greater level of uncertainty, whose effect will be the most dominant in the production process. That is apparent from Figure 25 as well, which outlines the deviation from the estimated values for each parameter. Note that the values for the standard deviation and the range between the minimum and maximum values in that plot were estimated based on a sample size of 1000, for a 95% interval ($\alpha=0.05$).

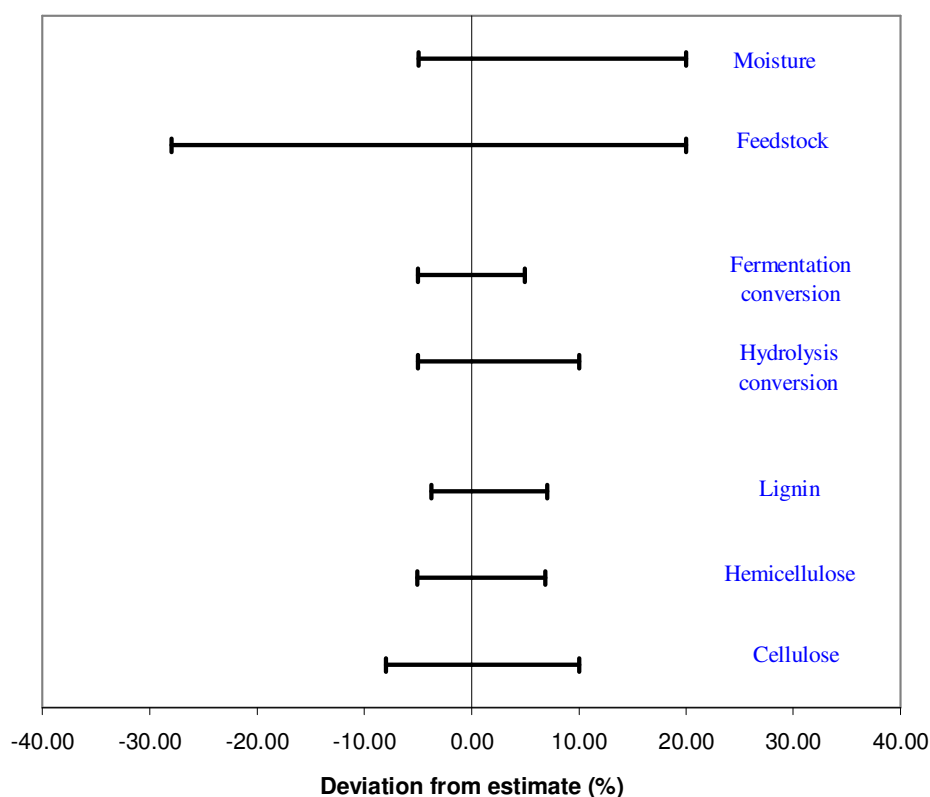


Figure 26: Deviation from nominal value (%) for various process parameters

Figure 27 is a histogram for the total amount of ethanol produced in the biorefinery. From this histogram, and using Excel (results on Table 44), we can estimate the probability of producing above or below a specific amount of biofuels. For instance, the probability of producing less than 18.0 MT/hr ethanol is 6.4%, 20.0 MT/hr or higher, ~71%, and within this range, the probability is ~ 23%.

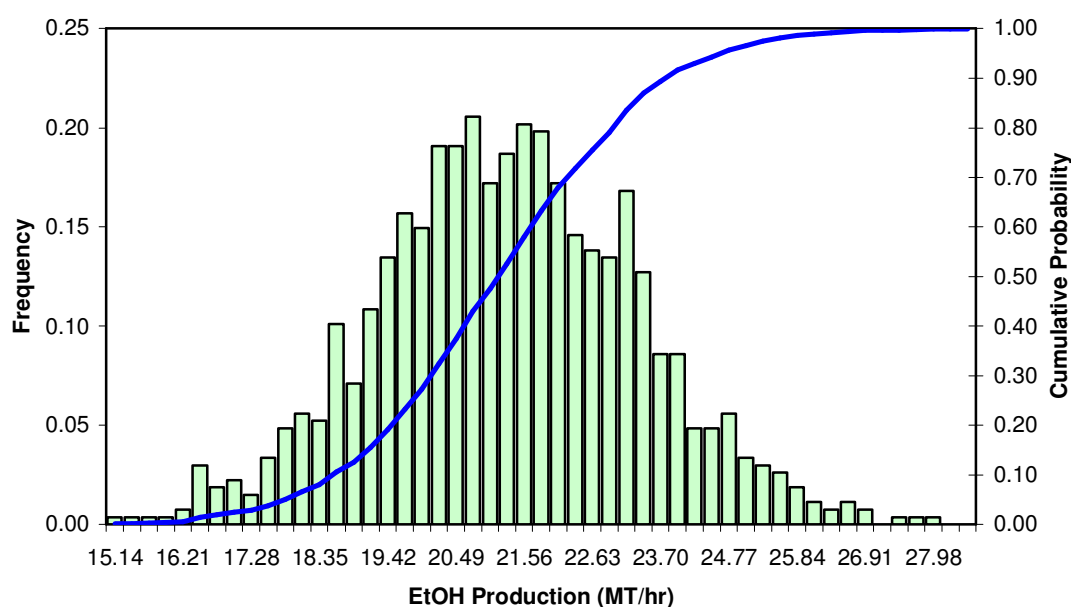


Figure 27: Histogram for the distribution of ethanol production data, and the cumulative probability

Table 44: Statistics for ethanol production

Mean	21.14	Min	13.37
St.dev.	1.99	Max	27.23
Probabilities			
P (y < 18.0)		6.40 %	
P (y > 20.0)		70.90 %	
P (18.00 < y < 20.0)		22.80 %	

The sensitivity analysis and the results obtained from this section demonstrated the necessity to further explore the effect of feedstock in ethanol production process, not only with respect to the amount of biofuel produced, but also with respect to the energy inputs for the process. Based on the outcome, we designed a series of simulations to determine the effect the aforementioned parameters more thoroughly, as shown in detail in the following sections.

4.5. Feedstock Composition

The effect of feedstock composition has been extensively studied. Based on our initial assumption for the biomass (see Table 33), we have considered three additional scenarios:

- Case I: Corn stover with increased carbohydrate content;
- Case II: Corn stover with increased lignin content; and
- Case II: Various feedstocks.

For the first two cases, the amounts of ash and other solids have remained constant, while carbohydrate and lignin content has been changed by a constant ratio. For the third scenario, we gathered data from the NREL database (Biomass Feedstock Composition and Property Database) for corn stover and three herbaceous crops: switchgrass (Case III-a), Big bluestem (*Andropogon gerardii*) (Case III-b), and *Sericea Lespedeza* (Case III-c).

In all cases, we calculated the metrics developed in Chapter 2. The steam requirements per section and the total power demand for the process were also evaluated. Additionally, the environmental impact of ethanol production was accounted by calculating the CO₂ emissions.

4.5.1. Case I: Increased Carbohydrate Content

In Case I, the carbohydrate content of the feedstock has been assumed to vary from ~65% to 68%, lignin from 18.5% to 14.7%, while the rest of the biomass content has

been assumed to remain constant. Table 45 - Table 46 summarize the outcome of the simulations, and the calculation of the metrics, introduced in Chapter 2.

Table 45: Corn stover w/ increased carbohydrate scenario, w/ heat integration (Case I)

Carbohydrate Content (%)	Lignin Content (%)	Ethanol Production (MT/hr)	HP-steam Demand (MT/hr)	MP-steam Demand (MT/hr)	Natural Gas Demand (MT/hr)
64.49	18.48	20.12	(5.36)	-16.64	2.04
64.96	18.02	20.30	(4.99)	-17.56	2.16
65.41	17.56	20.49	(4.59)	-19.54	2.40
65.86	17.11	20.66	(4.23)	-20.51	2.52
66.29	16.68	20.84	(3.85)	-22.44	2.76
66.71	16.26	21.00	(3.51)	-23.25	2.86
67.13	15.85	21.18	(3.15)	-25.22	3.10
67.53	15.44	21.33	(2.82)	-25.98	3.19
67.91	15.05	21.51	(2.46)	-27.95	3.43
68.29	14.66	21.65	(2.16)	-28.64	3.52

Table 46: Metrics estimation (Case I)

Carbohydrate Content (%)	Biorefinery Net Energy Value (MJ/L_{fuel})	Net Energy Ratio	Overall Efficiency
64.49	18.17	5.75	0.341
64.96	17.98	5.49	0.343
65.41	17.57	4.98	0.344
65.86	17.38	4.78	0.345
66.29	16.99	4.41	0.346
66.71	16.83	4.29	0.347
67.13	16.44	3.99	0.348
67.53	16.31	3.90	0.349
67.91	15.93	3.65	0.350
68.29	15.81	3.58	0.351

Schematic representations of the results are depicted in Figure 29 - Figure 31.

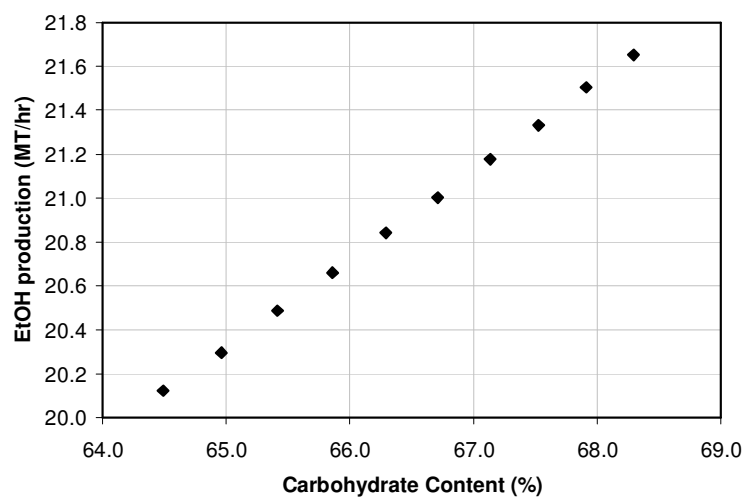


Figure 28: Ethanol production with respect to carbohydrate content of the biomass (Case I)

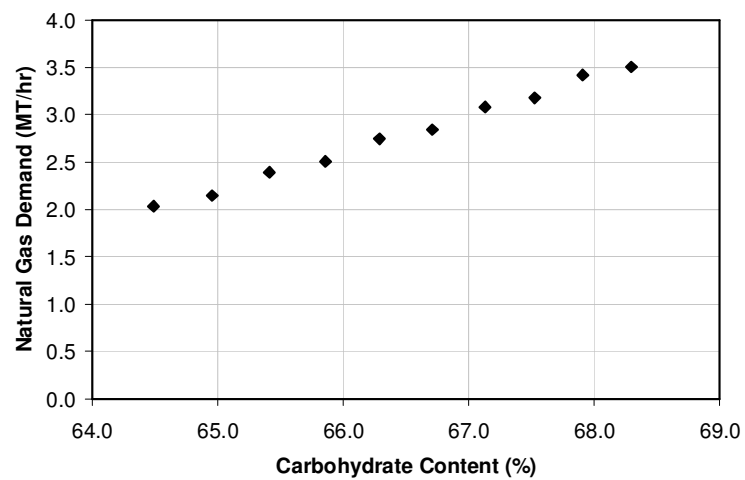


Figure 29: Natural gas demand with respect to carbohydrate content of the biomass (Case I)

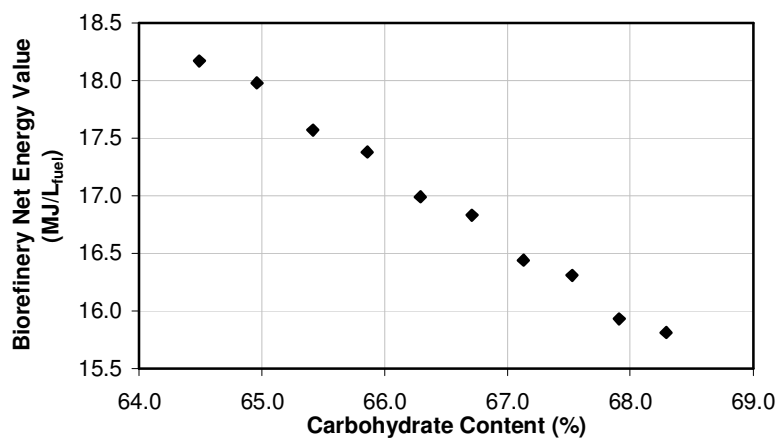


Figure 30: Biorefinery net energy value with respect to carbohydrate content of biomass (Case I)

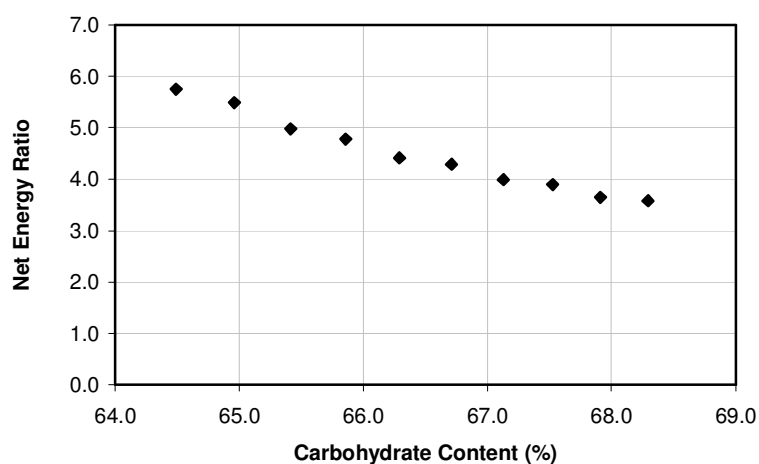


Figure 31: Net energy ratio with respect to carbohydrate content of biomass (Case I)

4.5.2. Case II: Increased Lignin Content

In Case II, the lignin content of the feedstock has been assumed to increase from ~19% to 22%, while cellulose and hemicellulose decrease from ~64% to 61%. The rest of the biomass content has been assumed to remain constant in this case as well. Tables 47 and 48 summarize the outcome of the simulations, and the calculation of the metrics.

Table 47: Corn stover w/ increased lignin scenario, w/ heat integration (Case II)

Carbohydrate Content (%)	Lignin Content (%)	Ethanol Production (MT/hr)	HP-steam Demand (MT/hr)	MP-steam Demand (MT/hr)	Natural Gas Demand (MT/hr)
63.73	19.24	19.82	(5.998)	-13.956	1.71
63.45	19.52	19.70	(6.257)	-12.674	1.56
63.15	19.82	19.59	(6.493)	-11.988	1.47
62.86	20.12	19.48	(6.727)	-11.056	1.36
62.55	20.42	19.36	(7.003)	-9.660	1.19
62.25	20.72	19.25	(7.238)	-9.041	1.11
61.93	21.04	19.12	(7.506)	-7.771	0.95
61.61	21.36	19.00	(7.761)	-7.001	0.86
61.30	21.68	18.89	(8.016)	-5.989	0.74
60.97	22.00	18.76	(8.295)	-4.603	0.57

Table 48: Metrics estimation (Case II)

Carbohydrate Content (%)	NEV (MJ/L_{fuel})	NER	Overall Efficiency
63.73	18.75	6.76	0.340
63.45	19.03	7.40	0.339
63.15	19.18	7.78	0.338
62.86	19.39	8.39	0.337
62.55	19.71	9.54	0.337
62.25	19.85	10.14	0.336
61.93	20.15	11.72	0.335
61.61	20.33	12.93	0.334
61.30	20.57	15.03	0.334
60.97	20.91	19.42	0.333

Schematic representations of the results are depicted in Figure 32 -Figure 35.

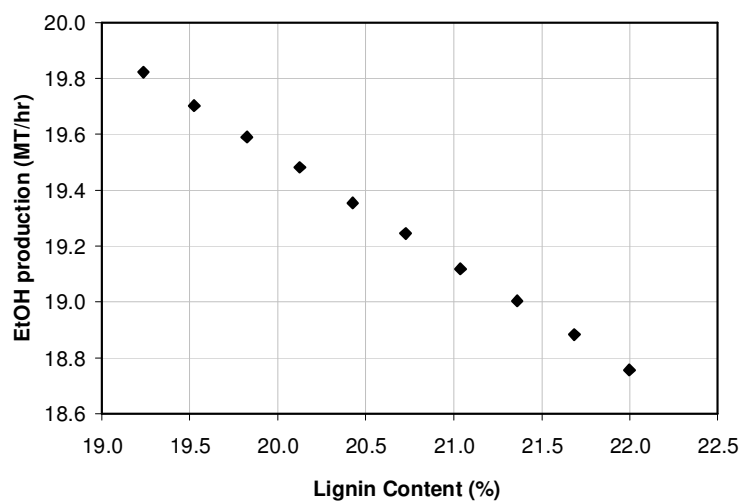


Figure 32: Ethanol production with respect to lignin content of the biomass (Case II).

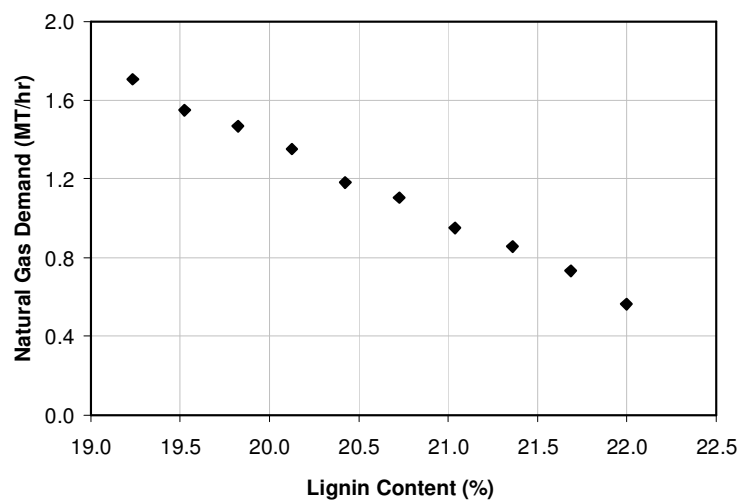


Figure 33: Natural gas demand with respect to lignin content of the biomass (Case II).

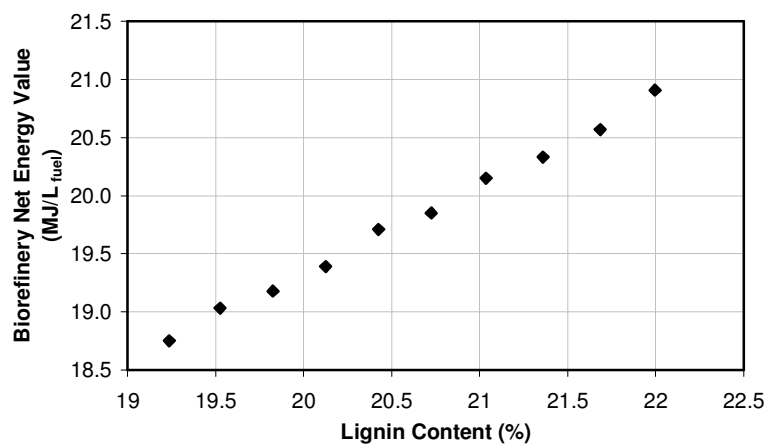


Figure 34: Biorefinery net energy value with respect to lignin content of biomass (Case II)

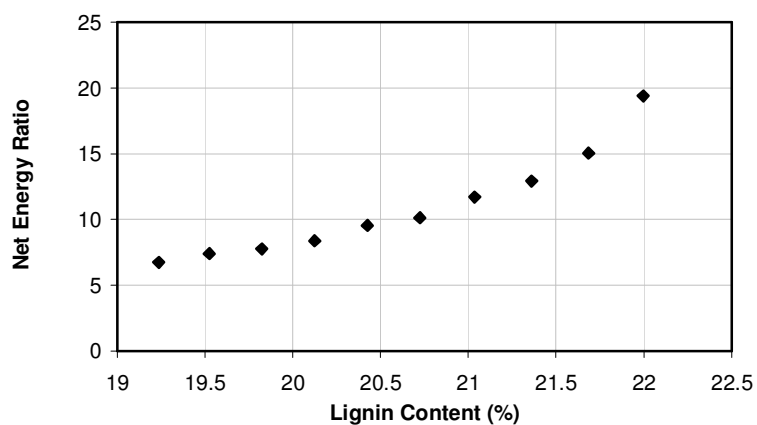


Figure 35: Net energy ratio with respect to lignin content of biomass (Case II)

Combining the results from Sections 2.3.1 and 2.3.2 (Figure 28 - Figure 35), we are able to determine whether corn stover is an attractive potential feedstock for ethanol production.

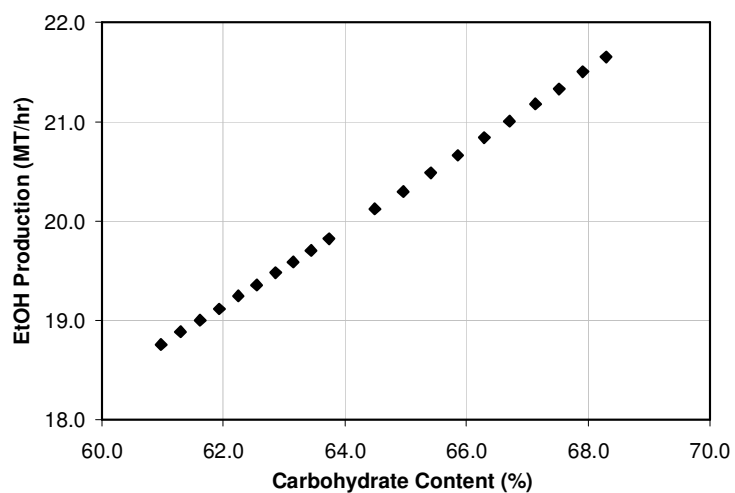


Figure 36: Ethanol production with respect to carbohydrate content for corn stover

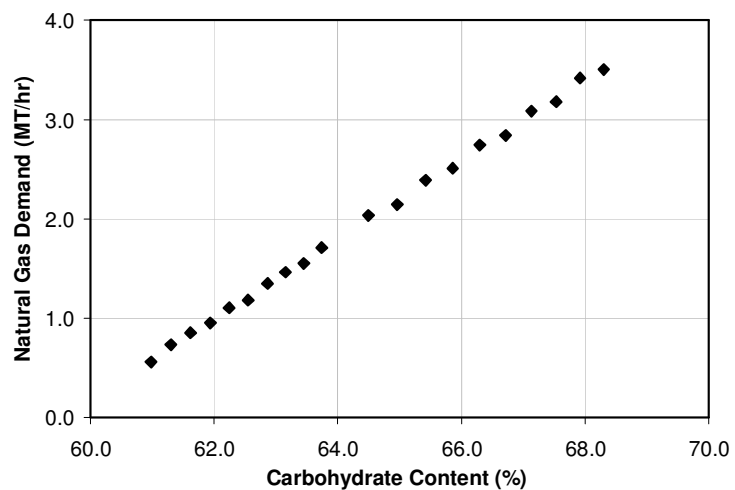


Figure 37: Natural gas demand with respect to carbohydrate content for corn stover

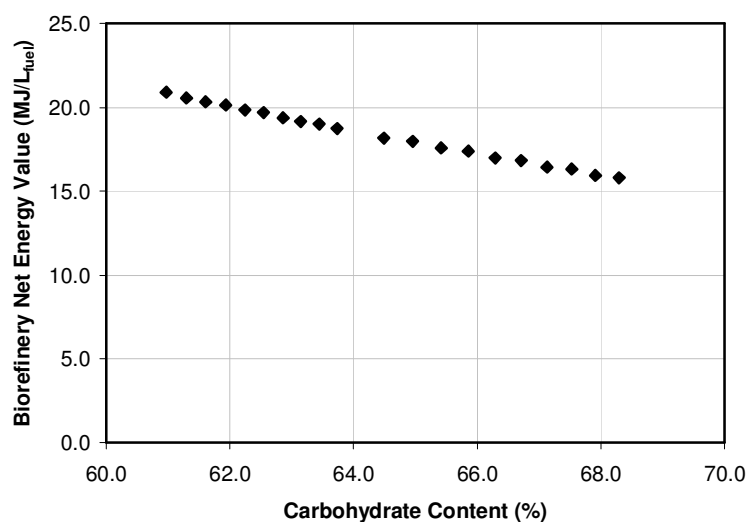


Figure 38: Biorefinery net energy value with respect to carbohydrate content for corn stover

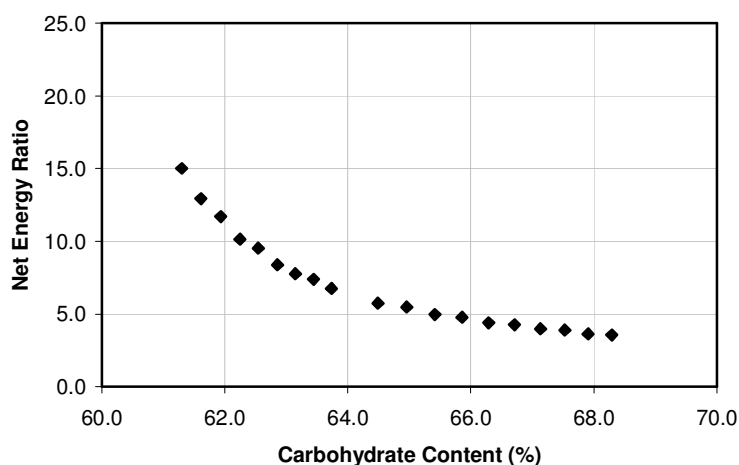


Figure 39: Net energy ratio with respect to carbohydrate content for corn stover

4.5.3. Case III: Corn stover (realistic scenario) & herbaceous crops

Data for the composition and properties of various herbaceous crops were collected from the database of the U.S. Department of Energy's Biomass Program. The ultimate objective was to explore and determine which amongst them would be the optimal crop

for ethanol production. Through this study and based on the data collected, we can further assess whether genetic improvements would be required in any of the herbaceous species in order to improve the feedstock quality.

The tables below include the simulation results for corn stover (Case III-a), and the following herbaceous crops: switchgrass (*Panicum virgatum L.*) (Case III-b), Big bluestem (*Andropogon gerardii*) (Case III-c), and Sericea Lespedeza (*Lespedeza cuneata*) (Case III-d). The datasets highlighted in the following tables indicate the median of the rest of the data, which have been selected as reference. It should also be noted that due to the lack of calculated values in the literature, the heating values for the samples were assumed constant among the samples (Table 49).

Table 49: Energy content of biomass feedstock

Variety	Energy Content (MJ/kg)
Corn Stover	18.36
Big bluestem	18.36
Sericea Lespedeza	19.66
Switchgrass	18.61

Table 50: Corn stover used as feedstock, w/ integration (Case III-a)

Carbohydrate Content (%)	Lignin Content (%)	Ethanol Production (MT/hr)	HP-steam Demand (MT/hr)	MP-steam Demand (MT/hr)	Natural Gas Demand (MT/hr)
58.71	18.38	17.49	(3.15)	-19.24	2.36
56.82	17.69	17.08	(5.38)	-10.61	1.30
58.86	17.77	17.76	(4.30)	-15.87	1.95
49.74	18.19	14.81	(9.62)	(7.65)	0.00
58.72	17.39	17.56	(3.01)	-19.40	2.38
59.33	19.25	17.62	(2.84)	-20.68	2.54
58.17	17.12	17.45	(3.66)	-17.06	2.10
61.30	18.14	18.19	(0.44)	-29.56	3.63
57.03	19.68	16.72	(2.86)	-18.94	2.33
56.25	21.25	16.33	(3.49)	-15.09	1.85
58.72	18.96	17.26	(1.47)	-24.80	3.05
61.55	20.24	18.20	(1.35)	-26.89	3.30
62.98	18.59	18.94	(1.36)	-28.11	3.45

Table 51: Metrics estimation (Case III-a)

Carbohydrate Content (%)	NEV (MJ/L _{fuel})	NER	Overall Efficiency
58.71	16.97	4.34	0.295
56.82	19.20	7.69	0.297
58.86	17.92	5.33	0.303
49.74	22.31		0.271
58.72	16.94	4.32	0.296
59.33	16.63	4.06	0.295
58.17	17.54	4.88	0.296
61.30	14.51	2.93	0.295
57.03	16.85	4.22	0.282
56.25	17.83	5.17	0.280
58.72	15.42	3.32	0.285
61.55	15.21	3.23	0.298
62.98	15.15	3.21	0.309

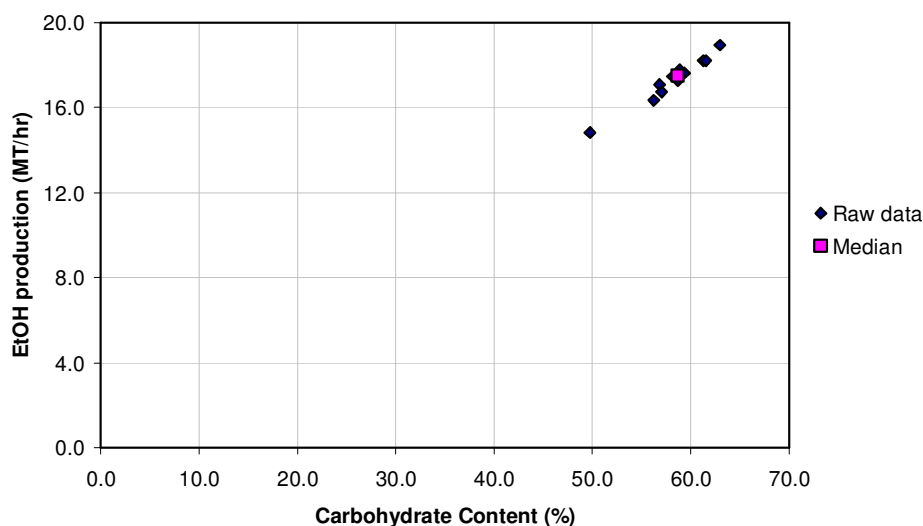


Figure 40: Ethanol production with respect to carbohydrate content of the biomass (Case III-a).

Table 54 -Table 55 summarize the steam demand and CO₂ emissions per sector. As expected, pretreatment section is the least energy intensive section of the biorefinery, compared to the fermentation and purification sections.

Table 52: Steam requirements per sector (MT/hr) (Case III-a)

Lignin Content (%)	Pretreatment Section	Purification Section	Utilities Section
18.38	20.46	57.30	45.07
17.69	20.21	57.30	43.64
17.77	20.21	58.12	44.74
18.19	20.31	55.16	40.69
17.39	20.31	57.45	44.8
19.25	20.59	57.24	45.48
17.12	20.22	57.55	44.48
18.14	20.56	57.63	46.49
19.68	20.86	55.89	44.88
21.25	21.1	54.68	43.96
18.96	20.78	56.56	45.79
20.24	20.77	57.46	46.62
18.59	20.41	58.86	46.84

Table 53: CO₂ emissions per sector (MT/hr) (Case III-a)

Lignin Content (%)	Fermentation Section	Utilities Section	Auxiliary CHP Section
18.38	24.27	75.02	6.49
17.69	23.70	79.54	3.58
17.77	24.63	77.06	5.37
18.19	20.56	89.14	<i>not operating</i>
17.39	24.37	74.73	6.55
19.25	24.46	74.31	6.98
17.12	24.22	76.05	5.75
18.14	25.23	69.43	9.98
19.68	23.18	75.02	6.38
21.25	22.67	76.39	5.08
18.96	23.94	72.03	8.37
20.24	25.27	71.07	9.07
18.59	26.26	70.66	9.50

In the case of switchgrass, we examined 8 different populations: Alamo whole plant, Kanlow leaves, Cave-in-Rock leaves (regular and high yield), Blackwell whole plant, Trailblazer whole plant, EY x FF high yield cycle 3, EY x FF low yield cycle 1. As shown in Table 54, the variability among the species with respect to their composition appears to be minimal, resulting in minor differences in ethanol production. Moreover, in all cases, the lignin content of switchgrass is such that additional natural gas is required for the operation of the biorefinery.

Table 54: Switchgrass used as feedstock, w/ heat integration (Case III-b)

Carbohydrate Content (%)	Lignin Content (%)	Ethanol Production (MT/hr)	HP-steam Demand (MT/hr)	MP-steam Demand (MT/hr)	Natural Gas Demand (MT/hr)
59.47	17.99	18.39	(7.23)	-6.71	0.82
59.41	17.63	18.40	(7.21)	-6.79	0.83
59.45	18.05	18.43	(7.54)	-5.70	0.70
60.97	19.14	18.68	(5.39)	-14.19	1.74
59.47	17.74	18.27	(6.11)	-10.29	1.26
61.15	17.94	19.12	(7.60)	-7.02	0.86
59.94	17.77	18.47	(6.34)	-9.62	1.18
59.10	19.04	18.07	(6.58)	-8.87	1.09

Table 55: Metrics estimation (Case III-b)

Carbohydrate Content (%)	NEV (MJ/L_{fuel})	NER	Overall Efficiency
59.47	20.35	13.05	0.324
59.41	20.33	12.90	0.324
59.45	20.61	15.41	0.326
60.97	18.52	6.27	0.320
59.47	19.43	8.46	0.318
61.15	20.32	12.96	0.336
59.94	19.62	9.15	0.322
59.10	19.78	9.71	0.316

The steam demand and CO₂ emissions per sector for ethanol production from switchgrass are displayed in Tables 56 – 57.

Table 56: Steam requirements per sector (MT/hr) (Case III-b)

Lignin Content (%)	Pretreatment Section	Purification Section	Utilities Section
17.99	19.90	59.45	43.70
17.63	19.84	59.57	43.66
18.05	19.89	59.54	43.57
19.14	20.24	59.35	45.18
17.74	20.00	59.08	44.06
17.94	19.70	60.68	44.13
17.77	19.94	59.30	43.94
19.04	20.19	58.76	44.21

Table 57: CO₂ emissions per sector (MT/hr) (Case III-b)

Lignin Content (%)	Fermentation Section	Utilities Section	Auxiliary CHP Section
17.99	25.43	82.31	2.27
17.63	25.46	82.29	2.29
18.05	25.50	82.89	1.91
19.14	25.82	78.58	4.79
17.74	25.27	80.27	3.47
17.94	26.48	82.54	2.37
17.77	25.56	80.55	3.25
19.04	25.00	81.22	2.99

Data for two different populations of Big bluestem were used: plants of Baldwin County, GA, and Greene County, AL. These varieties were further categorized in "leaves" and "stems". The first three datasets appearing in Table 58 are used as reference: the first one is the median of all data, the second represents the median of the plants of Baldwin County, GA, and the third the median of Big bluestem plants from Greene County, AL.

Table 58: Big bluestem used as feedstock, w/ heat integration (Case III-c)

Variety	Carbohydrate Content (%)	Lignin Content (%)	Ethanol Production (MT/hr)	HP-steam Demand (MT/hr)	MP-steam Demand (MT/hr)	Natural Gas Demand (MT/hr)
Median (all)	58.23	19.27	18.12	(10.11)	(3.17)	0.00
Median (Baldwin County, GA)	55.11	19.30	17.12	(12.15)	(11.99)	0.00
Median (Greene County, AL)	58.74	19.27	18.29	(9.74)	(1.48)	0.00
Genotype, Baldwin County, GA (leaves)	50.37	17.93	15.62	(14.62)	(24.07)	0.00
	49.48	18.79	15.27	(15.01)	(25.19)	0.00
Genotype, Baldwin County, GA (stems)	59.85	19.81	18.66	(9.58)	(0.52)	0.00
	60.06	20.24	18.74	(9.84)	(1.30)	0.00
Genotype, Greene County, AL (leaves)	57.15	19.34	17.61	(9.57)	(2.39)	0.00
	56.70	23.79	17.33	(11.79)	(9.24)	0.00
Genotype, Greene County, AL (stems)	60.03	17.09	18.85	(8.53)	-2.40	0.29
	63.01	19.19	19.67	(6.98)	-10.34	1.27

Table 59: Metrics estimation (Case III-c)

Carbohydrate Content (%)	NEV (MJ/L _{fuel})	NER	Overall Efficiency
58.23	22.10	Inf	0.328
55.11	22.28	Inf	0.313
58.74	22.08	Inf	0.331
50.37	22.54	Inf	0.289
49.48	22.59	Inf	0.283
59.85	22.05	Inf	0.337
60.06	22.06	Inf	0.339
57.15	22.11	Inf	0.319
56.70	22.25	Inf	0.316
60.03	21.43	37.46	0.337
63.01	19.58	9.05	0.341

From the two genotypes of Big bluestem compared, the leaves had significantly lower carbohydrate content, resulting in potentially lower ethanol yields, as displayed in Table

58. It should also be noted that AL stems are the only variety that, when used as feedstock, required additional natural gas for the operation of the biorefinery.

As indicated from the following figures, ethanol production is lower for the leaves varieties, resulting in higher net energy values for the biorefinery. Therefore, the outcome signifies the importance of targeting plant development research in this case towards the production of plants with more stem mass, a result which is in agreement with other literature findings (NREL, 1995).

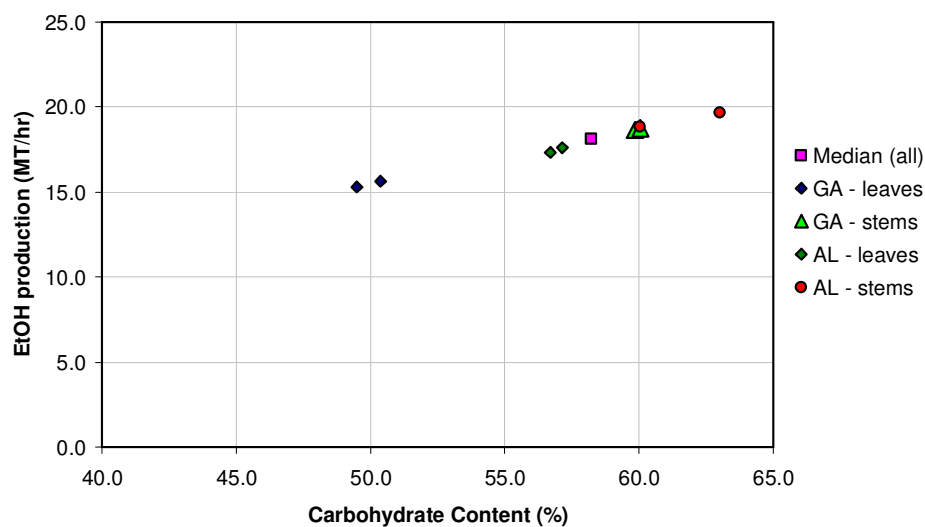


Figure 41: Ethanol production with respect to carbohydrate content of the biomass (Case III-c).

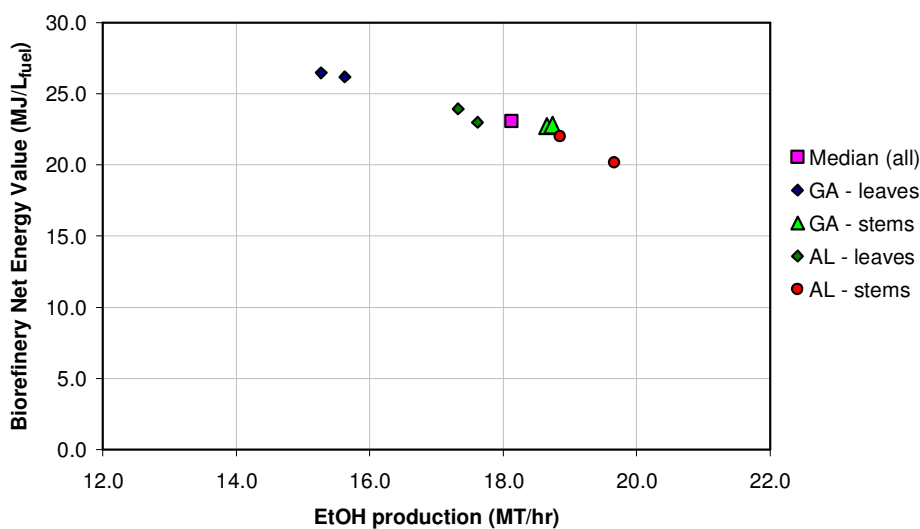


Figure 42: Biorefinery net energy value with respect to ethanol production (Case III-c).

Tables 60 - 61 present the steam demand and CO₂ emissions per sector for Case III-c. Once more, the purification section is the most energy intensive stage of the biorefinery.

Table 60: Steam requirements per sector (MT/hr) (Case III-c)

Variety	Lignin Content (%)	Pretreatment Section	Purification Section	Utilities Section
Median (all)	19.27	19.84	59.6	42.74
Median (Baldwin County, GA)	19.30	19.82	58.66	41.22
Median (Greene County, AL)	19.27	19.85	59.79	43.07
Genotype, Baldwin County, GA (leaves)	17.93	19.64	57.20	38.54
	18.79	19.81	56.89	38.76
Genotype, Baldwin County, GA (stems)	19.81	19.86	60.01	43.30
	20.24	19.89	60.05	43.28
Genotype, Greene County, AL (leaves)	19.34	19.99	58.68	42.59
	23.79	20.51	58.06	42.79
Genotype, Greene County, AL (stems)	17.09	19.52	60.39	42.89
	19.19	19.83	61.02	45.05

Table 61: CO₂ emissions per sector (MT/hr) (Case III-c)

Variety	Lignin Content (%)	Fermentation Section	Utilities Section	Auxiliary CHP Section
Median (all)	19.27	25.11	87.92	<i>not operating</i>
Median (Baldwin County, GA)	19.30	23.72	92.48	<i>not operating</i>
Median (Greene County, AL)	19.27	25.34	87.12	<i>not operating</i>
Genotype, Baldwin County, GA (leaves)	17.93	21.64	98.29	<i>not operating</i>
	18.79	21.15	99.23	<i>not operating</i>
Genotype, Baldwin County, GA (stems)	19.81	25.85	86.51	<i>not operating</i>
	20.24	25.98	86.94	<i>not operating</i>
Genotype, Greene County, AL (leaves)	19.34	24.40	87.19	<i>not operating</i>
	23.79	24.02	91.39	<i>not operating</i>
Genotype, Greene County, AL (stems)	17.09	26.11	84.56	0.80
	19.19	27.25	80.89	3.50

Sericea Lespedeza was the only variety where the data referred to crops stored in large round bales, according to the Biomass Feedstock Composition and Property Database. In all cases, the lignin content was significantly higher from the rest of the herbaceous crops examined, which justifies the lower ethanol production. Moreover, when Sericea Lespedeza was chosen as feedstock, the net energy values for the biorefinery were more than 40% higher than the corresponding values for corn stover, approximately 25% higher compared to switchgrass varieties, and only 10% greater than Big bluestem's.

Table 62: Sericea Lespedeza used as feedstock, w/ heat integration (Case III-d)

Carbohydrate Content (%)	Lignin Content (%)	Ethanol Production (MT/hr)	HP-steam Demand (MT/hr)	MP-steam Demand (MT/hr)	Natural Gas Demand (MT/hr)
53.88	28.47	16.16	(15.02)	(21.18)	0.00
54.95	24.09	16.72	(13.50)	(15.99)	0.00
52.35	25.20	15.77	(14.80)	(22.28)	0.00
56.76	24.43	17.34	(12.89)	(12.75)	0.00
57.17	24.43	17.43	(12.25)	(10.45)	0.00
51.60	24.89	15.67	(16.16)	(26.82)	0.00
50.16	30.36	14.82	(17.09)	(31.46)	0.00
56.31	27.45	16.98	(13.40)	(14.68)	0.00
48.75	28.65	14.39	(16.98)	(32.06)	0.00
53.25	28.83	15.93	(15.61)	(24.44)	0.00
52.15	26.65	15.71	(16.05)	(26.19)	0.00
49.44	30.93	14.59	(17.93)	(34.60)	0.00
57.29	27.61	17.29	(12.97)	(12.55)	0.00
55.07	30.12	16.44	(14.69)	(20.41)	0.00
57.78	28.26	17.40	(12.55)	(10.68)	0.00
52.74	31.95	15.61	(16.40)	(27.31)	0.00
53.38	31.93	15.80	(15.94)	(25.26)	0.00
50.73	31.61	14.95	(17.07)	(30.84)	0.00
56.11	28.89	16.81	(13.55)	(16.29)	0.00

Table 63: Metrics estimation (Case III-d)

Carbohydrate Content (%)	NEV (MJ/L_{fuel})	NER	Overall Efficiency
53.88	22.53	n/a	0.298
54.95	22.39	n/a	0.307
52.35	22.55	n/a	0.291
56.76	22.31	n/a	0.317
57.17	22.27	n/a	0.318
51.60	22.64	n/a	0.291
50.16	22.80	n/a	0.277
56.31	22.37	n/a	0.311
48.75	22.84	n/a	0.269
53.25	22.59	n/a	0.295
52.15	22.63	n/a	0.291
49.44	22.88	n/a	0.274
57.29	22.32	n/a	0.316
55.07	22.49	n/a	0.303
57.78	22.29	n/a	0.318
52.74	22.67	n/a	0.290
53.38	22.62	n/a	0.293
50.73	22.78	n/a	0.279
56.11	22.40	n/a	0.3084

The steam requirements and CO₂ emissions per sector for Case III-d are summarized in Tables 64 - 65.

Table 64: Steam requirements per sector (MT/hr) (Case III-d)

Lignin Content (%)	Pretreatment Section	Purification Section	Utilities Section
28.47	21.04	56.42	42.04
24.09	20.36	57.67	41.91
25.20	20.60	56.28	40.84
24.43	20.36	58.3	42.61
24.43	20.42	58.24	42.91
24.89	20.45	56.66	40.32
30.36	21.40	54.21	40.08
27.45	20.86	57.26	42.83
28.65	21.22	53.98	39.53
28.83	21.08	55.81	41.22
26.65	20.70	56.27	40.73
30.93	21.45	53.99	39.74
27.61	20.89	57.57	43.28
30.12	21.30	55.92	42.03
28.26	21.02	57.55	43.72
31.95	21.58	54.85	41.25
31.93	21.59	55.06	41.63
31.61	21.60	54.17	40.48
28.89	21.14	56.33	42.34

Table 65: CO₂ emissions per sector (MT/hr) (Case III-d)

Lignin Content (%)	Fermentation Section	Utilities Section	Auxiliary CHP Section
28.47	22.50	98.00	<i>not operating</i>
24.09	23.32	94.87	<i>not operating</i>
25.20	21.98	97.94	<i>not operating</i>
24.43	24.19	93.28	<i>not operating</i>
24.43	24.30	92.00	<i>not operating</i>
24.89	21.83	100.65	<i>not operating</i>
30.36	20.62	102.77	<i>not operating</i>
27.45	23.66	94.38	<i>not operating</i>
28.65	20.05	102.89	<i>not operating</i>
28.83	22.20	99.23	<i>not operating</i>
26.65	21.91	100.27	<i>not operating</i>
30.93	20.31	104.49	<i>not operating</i>
27.61	24.09	93.33	<i>not operating</i>
30.12	22.88	97.12	<i>not operating</i>
28.26	24.23	92.48	<i>not operating</i>
31.95	21.70	100.89	<i>not operating</i>
31.93	21.98	99.88	<i>not operating</i>
31.61	20.79	102.64	<i>not operating</i>
28.89	23.39	94.74	<i>not operating</i>

Taken as a whole, ethanol production has a linear dependence on the carbohydrate content of biomass feedstock, as depicted in Figure 43. The corresponding net energy values for each case are schematically represented in Figure 44.

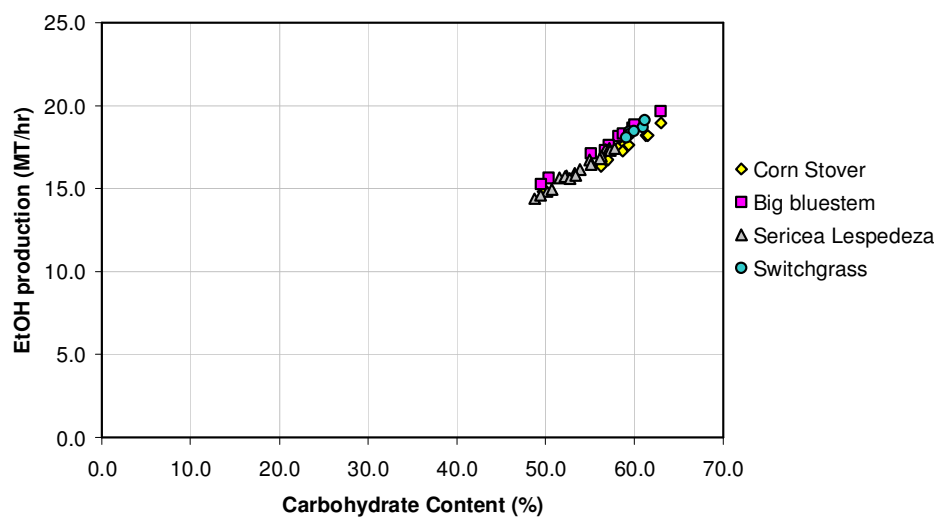


Figure 43: Ethanol production with respect to carbohydrate content for all herbaceous crops

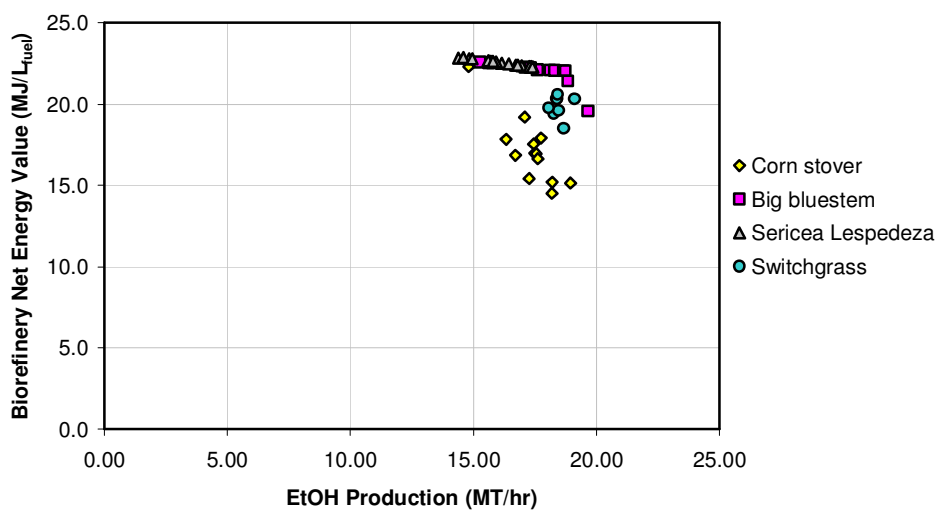


Figure 44: Biorefinery net energy values with respect to ethanol production for all herbaceous crops

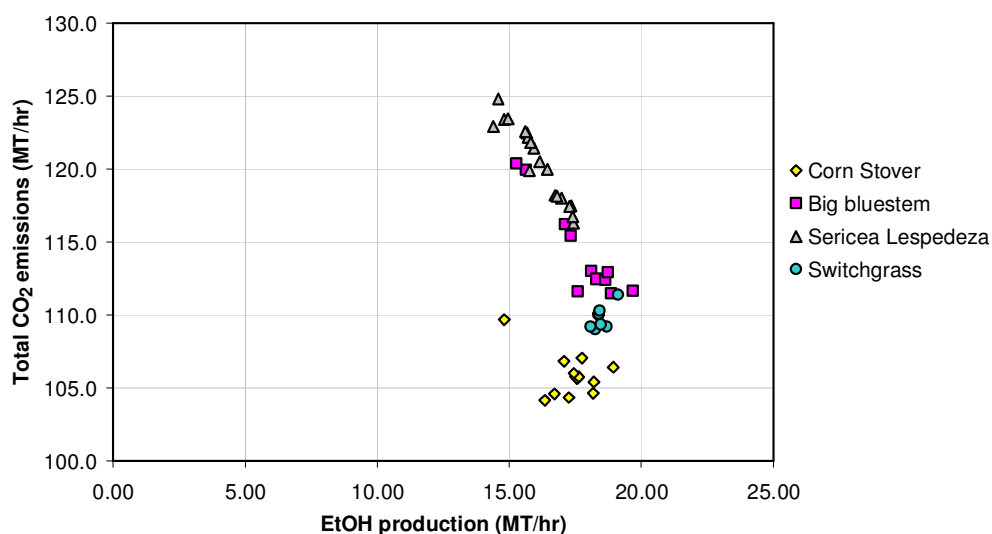


Figure 45: Total CO₂ emissions values with respect to ethanol production for all herbaceous crops

Table 66 is a comparative representation of the feedstock varieties, as obtained from the results of this section. The outcome indicates that Big bluestem is the optimum choice for ethanol production. It should be emphasized however, that this result only reflects the contribution of the biorefinery, and does not include contributions from the agricultural phase.

Table 66: Comparison between different varieties of feedstock (*) for ethanol production

Variety	Ethanol Production (MT/hr)	Natural Gas Demand (MT/hr)	CO ₂ emissions (MT/hr)	NEV (MJ/L _{fuel})	Overall Efficiency
Corn Stover	17.33	2.32	105.9	17.13	0.29
Big bluestem	17.72	0.16	114.4	21.90	0.32
Sericea Lespedeza	16.10	0.00	120.4	22.56	0.28
Switchgrass	18.49	1.10	109.8	19.80	0.32

(*) The compositions of the samples have been based on the mean compositions for each species.

If additional metrics are considered, for instance, the conversion of biomass to ethanol for a certain type of feedstock, or carbon efficiency, then we may obtain

additional results that strengthen the assumption that Big bluestem would be the optimum choice for biofuel production, in terms of carbon efficiency.

Apart from Big bluestem, switchgrass appears to be an attractive option, especially taking into account its lower environmental impact compared to the other biomass samples (Table 66).

Table 67: Comparison between different varieties of feedstock for ethanol production (II)

Variety	Ethanol Production (MT/hr)	Maximum (Theoretical) Ethanol Production (MT/hr)	Biomass to Ethanol Conversion (%)	Carbon Efficiency (%)
Corn Stover	17.33	28.03	61.83	41.60
Big bluestem	17.72	27.81	63.72	43.43
Sericea Lespedeza	16.10	25.69	62.67	41.93
Switchgrass	18.49	28.43	65.04	43.13

4.6. Effect of fuel used in the auxiliary CHP section

The results presented in the previous sections were obtained under the assumption that natural gas was used for additional steam and power production in the CHP unit. If natural gas is substituted with coal however, we observe a significant decrease in biorefinery's net energy values, combined with increased CO₂ emissions, when the auxiliary CHP unit is operating.

The coal sample selected for this case study was the Wyodak-Anderson coal. Its elemental composition is shown in Table 68. Table 69 includes results from the proximate analysis. Based on data collected from the Users Handbook for the Argonne

Premium Coal Samples, the coal's molecular type was estimated $C_{100}H_{85.6}O_{18}N_{1.28}S_{0.23}$ (MW = 1598.88 g/gmol), and its heating value 29.87 MJ/kg (12843 Btu/lb).

Table 68: Wyodak-Anderson coal – elemental analysis (wt. %)
(MAF: moisture- & ash-free, Dmmf: Dry, mineral matter free)

	Carbon	Hydrogen	Oxygen	Nitrogen	Sulfur	Chlorine
Dry	68.43	4.88	25.01	1.02	0.63	0.03
MAF	75.01	5.35	18.02	1.12	0.47	0.03
Dmmf	76.04	5.42	16.90	1.13	0.48	0.03

Table 69: Wyodak-Anderson coal – proximate analysis (wt. %)
(AR: as received)

	Fixed Carbon	Moisture	Ash	Volatile	Sulfur
AR	33.43	28.09	6.31	32.17	0.45
Dry	46.5	0.00	8.77	44.73	0.63

From the cases presented in Section 2.3.3, corn stover and switchgrass were the ones for which additional steam and power was unquestionably required for the operation of the biorefinery. Table 70 - Table 72 summarize the outcome for the case of corn stover (Case IV-a). The corresponding results for switchgrass are presented in Table 73 - Table 75.

Table 70: Corn stover used as feedstock, w/ integration (Case IV-a)

Carbohydrate Content (%)	Lignin Content (%)	Ethanol Production (MT/hr)	HP-steam Demand (MT/hr)	MP-steam Demand (MT/hr)	Coal Demand (MT/hr)
58.71	18.38	17.49	(3.15)	-19.24	6.57
56.82	17.69	17.08	(5.38)	-10.61	3.62
58.86	17.77	17.76	(4.30)	-15.87	5.42
49.74	18.19	14.81	(9.62)	(7.65)	0.00
58.72	17.39	17.56	(3.01)	-19.40	6.62
59.33	19.25	17.62	(2.84)	-20.68	7.06
58.17	17.12	17.45	(3.66)	-17.06	5.82
61.30	18.14	18.19	(0.44)	-29.56	10.09
57.03	19.68	16.72	(2.86)	-18.94	6.46
56.25	21.25	16.33	(3.49)	-15.09	5.15
58.72	18.96	17.26	(1.47)	-24.80	8.46
61.55	20.24	18.20	(1.35)	-26.89	9.18
62.98	18.59	18.94	(1.36)	-28.11	9.59

Table 71: Metrics estimation (Case IV-a)

Carbohydrate Content (%)	NEV (MJ/L _{fuel})	NER	Overall Efficiency
58.71	13.20	2.50	0.28
56.82	17.08	4.43	0.29
58.86	14.86	3.07	0.29
49.74	22.21	Inf	0.27
58.72	13.15	2.48	0.28
59.33	12.61	2.34	0.28
58.17	14.18	2.81	0.28
61.30	8.94	1.69	0.27
57.03	12.96	2.43	0.27
56.25	14.66	2.98	0.27
58.72	10.50	1.91	0.27
61.55	10.14	1.86	0.28
62.98	10.06	1.85	0.29

Table 72: CO₂ emissions per sector (MT/hr) (Case IV-a)

Lignin Content (%)	Fermentation Section	Utilities Section	Auxiliary CHP Section
18.38	24.27	75.02	11.85
17.69	23.70	79.54	6.53
17.77	24.63	77.06	9.78
18.19	20.56	89.14	<i>not operating</i>
17.39	24.37	74.73	11.95
19.25	24.46	74.31	12.73
17.12	24.22	76.05	10.50
18.14	25.23	69.43	18.20
19.68	23.18	75.02	11.65
21.25	22.67	76.39	9.28
18.96	23.94	72.03	15.27
20.24	25.27	71.07	16.56
18.59	26.26	70.66	17.32

Table 73: Switchgrass used as feedstock, w/ heat integration (Case IV-b)

Carbohydrate Content (%)	Lignin Content (%)	Ethanol Production (MT/hr)	HP-steam Demand (MT/hr)	MP-steam Demand (MT/hr)	Coal Demand (MT/hr)
59.47	17.99	18.39	(7.23)	-6.71	1.43
59.41	17.63	18.40	(7.21)	-6.79	1.45
59.45	18.05	18.43	(7.54)	-5.70	1.22
60.97	19.14	18.68	(5.39)	-14.19	3.03
59.47	17.74	18.27	(6.11)	-10.29	2.20
61.15	17.94	19.12	(7.60)	-7.02	1.50
59.94	17.77	18.47	(6.34)	-9.62	2.06
59.10	19.04	18.07	(6.58)	-8.87	1.89

Table 74: Metrics estimation (Case IV-b)

Carbohydrate Content (%)	NEV (MJ/L_{fuel})	NER	Overall Efficiency
59.47	19.10	7.52	0.32
59.41	19.06	7.44	0.32
59.45	19.55	8.88	0.32
60.97	15.91	3.61	0.31
59.47	17.50	4.87	0.31
61.15	19.06	7.47	0.33
59.94	17.84	5.27	0.32
59.10	18.10	5.60	0.31

Table 75: CO₂ emissions per sector (MT/hr) (Case IV-b)

Lignin Content (%)	Fermentation Section	Utilities Section	Auxiliary CHP Section
17.99	25.43	82.31	3.95
17.63	25.46	82.29	3.99
18.05	25.50	82.89	3.34
19.14	25.82	78.58	8.34
17.74	25.27	80.27	6.05
17.94	26.48	82.54	4.13
17.77	25.56	80.55	5.65
19.04	25.00	81.22	5.21

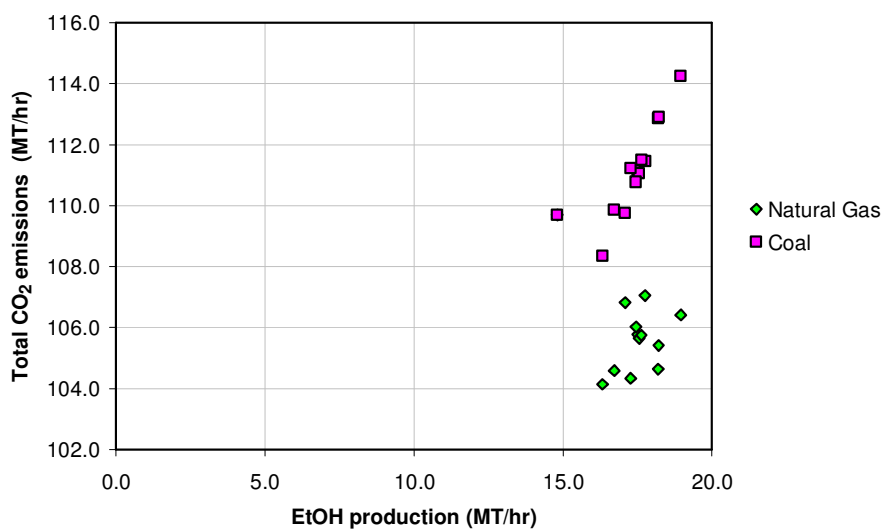


Figure 46: Effect of fuel input at CHP auxiliary unit on the total CO₂ emissions (corn stover)

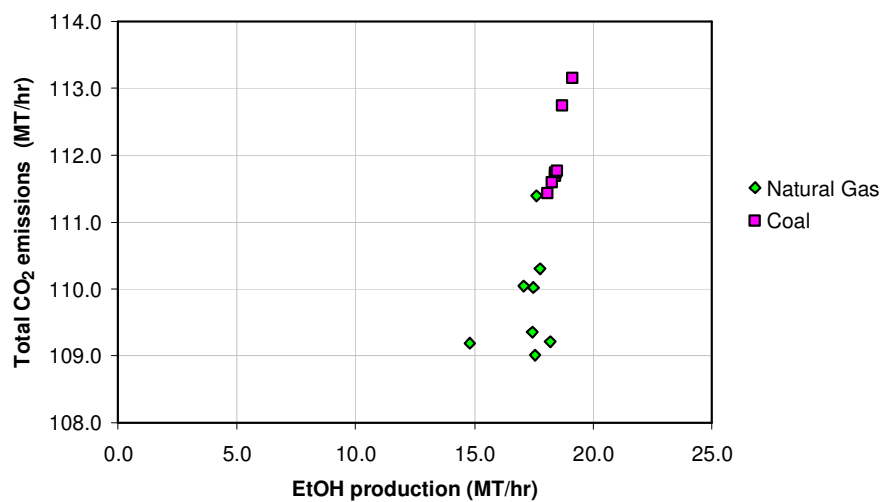


Figure 47: Effect of fuel input at CHP auxiliary unit on the total CO₂ emissions (switchgrass)

Based on the environmental impact of the two alternatives presented, natural gas should be the fuel that should be used for the operation of the biorefinery. This decision could be further supported when exploring the economic aspect for the two fuels: given the cost of natural gas for industrial use (\$2.7 \$/MMBtu, or \$0.02 \$/MT), and coal

(\$12.4/short tone, or \$13.7/MT), natural gas would be the optimal choice for the operation of the CHP unit.

4.7. Effect of conversion during enzymatic hydrolysis

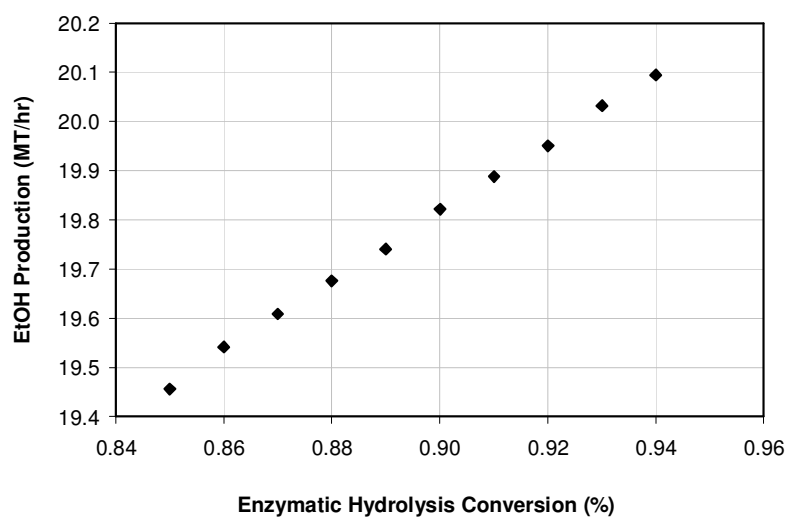
The effect of the conversion of cellulose to 6-carbon sugars was also studied more thoroughly. In the base-case scenario, 90% of the cellulose content of corn stover is converted to glucose. In the tables that follow, saccharification yield varies from 85% to 94%. The outcome is also depicted in Figure 48 - Figure 51.

Table 76: Effect of cellulose conversion during hydrolysis on ethanol production

Conversion (%)	EtOH Production (MT/hr)	HP-steam Demand (MT/hr)	MP-steam Demand (MT/hr)	Natural Gas Demand (MT/hr)
0.85	19.46	(6.49)	-11.50	1.41
0.86	19.54	(6.37)	-12.70	1.56
0.87	19.61	(6.28)	-12.81	1.57
0.88	19.68	(6.20)	-13.00	1.60
0.89	19.74	(6.11)	-13.10	1.61
0.90	19.82	(6.00)	-13.96	1.71
0.91	19.89	(5.91)	-14.12	1.73
0.92	19.95	(5.83)	-14.23	1.75
0.93	20.03	(5.71)	-15.45	1.90
0.94	20.10	(5.63)	-15.54	1.91

Table 77: Effect of cellulose conversion during hydrolysis at metrics estimation

Conversion (%)	Natural Gas Demand (MT/hr)	NEV (MJ/L _{fuel})	NER	Overall Efficiency
0.85	1.41	19.28	8.06	0.341
0.86	1.56	19.01	7.33	0.341
0.87	1.57	18.99	7.29	0.342
0.88	1.60	18.96	7.21	0.343
0.89	1.61	18.94	7.18	0.344
0.90	1.71	18.75	6.76	0.344
0.91	1.73	18.72	6.71	0.345
0.92	1.75	18.70	6.67	0.346
0.93	1.90	18.43	6.17	0.346
0.94	1.91	18.42	6.16	0.347

**Figure 48: Ethanol production with respect to cellulose conversion during hydrolysis**

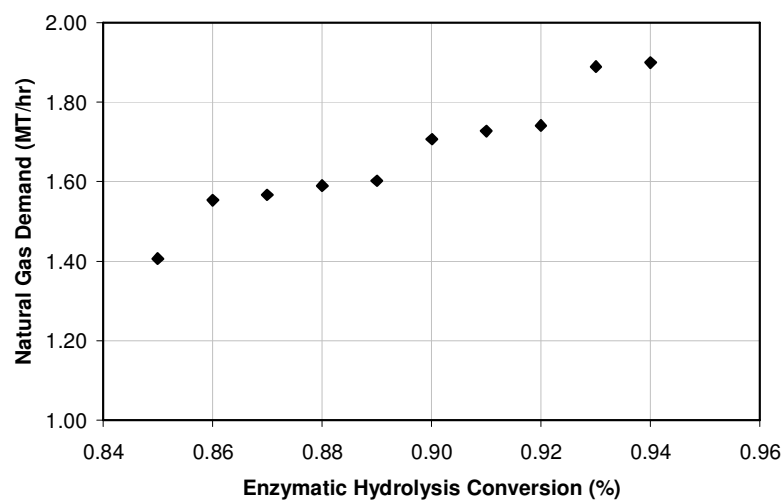


Figure 49: Natural gas demand with respect to cellulose conversion during hydrolysis

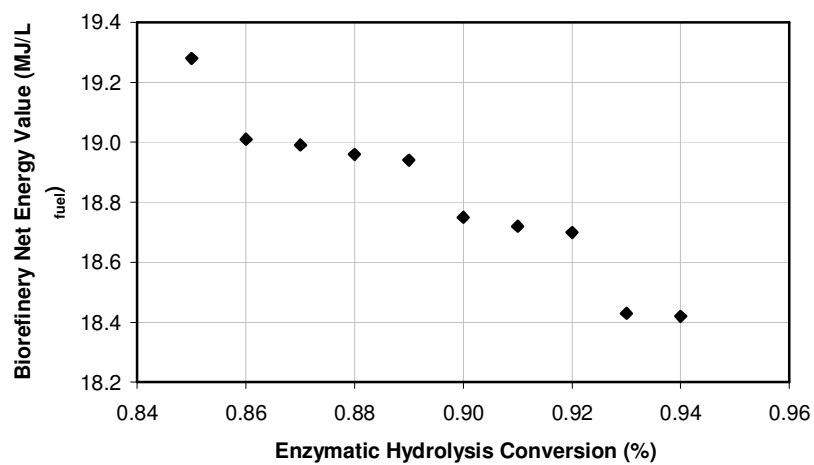


Figure 50: Biorefinery net energy value with respect to cellulose conversion during hydrolysis

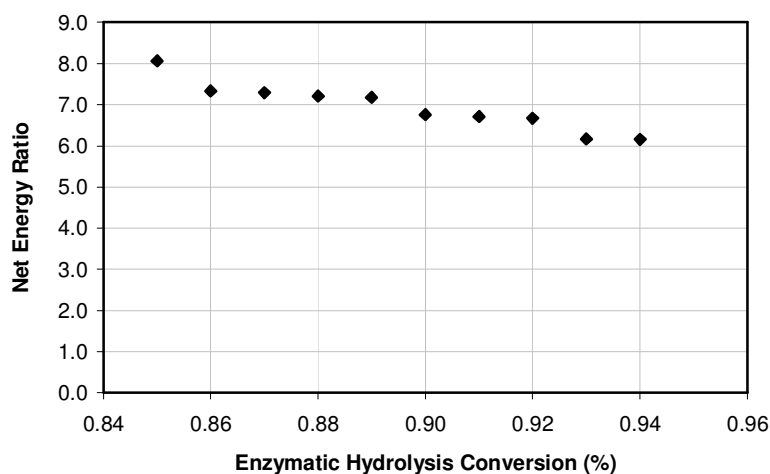


Figure 51: Net energy ratio with respect to cellulose conversion during saccharification

From the figures above, it can be deduced that increased conversion levels result in higher amounts of ethanol produced. However, the increased amount of final product (~3%) is accompanied a significantly greater natural gas demand (~25%). The increased natural gas requirement combined with the fact that the total amount of power and steam produced remains constant, leads to the lower values for the estimated metrics.

4.8. Effect of fermentation conversion

A systematic analysis of the effect of the conversion levels during fermentation was conducted. In the base-case scenario, where corn stover was used for ethanol production, the fermentation yields for glucose and xylose to ethanol were 95% each. Here, the conversion values varied from 90% to 99%. The simulation results are presented in Table 78 - Table 79. Note that the biomass composition is the same as in the base-case scenario described in Section 2.1 (lignin 19.24%, carbohydrates 63.73%).

Table 78: Effect of the fermentation conversion at ethanol production

Conversion (%)	EtOH Production (MT/hr)	HP-steam Demand (MT/hr)	MP-steam Demand (MT/hr)	Natural Gas Demand (MT/hr)
0.90	18.78	(6.99)	-8.55	1.05
0.91	18.99	(6.79)	-9.63	1.18
0.92	19.20	(6.59)	-10.71	1.32
0.93	19.41	(6.39)	-11.81	1.45
0.94	19.61	(6.20)	-12.88	1.58
0.95	19.82	(6.00)	-13.96	1.71
0.96	20.03	(5.80)	-15.04	1.85
0.97	20.24	(5.60)	-16.12	1.98
0.98	20.45	(5.37)	-17.17	2.11
0.99	20.66	(5.14)	-18.23	2.24

Table 79: Effect of the fermentation conversion at metrics estimation

Conversion (%)	Natural Gas Demand (MT/hr)	NEV (MJ/L _{fuel})	NER	Overall Efficiency
0.90	1.05	19.92	10.47	0.333
0.91	1.18	19.68	9.39	0.335
0.92	1.32	19.44	8.54	0.338
0.93	1.45	19.20	7.84	0.340
0.94	1.58	18.97	7.25	0.342
0.95	1.71	18.75	6.76	0.344
0.96	1.85	18.53	6.34	0.346
0.97	1.98	18.32	5.98	0.349
0.98	2.11	18.11	5.67	0.351
0.99	2.24	17.91	5.39	0.353

Figure 52 - Figure 55 are schematic representations of the aforementioned results.

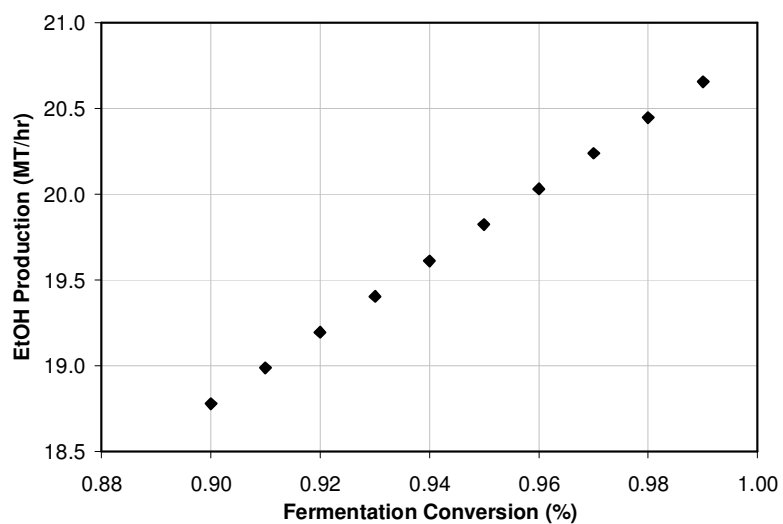


Figure 52: Ethanol production with respect to fermentation conversion, for constant biomass input

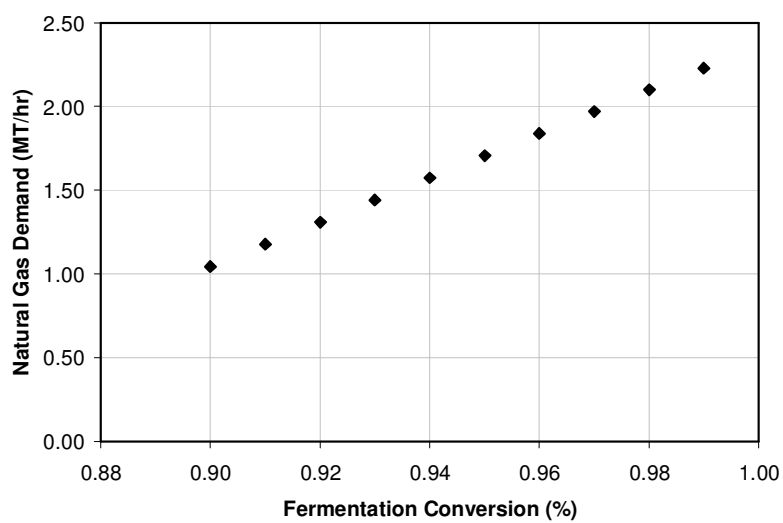


Figure 53: Natural gas demand with respect to fermentation conversion, for constant biomass input

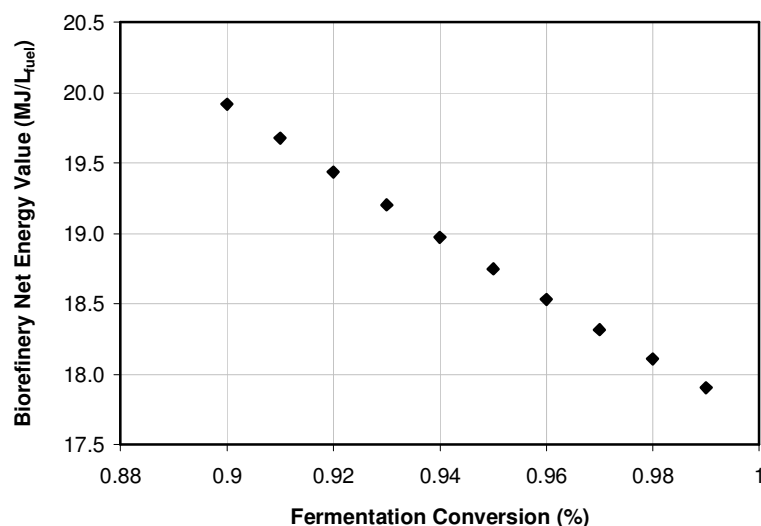


Figure 54: Biorefinery net energy value with respect to fermentation conversion, for constant biomass input

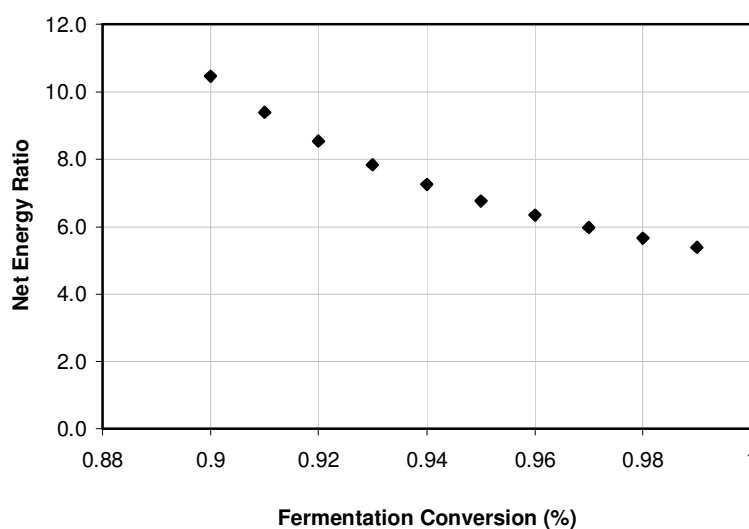


Figure 55: Net energy ratio with respect to fermentation conversion, for constant biomass input

The outcome above indicates that increased fermentation conversion, leads to higher ethanol production (~9.1%). However, the operation of the biorefinery requires more steam and power, which is translated into a significantly higher amount of natural gas to operate the auxiliary CHP unit (more than 50%).

4.9. Effect of heat integration

The effect of heat integration in the overall process has also been explored while varying the feedstock content. The comparative results for varying biomass content are depicted in Figure 56 - Figure 58 that follow.

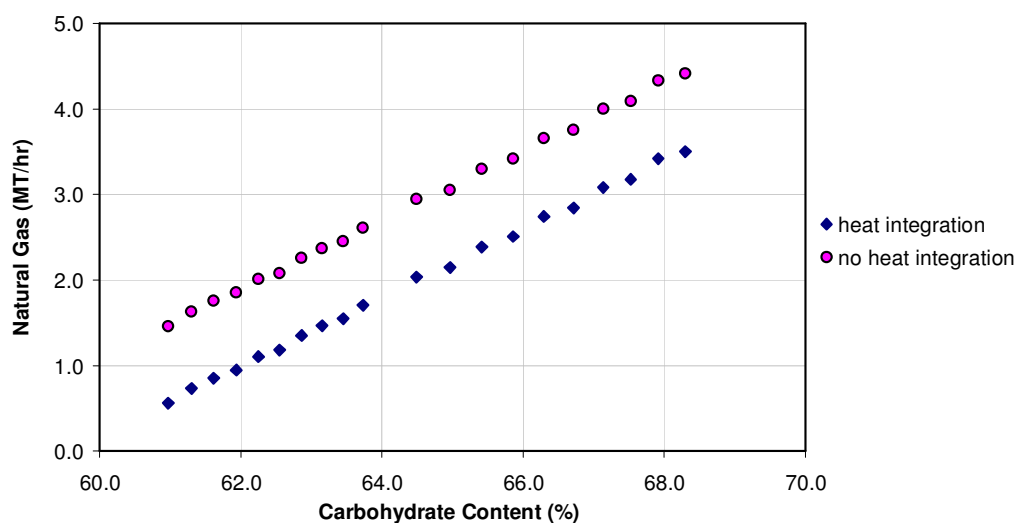


Figure 56: Natural gas requirements with respect to carbohydrate content of the biomass, for biorefinery operation with and without heat integration

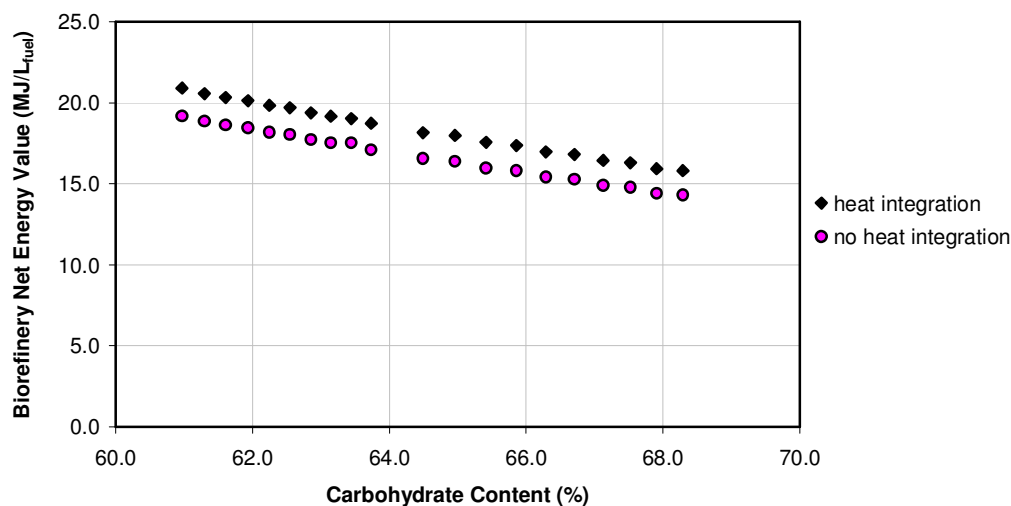


Figure 57: Biorefinery net energy value with respect to carbohydrate content of the biomass, for biorefinery operation with and without heat integration

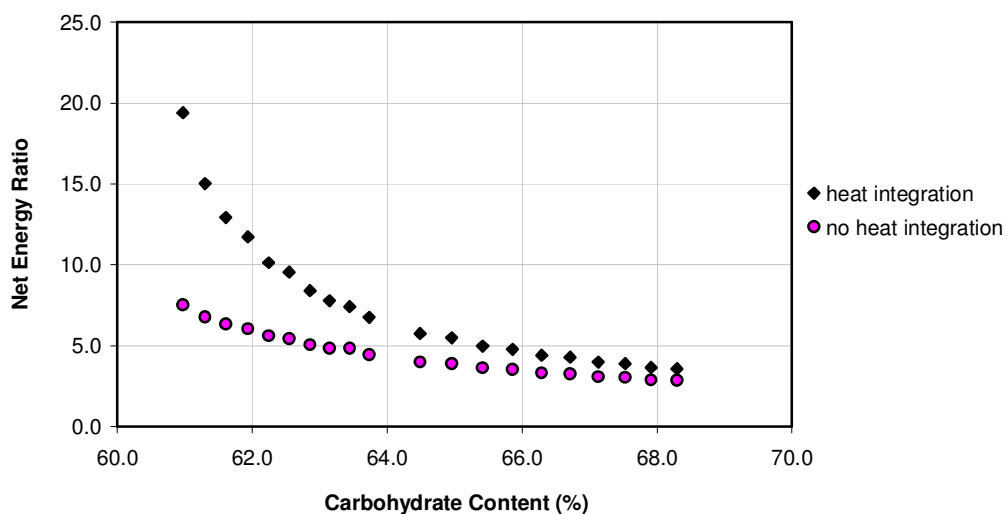


Figure 58: Net energy ratios with respect to carbohydrate content of the biomass, for biorefinery operation with and without heat integration

Without heat integration during the operation of the biorefinery, we would expect higher natural gas requirements for ethanol production, yielding in lower net energy values and net energy ratios, when increasing the carbohydrate content of the biomass (or decreasing lignin). The outcome is in accordance with the assumption, as shown in the plots above.

Chapter 5

Concluding Remarks and Future Directions

Based on published experimental data and technical studies, the work presented in this thesis incorporates and improves existing technologies for biofuel production. The core of our research was to provide a detailed and rigorous analysis of biofuel production in order to critically assess the validity of previous studies. The major contribution of this work was the development of a comprehensive simulation framework for the optimal design of biofuel production facilities using a system-based approach that considered all the critical components of a biorefinery. More specifically:

a) By incorporating rigorous reactor models into process simulation, we developed a comprehensive framework that can be used for the optimal design of biodiesel plants.

b) In bioethanol production, we explored the effect of feedstock composition on the overall process. Using cellulosic feedstock with varying cellulose, hemicellulose and lignin contents, we rigorously assessed how biomass composition affects the overall energy balance of the process. The findings point out a potential unintended consequence of efforts to develop genetically modified crops: increased ethanol yields may lower the net energy values of the biofuel and, consequently, increase its cost.

c) We also estimated the effect of the conversion levels during hydrolysis and fermentation in the overall process. Our simulation results illustrated the significant effect of these parameters on product yield, energy efficiency, and environmental impact.

Moreover, these findings underlined the importance of exploring and developing advanced technologies to improve ethanol yield and lower carbon dioxide emissions during the fermentation stage.

d) In order to meet the energy demands of the biorefineries, combined heat and power (CHP) units were integrated in the main process. For an ethanol plant, the main CHP unit operated with lignin and the insoluble solids of the biomass. If this unit did not produce sufficient amounts of steam and power, an auxiliary CHP unit was introduced that operated using natural gas or coal. For the base case of biodiesel production, the CHP unit used natural gas as its only fuel source. An additional scenario was explored, where an auxiliary CHP unit was integrated into the facility. The co-products of the main process (mainly glycerin) were fed to the auxiliary CHP to produce the steam and power necessary for the operation of the biorefinery thus, increasing the energy efficiency of biodiesel production.

e) Some of the scenarios simulated for biodiesel production included purification of the co-product (glycerin), fermentation for ethanol production, or glycerin's utilization for the operation of the CHP unit. The results indicated that the third case was the most beneficial, as it combined higher energy efficiency and lower emissions compared to the others.

The current framework could be further expanded. As a first step, future studies should carry out an economic analysis of the biorefinery that accounts for essential input

parameters: raw materials, capital and operating costs, and utility expenses. The economics of biofuel production can be analyzed for several combinations of feedstock, plant capacity, and technological improvements that may result in substantially lower production costs. The following are some of the points that should be considered for the economic analysis:

- The (fixed) capital cost of raw materials, reactors, separators, and all other units included in the design. For the raw materials, the quality of each component should be taken into account. For the pricing of the equipment, the cost will be based mainly on the size and manufacturing material of each unit. Data and empirical formulas to estimate the purchased and installed prices of the equipment can be obtained from standard sources (Walas, 1990, Peters *et al.*, 2002, Perry and Green, 1997).
- The (variable) operating cost of the process. The net cost of the utilities (cooling water, steam, electricity) will be estimated, depending on their quantity, and the quality of the steam. The revenue from the biofuel produced and the co-products should also be accounted for.

Since scale-up is a critical aspect during the design of a facility, we propose exploring the performance of different scenarios involving small- and large-scale facilities. Process integration will be of key importance when designing the production facilities. The heating, cooling, and power requirements of the units need to be taken into account, to ensure a rigorous design of energy and economically efficient systems.

Furthermore, consideration could be given to the water balance of the facility. Cooling water is essential for biofuel production process. Yet after its use, it needs to be discarded to the environment (in the case of cellulosic ethanol production, approximately $4.8 L_{\text{water}}/L_{\text{fuel}}$ are discarded to the environment). In our simulations a significant amount of water is recycled in the biorefinery, and used e.g. at the pretreatment section of the bioethanol production facility. Even though water balance was not accounted for in the work of this thesis, we tried to minimize the environmental impact by "disposing" it to the environment at an appropriate temperature (so that it wouldn't disturb the ecosystem of the area). A cooling tower was used to lower the temperature of the water. If more rigorous calculations on this topic are to be done, it should be taken into consideration that while water recycling reduces the cost of utilities, it increases the capital and the operational cost of the process as more units must be purchased and commissioned.

On the environmental aspect of the proposed future work, CO₂ provision would be of critical importance, particularly during the production of bioethanol. Carbon capture and storage (CCS) technologies usually involve chemical absorption of carbon dioxide. Various solvents have been proposed, with monoethanol amine (MEA) as the most used amine for the removal process (Singh *et al.*, 2003; Abu-Zahra *et al.*, 2007; Alie *et al.*, 2005). Other solvents proposed for CO₂ capture are potassium carbonate and chilled ammonia (Bai and Yeh, 1997; Yeh and Bai, 1999; Yeh *et al.*, 2005). To our knowledge, these technologies have been simulated, but so far, not integrated to bioethanol production process.

Finally, more rigorous models could be developed to estimate the energy requirements and subsequently, the cost of glycerol's fermentation, based on the metabolic model of glycerin's fermentation. Additional consideration could also be given to the separation of the components in the fermentation broth, as mentioned in earlier sections of this thesis.

.

References

1. *National Biodiesel Board* (www.biodiesel.org/).
2. *Ethanol Producer Magazine* (www.ethanolproducer.com/plant-list.jsp).
3. *GreenTech America* (www.greentechamerica.com).
4. *Argonne GREET Model*
(www.transportation.anl.gov/modeling_simulation/GREET).
5. *Biomass Feedstock Composition and Property Database*, National Renewable Energy Laboratory (www.eere.energy.gov/biomass/feedstock_databases.html).
6. *U.S. Department of Energy's Biomass Program Database*.
(www.afdc.energy.gov/biomass/progs/search1.cgi).
7. *National Renewable Energy Laboratory (NREL): Second biomass conference of the Americas: Energy, environment, agriculture, and industry. Portland, OR (1995).*
8. *Users Handbook for the Argonne Premium Coal Samples*
(www.anl.gov/PCS/report/part1.html).
9. Abu-Zahra, M.R.M., Schneiders, L.H.J. , Niederer, J.P.M., Feron, P.H.M., and Versteeg, G.F., "CO₂ capture from power plants: Part I. A parametric study of the technical performance based on monoethanolamine". *International Journal of Greenhouse Gas Control*, **1** (1): p. 37-46 (2007)
10. Aden, A., Ruth, M., Ibsen, K., Jechura, J., Neeves, K., Sheehan, J., and Wallace, B., *Lignocellulosic biomass to ethanol: Process design and economics utilizing co-current dilute acid prehydrolysis and enzymatic hydrolysis for corn stover*, National Renewable Energy Laboratory (2002).

11. Agarwal, A.K., "Biofuels (alcohols and biodiesel) applications as fuels for internal combustion engines". *Prog. Energ. Combust. Sci.*, **33**: p. 233-271 (2007)
12. Alie, C., Backham, L., Croiset, E., and Douglas, P.L. , "Simulation of CO₂ capture using MEA scrubbing: a flowsheet decomposition method". *Energy Conversion and Management*, **46** (3): p. 475-487 (2005)
13. Al-Zuhair, S., "Production of biodiesel by lipase-catalyzed transesterification of vegetable oils: a kinetic study". *Biotechnol. Progr.*, **21**: p. 1442-1448 (2005)
14. Aravindhakshan, S.C., Epplin, F.M., and Taliaferro, C.M., "Economics of switchgrass and miscanthus relative to coal as feedstock for generating electricity". *Biomass & Bioenergy*, **34** (9): p. 1375-1383 (2010)
15. AspenTech. [cited; Available from: <http://www.aspentech.com/>.
16. Ataei, S.A., and Vasheghani-Farahani, E., "In situ separation of lactic acid from fermentation broth using ion exchange resins". *Journal of Industrial Microbiology & Biotechnology for Biofuels*, **35** (11): p. 1229-1233 (2007)
17. Avila, A., Bula, A. Sanjuan, H. , "Kinetics of African palm olein transesterification with ethanol" (in Spanish)". *Interciencia – Caracas*, **33** (3): p. 232-236 (2008)
18. Bai, H.L., Yeh, A.C. , "Removal of CO₂ greenhouse gas by ammonia scrubbing". *Industrial & Engineering Chemistry Research*, **36** (6): p. 2490-2493 (1997)
19. Bambase, M.E., Nakamura, N., Tanaka, J., and Matsumura, M., "Kinetics of hydroxide-catalyzed methanolysis of crude sunflower oil for the production of fuel-grade methyl esters". *Journal of Chemical Technology and Biotechnology*, **82** (3): p. 273-280 (2007)

20. Barbosa, M., Beck, M., Fein, J., Potts, D., and Ingram, L., "Efficient fermentation of *Pinus* sp. acid hydrolysates by an ethanologenic strain of *Escherichia coli*". *Appl. Environ. Microbiol.*, **58** (4): p. 1382-1384 (1992)
21. Berg, J.M., "Biochemistry". 6th ed. New York: W.H. Freeman. 303-325 (2007)
22. Bikou, E., Louloudi, A., and Papayannakos, N., "The effect of water on the transesterification kinetics of cotton seed oil with ethanol". *Chem. Eng. Technol.*, **22**: p. 70-75 (1999)
23. Blankenship, R.E., Tiede, D.M., Barber, J., Brudvig, G.W., Fleming, G., Ghirardi, M., Gunner, M.R., Junge, W., et al., "Comparing Photosynthetic and Photovoltaic Efficiencies and Recognizing the Potential for Improvement". *Science*, **332** (6031): p. 805-809 (2011)
24. Boyce, M., "Handbook for cogeneration and combined cycle power plants". ASME Press (2002)
25. Brown, R., "Biorenewable resources: Engineering new products from agriculture". Iowa State Press (2003)
26. Butnar, I., Rodrigo, J., Gasol, C.M., and Castells, F., "Life-cycle assessment of electricity from biomass: Case studies of two biocrops in Spain". *Biomass & Bioenergy*, **34** (12): p. 1780-1788 (2010)
27. Caserini, S., Livio, S., Giugliano, M., Grosso, M., and Rigamonti, L., "LCA of domestic and centralized biomass combustion: The case of Lombardy (Italy)". *Biomass & Bioenergy*, **34** (4): p. 474-482 (2010)
28. Charusiri, W. and Vitidsant, T., "Kinetic study of used vegetable oil to liquid fuels over sulfated zirconia". *Energy & Fuels*, **19**: p. 1783-1789 (2005)

29. Cheryan, M., and Parekh, S.R., "Separation of glycerol and organic acids in model ethanol stillage by electrodialysis and precipitation". *Process Biochemistry*, **30** (1): p. 17-23 (1995)
30. Cho, A., "Energy's Tricky Tradeoffs". *Science*, **329** (5993): p. 786-787 (2010)
31. Chuck, G.S., Tobias, C., Sun, L., Kraemer, F., Li, C.L., Dibble, D., Arora, R., Bragg, J.N., et al., "Overexpression of the maize Corngrass1 microRNA prevents flowering, improves digestibility, and increases starch content of switchgrass". *Proceedings of the National Academy of Sciences of the United States of America*, **108** (42): p. 17550-17555 (2011)
32. Danielo, O., "An algae-based fuel". *Biofutur*, **255** (2005)
33. Darnoko, D. and Cheryan, M., "Kinetics of palm oil transesterification in a batch reactor". *Journal of the American Oil Chemists Society*, **77** (12): p. 1263-1267 (2000)
34. Darnoko, D. and Cheryan, M., "Continuous production of palm methyl esters". *Journal of the American Oil Chemists Society*, **77** (12): p. 1269-1272 (2000)
35. Demirbas, A., Kara, H. , "New options for conversion of vegetable oils to alternative fuels". *Energy Sources Part A: Recovery, Utilization & Environmental Effects*, (Taylor & Francis Ltd): p. 619-626 (2006)
36. Diasakou, M., Louloudi, A., and Papayannakos, N., "Kinetics of the non-catalytic transesterification of soybean oil". *Fuel*, **77** (12): p. 1297-1302 (1998)
37. Edgar, T., Himmelblau, D., and Lasdon, L., "Optimization of chemical processes". 2nd ed. ed. M.-H.C.E. Series (2001)
38. Fargione, J., Hill, J., Tilman, D., Polasky, S., and Hawthorne, P., "Land clearing and the biofuel carbon debt". *Science*, **319** (5867): p. 1235-1238 (2008)

39. Farrell, A.E., Plevin, R.J., Turner, B.T., Jones, A.D., O'Hare, M., and Kammen, D.M., "Ethanol can contribute to energy and environmental goals". *Science*, **311** (5760): p. 506-8 (2006)
40. Foon, C.S., May, C.Y., Ngan, Ma Ah, Hock, C.C., "Kinetic study on transesterification of palm oil". *Journal of Oil Palm Research* **16** (2): p. 19-29 (2004)
41. França, B.B., Pinto, F.M., Pessoa, F.L., Uller, A.M., "Liquid-liquid equilibria for castor oil biodiesel + glycerol + alcohol". *J. Chem. Eng. Data*, (54): p. 2359-2364 (2009)
42. Freedman, B., Butterfield, R., and Pryde, E., "Transesterification kinetics of soybean oil". *JAOCs*, **63** (10): p. 1375-1380 (1986)
43. Fu, C.X., Mielenz, J.R., Xiao, X.R., Ge, Y.X., Hamilton, C.Y., Rodriguez, M., Chen, F., Foston, M., et al., "Genetic manipulation of lignin reduces recalcitrance and improves ethanol production from switchgrass". *Proceedings of the National Academy of Sciences of the United States of America*, **108** (9): p. 3803-3808 (2011)
44. Fu, C.X., Xiao, X.R., Xi, Y.J., Ge, Y.X., Chen, F., Bouton, J., Dixon, R.A., and Wang, Z.Y., "Downregulation of Cinnamyl Alcohol Dehydrogenase (CAD) Leads to Improved Saccharification Efficiency in Switchgrass". *Bioenergy Research*, **4** (3): p. 153-164 (2011)
45. Galbe, M., and Zacchi, G., "A review of the production of ethanol from softwood". *Appl. Microbiol. Biotechnol.* , **59**: p. 618–628 (2002)
46. Gallagher, E., "The Gallagher Review of the indirect effects of biofuels production". Renewable Fuels Agency (2008)

47. Gonzalez, R., Murarka, A., Dharmadi, Y., Yazdani, S.S., "A new model for the anaerobic fermentation of glycerol in enteric bacteria: trunk and auxiliary pathways in *Escherichia coli*". *Metabolic Engineering*, **10** (5): p. 234-245 (2008)
48. Haas, M.J., McAloon, A.J., Yee, W.C., Foglia, T.A., "A process model to estimate biodiesel production costs". *Bioresource Technology*, **97**: p. 671-678 (2006)
49. Hábová, V., Melzoch, K., Rychtera, M., Sekavová, B., "Electrodialysis as a useful technique for lactic acid separation from a model solution and a fermentation broth". *Desalination, Elsevier*, (2004)
50. Hamelinck, C., van Hooijdonk, G., and Faaij, A., "Ethanol from lignocellulosic biomass: techno-economic performance in short-, middle- and long-term". *Biomass & Bioenergy*, **28**: p. 384-410 (2005)
51. Harding, K.G., Dennis, J.S., von Blottnitz, H., and Harrison, S.T.L., "A life-cycle comparison between inorganic and biological catalysis for the production of biodiesel". *Journal of Cleaner Production*, **16** (13): p. 1368-1378 (2008)
52. Harington, T., Hossain, M.M., "Extraction of lactic acid into sunflower oil and its recovery into an aqueous solution ". *Desalination*, **218**: p. 287-296 (2008)
53. Harwood, H.J., "Oleochemicals as a fuel: Mechanical and economic feasibility". *JAACS*, **61**: p. 315-324 (1984)
54. He, H., Sun, S., Wang, T., and Zhu, S., "Transesterification kinetics of soybean oil for production of biodiesel in supercritical methanol". *JAACS*, **84**: p. 399-404 (2007)
55. Hill, J., Nelson, E., Tilman, D., Polasky, S., and Tiffany, D., "Environmental, economic, and energetic costs and benefits of biodiesel and ethanol biofuels". *PNAS*, **103** (30): p. 11206-11210 (2006)

56. Hinman, N., Schell, D., Riley, J., Bergeron, P., and Walter, P., "Preliminary estimate of the cost of ethanol production for SSF technology". *Applied Biochemistry and Biotechnology*, **34/35**: p. 639-649 (1992)
57. Hohenstein, W. and Wright, L., "Biomass Energy Production in the United States: An Overview". *Biomass and Bioenergy*, **6**: p. 161-173 (1994)
58. Horton, G., Rivers, D., and Emert, G., "Preparation of cellulose for enzymatic conversion". *Ind. Eng. Chem. Prod. Res. Dev.*, **19**: p. 422-429 (1980)
59. Humbird, D., Davis, R., Tao, L., Kinchin, C., Hsu, D., and Aden, A., *Process design and economics for biochemical conversion of lignocellulosic biomass to ethanol*, NREL/TP-5100-47764. National Renewable Energy Laboratory (2011).
60. Jansri, S., Ratanawilai, S.B., Allen, M.L., Prateepchaikul, G., "Kinetics of methyl ester production from mixed crude palm oil by using acid-alkali catalyst". *Fuel Processing Technology*, **92** (8) (2011)
61. Kang, S.H., and Chang Y.K., "Removal of organic acid salts from simulated fermentation broth containing succinate by nanof". *J. Memb. Sci.*, **246** (1): p. 49-57 (2005)
62. Kapilakarn, K. and Peugtong, A., "A comparison of costs of biodiesel production from transesterification". *International Energy Journal*, **8**: p. 1-6 (2007)
63. Karmee, S., Chandna, D., Ravi, R., and Chadha, A., "Kinetics of base-catalyzed transesterification of triglycerides from Pongamia oil". *JAOCs*, **83** (10): p. 873-877 (2006)

64. Khan, A., Labrie, J., and McKeown, J., "Electron beam irradiation pretreatment and enzymatic saccharification of used newsprint and paper mill wastes". *Rad. Phys. Chem.*, **29** (2): p. 117-120 (1987)
65. Kim, Y.H., Moon, S.H., "Lactic acid recovery from fermentation broth using one-stage electrodialysis". *Journal of Chemical Technology & Biotechnology*, **76** (2): p. 169-178 (2001)
66. Knothe, G., Krahl, J., and Gerpen, J.v., "The biodiesel handbook". AOCS Press (2005)
67. Komers, K., Skopal, F., Stloukal, R., and Machek, J., "Kinetics and mechanism of the KOH-catalyzed methanolysis of rapeseed oil for biodiesel production". *Eur. J. Lipid Sci. Technol.*, **104**: p. 728-737 (2002)
68. Kumar, P., Barrett, D.M., Delwiche, M.J., and Stroeve, P., "Methods for Pretreatment of Lignocellulosic Biomass for Efficient Hydrolysis and Biofuel Production". *Industrial & Engineering Chemistry Research* **48** (8): p. 3713-3729 (2009)
69. Kusdiana, D. and Saka, S., "Kinetics of transesterification in rapeseed oil to biodiesel fuel as treated in supercritical methanol". *Fuel*, **80**: p. 693-698 (2001)
70. Kusdiana, D. and Saka, S., "Methyl esterification of free fatty acids of rapeseed oil as treated in supercritical methanol". *Journal of Chemical Engineering of Japan*, **34** (3): p. 383-387 (2001)
71. Kwiatkowski, J.R., McAloon, A.J., Taylor, F., Johnston, D.B., "Modeling the process and costs of fuel ethanol production by the corn dry-grind process". *Industrial Crops and Products*, **23**: p. 288-296 (2006)

72. Lamsal, B.P., Wang, H., Johnson, L.A., "Effect of corn preparation methods on dry-grind ethanol production by granular starch hydrolysis and partitioning of spent beer solids". *Bioresource Technology*, **102**: p. 6680–6686 (2011)
73. Liang, Y.C., May, C.Y., Foon, C.S., Ngan, M.A., Chuah, C.H., and Basiron, Y., "The effect of natural and synthetic antioxidants on the oxidative stability of palm diesel". *Fuel*, **85** (5-6): p. 867-870 (2006)
74. Liebig, M.A., Schmer, M.R., Vogel, K.P., and Mitchell, R.B., "Soil Carbon Storage by Switchgrass Grown for Bioenergy". *Bioenergy Research*, **1** (3-4): p. 215-222 (2008)
75. Lin, Y. and Tanaka, S., "Ethanol fermentation from biomass resources: current state and prospects". *Appl. Microbiol. Biotechnol.*, **69**: p. 627-642 (2006)
76. Lu, J., Deng, Li, Zhao, R., Zhang, R., Wang, F., Tan, T., "Pretreatment of immobilized *Candida* sp. 99-125 lipase to improve its methanol tolerance for biodiesel production", *J. of Mol. Catalysis B: Enzymatic*, **62** (1): p. 15-18 (2010)
77. Lynd, L., "Overview and evaluation of fuel ethanol from cellulosic biomass: Technology, economics, the environment, and policy". *Annu. Rev. Energy Environ.*, **21**: p. 403-65 (1996)
78. Lynd, L., Elander, R., and Wyman, C., "Likely features and costs of mature biomass ethanol technology". *Applied Biochemistry and Biotechnology*, **57/58**: p. 741-761 (1996)
79. Lynd, L.R., Laser, M.S., Brandsby, D., Dale, B.E., Davison, B., Hamilton, R., Himmel, M., Keller, M., et al., "How biotech can transform biofuels". *Nature Biotechnology*, **26** (2): p. 169-172 (2008)

80. Ma, F. and Hanna, M., "Biodiesel production: a review". *Bioresource Technology*, **70**: p. 1-15 (1999)
81. Mani, S., Sokhansanj, S., Tagore, S., and Turhollow, A.F., "Techno-economic analysis of using corn stover to supply heat and power to a corn ethanol plant - Part 2: Cost of heat and power generation systems". *Biomass & Bioenergy*, **34** (3): p. 356-364 (2010)
82. May, C.Y., Liang, Y.C., Foon, C.S., Ngan, M.A., Chuah, C.H., and Basiron, Y., "Key fuel properties of palm oil alkyl esters". *Fuel*, **84** (12-13): p. 1717-1720 (2005)
83. McAloon, A., Taylor, F., Yee, W., Ibsen, K., and Wooley, R., "Determining the cost of producing ethanol from corn starch and lignocellulosic feedstocks". ed. N.R.E.L.-T. Report. NREL/TR-580-28893 (2000)
84. Mesquita, F.M., Feitosa, F.X., Sombra, N.E., de Santiago-Aguiar, R.S. and de Sant'Ana, H.B., "Liquid-liquid equilibrium for ternary mixtures of biodiesel (soybean or sunflower) + glycerol + ethanol at different temperatures". *J. Chem. Eng. Data*, (56): p. 4061–4067 (2011)
85. Morris, D., "The carbohydrate economy, biofuels and the net energy debate". Institute for Local Self-Reliance (ILSR) (2005)
86. Mousdale, D., "Biofuels: Biotechnology, chemistry, and sustainable development". CRC Press (2008)
87. Murarka, A., Dharmadi, Y., Yazdani, S.S., Gonzalez R., "Fermentative utilization of glycerol by *Escherichia coli* and its implications for the production of fuels and chemicals". *Applied and Environmental Microbiology*, **74** (4): p. 1124-1135 (2008)

88. Nouredдини, H. and Zhu, D., "Kinetics of transesterification of soybean oil". *JAACS*, **74** (11): p. 1457-1463 (1997)
89. Novozymes. [Available from: <http://www.novozymes.com>].
90. Olofsson, K., Bertilsson, M., and Lidén, G., "A short review on SSF - an interesting process option for ethanol production from lignocellulosic feedstocks". *Biotechnology for Biofuels*, **1** (7) (2008)
91. Omota, F., Dimian, A., and Blik, A., "Fatty acid esterification by reactive distillation: Part 2 - kinetics-based design for sulphated zirconia catalysts". *Chemical Engineering Science*, **58**: p. 3175-3185 (2003)
92. Ooshima, H., Aso, K., Harano, Y., and Yamamoto, T., "Microwave treatment of cellulosic materials for their enzymatic hydrolysis". *Biotech. Lett.*, **6** (5): p. 289-294 (1984)
93. Padukone, N., Evans, K., McMillan, J., and Wyman, C., "Characterization of recombinant E. coli ATCC 11303 (pLOI 297) in the conversion of cellulose and xylose to ethanol". *Appl. Microbiol. Biotechnol.*, **43**: p. 850-855 (1995)
94. Palmer, M., Downing, M., Kaufmann, R., Patzek, T., Farrell, A., Plevin, R., Turner, B., Jones, A., et al., "Energy returns on ethanol production". *Science*, **312** (5781): p. 1746 - 1748 (2006)
95. Patzek, T., "Thermodynamics of the corn-ethanol biofuel cycle". *Crit. Rev. Plant Sci.*, **23** (6): p. 519-567 (2004)
96. Patzek, T.W. and Pimentel, D., "Thermodynamics of energy production from biomass". *Critical Reviews in Plant Sciences*, **24** (5-6): p. 327-364 (2005)

97. Perrin, R., Vogel, K., Schmer, M., and Mitchell, R., "Farm-scale production cost of switchgrass for biomass". *Bioenergy Research*, **1** (1): p. 91-97 (2008)
98. Perry, R.H., Green, D.W., "Perry's Chemical Engineers' Handbook". 7th ed. McGraw-Hill (1997)
99. Peters M., T.K., West R., "Plant design and economics for chemical engineers". 5th ed. McGraw-Hill Science/Engineering/Math (2002)
100. Pimentel, D. and Patzek, T., "Ethanol production using corn, switchgrass, and wood; biodiesel production using soybean and sunflower". *Natural Resources Research*, **14** (1): p. 65-76 (2005)
101. Pimentel, D. and Patzek, T., "Green plants, fossil fuels, and now biofuels". *Bioscience*, **56** (11): p. 875-875 (2006)
102. Pimentel, D., Patzek, T., and Cecil, G., "Ethanol production: Energy, economic, and environmental losses". *Reviews of Environmental Contamination and Toxicology*, Vol 189, **189**: p. 25-41 (2007)
103. Pimentel, D., Patzek, T., Siegert, F., Giampietro, M., and Haberl, H., "Biofuel in question". *New Scientist*, **197** (2639): p. 18-18 (2008)
104. Pimentel, D. and Patzek, T.W., "Ethanol production using corn, switchgrass, and wood; Biodiesel production using soybean and sunflower". *Natural Resources Research*, **14** (1): p. 65-76 (2005)
105. Pitt, W.W.J., Haag, G.L., Lee, D.D., "Recovery of ethanol from fermentation broths using selective sorption-desorption". *Biotechnol. Bioeng.*, **25** (1): p. 123-131 (1983)
106. Predojevic, Z.J., "The production of biodiesel from waste frying oils: a comparison of different purification steps". *Fuel*, **87**: p. 3522-3528 (2008)

107. Ragauskas, A.J., Williams, C.K., Davison, B.H., Britovsek, G., Cairney, J., Eckert, C.A., Frederick, W.J., Hallett, J.P., et al., "The path forward for biofuels and biomaterials". *Science*, **311** (5760): p. 484-489 (2006)
108. Richard, T.L., "Challenges in scaling up biofuels infrastructure". *Science*, **329** (5993): p. 793-796 (2010)
109. Robertson, G.P., Dale, V.H., Doering, O.C., Hamburg, S.P., Melillo, J.M., Wander, M.M., Parton, W.J., Adler, P.R., et al., "Agriculture - Sustainable biofuels Redux". *Science*, **322** (5898): p. 49-50 (2008)
110. Rootzen, J.M., Berndes, G., Ravindranath, N.H., Somashekar, H.I., Murthy, I.K., Sudha, P., and Ostwald, M., "Carbon sequestration versus bioenergy: A case study from South India exploring the relative land-use efficiency of two options for climate change mitigation". *Biomass & Bioenergy*, **34** (1): p. 116-123 (2010)
111. Ropars, M., Marchal, R., Pourquie, J., and Vandecasteele, J. , "Large-scale enzymatic hydrolysis of agricultural lignocellulosic biomass. Part 1: Pretreatment procedures ". *Biores. Technol.*, **42**: p. 197-204 (1992)
112. Rubin, E.M., "Genomics of cellulosic biofuels". *Nature*, **454** (7206): p. 841-845 (2008)
113. Saka, S. and Kusdiana, D., "Biodiesel fuel from rapeseed oil as prepared in supercritical methanol". *Fuel*, **80** (2): p. 225-231 (2001)
114. Schmer, M.R., Vogel, K.P., Mitchell, R.B., and Perrin, R.K., "Net energy of cellulosic ethanol from switchgrass". *Proceedings of the National Academy of Sciences of the United States of America*, **105** (2): p. 464-469 (2008)

115. Searchinger, T., Heimlich, R., Houghton, R., Dong, F., Elobeid, A., Fabiosa, J., Tokgoz, S., Hayes, D., and Yu, T., "Use of U.S. croplands for biofuels increases greenhouse gases through emissions from land use change". *Scienceexpress*, **319** (5867): p. 1238-1240 (2008)
116. Shay, E.G., "Diesel fuel from vegetable oils - status and opportunities". *Biomass & Bioenergy*, **4**: p. 227-242 (1993)
117. Sheehan, J., Camobreco, V., Duffield, J., Graboski, M., and Shapouri, H., "Life cycle inventory of biodiesel and petroleum diesel for use in an urban bus". National Renewable Energy Laboratory - Final Report. NREL/SR-580-24089 (1998)
118. Singh, D., E. Croiset, P.L. Douglas, and Douglas, M.A., "Techno-economic study of CO₂ capture from an existing coal-fired power plant: MEA scrubbing vs. O₂/CO₂ recycle combustion". *Energy Conversion and Management*, **44** (19): p. 3073-3091 (2003)
119. Somerville, C., Youngs, H., Taylor, C., Davis, S.C., and Long, S.P., "Feedstocks for Lignocellulosic Biofuels". *Science*, **329** (5993): p. 790-792 (2010)
120. Speight, J., "Synthetic fuels handbook: Properties, process, and performance". McGraw-Hill (2008)
121. Sun, Y. and Cheng, J., "Hydrolysis of lignocellulosic materials for ethanol production: a review". *Bioresource Technology*, **83** (1): p. 1-11 (2002)
122. Tilman, D., Hill, J., and Lehman, C., "Carbon-negative biofuels from low-input high-diversity grassland biomass". *Science*, **314** (5805): p. 1598-1600 (2006)

123. Tilman, D., Hill, J., and Lehman, C., "Response to comment on "Carbon-negative biofuels from low-input high-diversity grassland biomass"". *Science*, **316** (5831): p. 1567 (2007)
124. Timmons, D. and Mejia, C.V., "Biomass energy from wood chips: Diesel fuel dependence?" *Biomass & Bioenergy*, **34** (9): p. 1419-1425 (2010)
125. Tock, L., Gassner, M., and Marechal, F., "Thermochemical production of liquid fuels from biomass: Thermo-economic modeling, process design and process integration analysis". *Biomass & Bioenergy*, **34** (12): p. 1838-1854 (2010)
126. Turner, T.L., "Modeling and simulation of reaction kinetics for biodiesel production". MS Thesis, Department of Mechanical Engineering, North Carolina State University (2005)
127. Van Gerpen, J., "Biodiesel processing and production". *Fuel Processing Technology*, (86): p. 1097– 1107 (2005)
128. Vane, L.M., "Separation technologies for the recovery and dehydration of alcohols from fermentation broths". *Biofuels, Bioprod. Bioref.*, **2**: p. 553–588 (2008)
138. Vicente, G., Martinez, M., Aracil, J., and Esteban, A., "Kinetics of sunflower oil methanolysis". *Ind. Eng. Chem. Res.*, **44**: p. 5447-5454 (2005)
139. Walas, S.M., "Chemical Process Equipment - Selection and Design". Elsevier (1990)
140. Wang, L., Du, W., Liu, D., Li, L., Dai, N., "Lipase-catalyzed biodiesel production from soybean oil deodorizer distillate with absorbent present in tert-butanol system". *J. Mol. Catal. B. Enzym.*, **43** (1–4): p. 29–32 (2006)

141. Wang, M., *Development and use of GREET 1.6 fuel-cycle model for transportation fuels and vehicle technologies*, Technical Report ANL/ESD/TM-163. Argonne National Laboratory (2001).
142. Wang, Z.Y., Fu, C.X., Mielenz, J., Xiao, X.R., Ge, Y.X., Hamilton, C.Y., and Bouton, J., "Redesigning lignocellulosic feedstocks: Genetic modification of lignin biosynthesis significantly improves ethanol production in switchgrass". *In Vitro Cellular & Developmental Biology-Animal*, **47**: p. S23-S23 (2011)
143. Wayman, M. and Parekh, S., "SO₂ hydrolysis for high yield ethanol production from biomass". *Applied Biochemistry and Biotechnology*, **17**: p. 33-43 (1988)
144. Wayman, M., Seagrave, C., and Parekh, S., "Ethanol fermentation by *Pichia stipitis* of combined pentose and hexose sugars from lignocellulosics prehydrolyzed by SO₂ and enzymatically saccharified". *Proc. Biochem.*, **22**: p. 55-59 (1987)
145. Wright, L. and Turhollow, A., "Switchgrass selection as a "model" bioenergy crop: A history of the process". *Biomass & Bioenergy*, **34** (6): p. 851-868 (2010)
146. Wyman, C., "Handbook on bioethanol: Production and utilization". Applied Energy Technology Series (1996)
147. Wyman, C., "Biomass ethanol: Technical progress, opportunities, and commercial challenges". *Annu. Rev. Energy Environ.*, **24**: p. 189-226 (1999)
148. Wyman, C., "What is (and is not) vital to advancing cellulosic ethanol". *Trends in Biotechnology*, **25** (4): p. 153-157 (2007)
149. Yazdani, S.S., Mattam, A.J., and Gonzalez, R., *Fuel and chemical production from glycerol, a biodiesel waste product*, in *Biofuels from agricultural wastes and*

- byproducts*, H. Blaschek, Ezeji, T., and Scheffran, J., Editor. 2010, Blackwell Publishing, Ames, IA.
150. Yeh, A.C., Bai, H.L., "Comparison of ammonia and monoethanolamine solvents to reduce CO₂ greenhouse gas emissions. " *Science of the Total Environment*, **228** ((2-3)): p. 121-133 (1999)
 151. Yeh, J.T., Resnik, K.P., Rygle, K., and Pennline, H.W., "Semi-batch absorption and regeneration studies for CO₂ capture by aqueous ammonia". *Fuel Processing Technology*, **86** ((14-15)): p. 1533-1546 (2005)
 152. Zhang, Y., "Design and economic assessment of biodiesel production from waste cooking oil". M.A.Sc. Thesis, Department of Chemical Engineering, University of Ottawa (2002)
 153. Zhang, Y., Dubé, M.A., McLean, D.D., and Kates, M., "Biodiesel production from waste cooking oil: 1. Process design and technology assessment". *Bioresource Technology*, **89** (1): p. 1-16 (2003)
 154. Zhang, Y., Dubé, M.A., McLean, D.D., and Kates, M., "Biodiesel production from waste cooking oil: 2. Economic assessment and sensitivity analysis". *Bioresource Technology*, **90**: p. 229-240 (2003)
 155. Zhou, H., Lu, H., Liang, B., "Solubility of multicomponent systems in the biodiesel production by transesterification of *Jatropha curcas* L. oil with methanol". *J. Chem. Eng. Data*, (51): p. 1130-1135 (2006)

Appendix A

Below are the results of the simulation for biodiesel production, using a single continuous stirred tank reactor, and obtaining glycerin of 80% purity.

Input Materials	(kg/hr)
HCl	10.60
Water	185.76
Methanol	411.15
NaOCH ₃	13.27
Soybean Oil	4250.16
Sodium Hydroxide	1.80
TOTAL	4872.74

Heat Transfer Agent	Total Heat Transfer Agent Demand (kg/h)
MP-Steam	2509.15
HP-Steam	1994.59
CT Water	53980.58
CT Water2	13727.18
CT Water3	69.01
Cooling Adjust	56120.17

Total Power Demand (kWh/hr)
112.03

Stream Name	Soybean Oil	S-130	S-106	S-103
Source	INPUT	P1	Storage Tank 3	P4
Destination	P1	Storage Tank 3	P4	HX1
Stream Properties				
Temperature (°C)	25.00	25.08	25.08	25.16
Pressure (bar)	1.01	4.46	1.01	4.46
Density (g/L)	898.80	898.80	898.80	898.80
Component Flowrates (kg/h averaged)				
Soybean Oil	4250.16	4250.16	4250.16	4250.16
TOTAL (kg/h)	4250.16	4250.16	4250.16	4250.16

Stream Name	S-131	Catalyst	S-128	S-110
Source	HX1	INPUT	P2	Storage Tank 2
Destination	REACTOR 1	P2	Storage Tank 2	P5
Stream Properties				
Temperature (°C)	60.00		25.00	25.07
Pressure (bar)	4.46		1.01	4.46
Density (g/L)	898.80		925.50	925.43
Component Flowrates (kg/h averaged)				
Methanol	0.00		39.80	39.80
NaOCH ₃	0.00		13.27	13.27
Soybean Oil	4250.16		0.00	0.00
TOTAL (kg/h)	4250.16		53.07	53.07

Stream Name	S-127	Methanol	S-125	NAOH
Source	P5	INPUT	P3	INPUT
Destination	Mixer1	P3	Storage Tank 1	P11
Stream Properties				
Temperature (°C)	25.14	25.00	25.07	25.00
Pressure (bar)	4.46	1.01	4.46	1.01
Density (g/L)	925.36	789.61	789.54	1913.35
Component Flowrates (kg/h averaged)				
Methanol	39.80	371.34	371.34	0.00
NaOCH ₃	13.27	0.00	0.00	0.00
Sodium Hydroxid	0.00	0.00	0.00	1.80
TOTAL (kg/h)	53.07	371.34	371.34	1.80

Stream Name	S-141	WATER	HCL	S-145
Source	P11	INPUT	INPUT	Mixer2
Destination	MIXING3	Mixer2	Mixer2	MIXING1
Stream Properties				
Temperature (°C)	25.04	25.00	25.00	25.00
Pressure (bar)	4.46	1.01	1.01	1.01
Density (g/L)	1913.33	994.70	4.25	94.57
Component Flowrates (kg/h averaged)				
HCl	0.00	0.00	2.47	2.47
Sodium Hydroxid	1.80	0.00	0.00	0.00
Water	0.00	166.08	4.59	170.67
TOTAL (kg/h)	1.80	166.08	7.07	173.15

Stream Name	S-122	REMEOH	S-118	S-132
Source	HX5	MEOH DISTILL	MEOH DISTILL	P15 Storage Tank 1
Destination	MEOH DISTILL	P15	P18	
Stream Properties				
Temperature (°C)	80.56	64.44	102.44	64.52
Pressure (bar)	4.46	1.01	1.01	4.46
Density (g/L)	17.27	751.82	1023.74	751.75
Component Flowrates (kg/h averaged)				
Biodiesel	0.72	0.00	0.72	0.00
Glycerin	332.65	0.00	332.65	0.00
HCl	0.29	0.00	0.29	0.00
Methanol	507.90	507.75	0.05	507.75
Sodium Chloride	16.13	0.00	16.13	0.00
Soybean Oil	0.01	0.00	0.01	0.00
Water	970.35	0.10	970.25	0.10
TOTAL (kg/h)	1828.04	507.85	1320.09	507.85

Stream Name	S-101	S-126	S-107	S-104
Source	Storage Tank 1	P6	Mixer1	REACTOR1
Destination	P6	Mixer1	REACTOR1	CFUGE1
Stream Properties				
Temperature (°C)	47.86	47.94	46.75	60.25
Pressure (bar)	1.01	4.46	4.46	4.46
Density (g/L)	767.71	767.64	775.35	882.67
Component Flowrates (kg/h averaged)				
Biodiesel	0.00	0.00	0.00	3580.37
Glycerin	0.00	0.00	0.00	370.69
Methanol	879.09	879.09	918.90	532.03
NaOCH ₃	0.00	0.00	13.27	13.27
Soybean Oil	0.00	0.00	0.00	685.98
Water	0.10	0.10	0.10	0.10
TOTAL (kg/h)	879.19	879.19	932.26	5182.42

Stream Name	S-102	S-146	S-114	S-147
Source	CFUGE 1	CFUGE 1	P17	P18
Destination	MIXING1	P17	MIXING2	H2O DISTILL
Stream Properties				
Temperature (°C)	25.00	25.00	25.06	102.48
Pressure (bar)	1.01	1.01	4.46	4.46
Density (g/L)	873.15	1031.21	1031.16	3.50
Component Flowrates (kg/h averaged)				
Biodiesel	3580.01	0.36	0.36	0.72
Glycerin	22.24	348.45	348.45	332.65
HCl	0.00	0.00	0.00	0.29
Methanol	319.22	212.81	212.81	0.05
NaOCH ₃	7.96	5.31	5.31	0.00
Sodium Chloride	0.00	0.00	0.00	16.13
Soybean Oil	685.29	0.69	0.69	0.01
Water	0.06	0.04	0.04	970.25
TOTAL (kg/h)	4614.77	567.65	567.65	1320.09

Stream Name	RWATER	S-137	S-111	S-119
Source	H2O DISTILL	H2O DISTILL	HX9	MIXING1
Destination	HX9	P13	MIXING1	CFUGE 3
Stream Properties				
Activity (U/ml)	0.00	0.00	0.00	0.00
Temperature (°C)	100.00	127.74	60.00	35.20
Pressure (bar)	1.01	1.01	1.01	1.01
Density (g/L)	918.95	1150.64	981.94	892.24
Component Flowrates (kg/h averaged)				
Biodiesel	0.00	0.72	0.00	3580.01
Glycerin	0.03	332.61	0.03	22.28
HCl	0.00	0.29	0.00	0.00
Methanol	0.05	0.00	0.05	321.44
NaOCH ₃	0.00	0.00	0.00	4.30
Sodium Chloride	0.00	16.13	0.00	3.96
Soybean Oil	0.00	0.01	0.00	685.29
Water	889.72	80.53	889.72	1060.45
TOTAL (kg/h)	889.81	430.28	889.81	5677.73

Stream Name	S-112	S-105	HCl2	S-115
Source	CFUGE 3	CFUGE 3	INPUT	MIXING 2
Destination	HX4	MIXING 2	MIXING 2	P10
Stream Properties				
Temperature (°C)	25.00	25.00	25.00	25.01
Pressure (bar)	1.01	1.01	1.01	1.01
Density (g/L)	879.45	942.32	4.25	586.85
Component Flowrates (kg/h averaged)				
Biodiesel	3579.65	0.36	0.00	0.72
Glycerin	1.11	21.16	0.00	369.61
HCl	0.00	0.00	8.13	1.93
Methanol	31.79	289.65	0.00	507.90
NaOCH ₃	0.43	3.87	0.00	0.00
Sodium Chloride	0.40	3.57	0.00	13.49
Soybean Oil	616.76	68.53	0.00	69.22
Water	106.05	954.41	15.09	969.54
TOTAL (kg/h)	4336.19	1341.54	23.22	1932.40

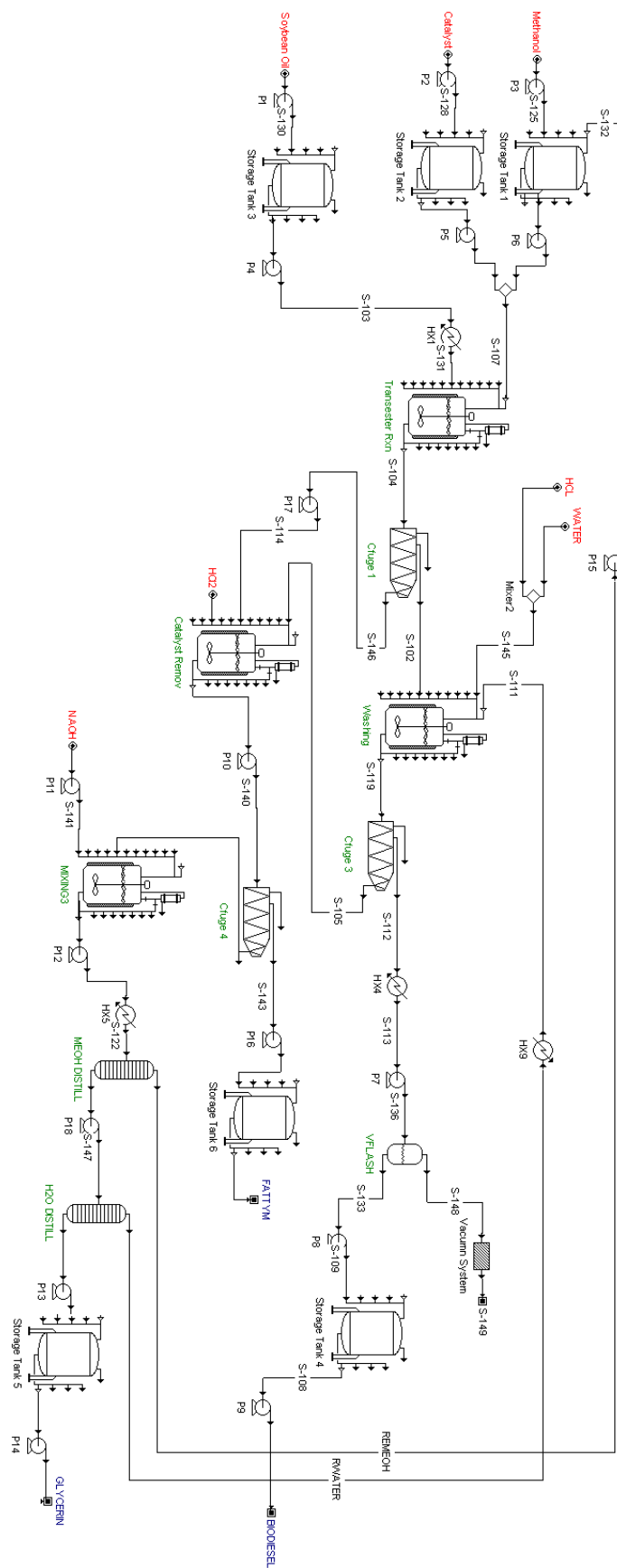
Stream Name	S-140	S-143	S-117	S-116
Source	P10	CFUGE 4	CFUGE 4	MIXING 3
Destination	CFUGE 4	P16	MIXING 3	P12
Stream Properties				
Temperature (°C)	25.06	25.00	25.00	25.00
Pressure (bar)	4.46	1.01	1.01	1.01
Density (g/L)	843.44	998.02	573.14	876.16
Component Flowrates (kg/h averaged)				
Biodiesel	0.72	0.00	0.72	0.72
Glycerin	369.61	36.96	332.65	332.65
HCl	1.93	0.00	1.93	0.29
Methanol	507.90	0.00	507.90	507.90
Sodium Chloride	13.49	0.00	13.49	16.13
Soybean Oil	69.22	69.21	0.01	0.01
Water	969.54	0.00	969.54	970.35
TOTAL (kg/h)	1932.40	106.17	1826.23	1828.04

Stream Name	S-142	S-129	S-139	GLYCERIN
Source	P12	P13	Storage Tank 5	P14
Destination	HX5	Storage Tank 5	P14	OUTPUT
Stream Properties				
Temperature (°C)		25.05	127.79	127.79
Pressure (bar)		4.46	4.46	1.01
Density (g/L)		944.01	12.75	2.92
Component Flowrates (kg/h averaged)				
Biodiesel		0.72	0.72	0.72
Glycerin		332.65	332.61	332.61
HCl		0.29	0.29	0.29
Methanol		507.90	0.00	0.00
Sodium Chloride		16.13	16.13	16.13
Soybean Oil		0.01	0.01	0.01
Water		970.35	80.53	80.53
TOTAL (kg/h)	1828.04	430.28	430.28	430.28

Stream Name	S-144	FATTYM	S-113	S-136
Source	P16	Storage Tank 6	HX4	P7
Destination	Storage Tank 6	OUTPUT	P7	Flash
Stream Properties				
Temperature (°C)		25.07	25.07	101.67
Pressure (bar)		4.46	1.01	1.01
Density (g/L)		998.01	998.01	20.02
Component Flowrates (kg/h averaged)				
Biodiesel		0.00	0.00	3579.65
Glycerin		36.96	36.96	1.11
Methanol		0.00	0.00	31.79
NaOCH ₃		0.00	0.00	0.43
Sodium Chloride		0.00	0.00	0.40
Soybean Oil		69.21	69.21	616.76
Water		0.00	0.00	106.05
TOTAL (kg/h)	106.17	106.17	4336.19	4336.19

Stream Name	S-148	S-133	S-109	S-108
Source	Flash	Flash	P8	Storage Tank 4
Destination	Vacumn Sys	P8	Storage Tank 4	P9
Stream Properties				
Temperature (°C)		120.00	120.00	120.10
Pressure (bar)		0.00	0.00	3.45
Density (g/L)		0.01	875.11	693.31
Component Flowrates (kg/h averaged)				
Biodiesel		0.00	3579.65	3579.65
Glycerin		0.01	1.11	1.11
Methanol		31.64	0.15	0.15
NaOCH ₃		0.00	0.43	0.43
Sodium Chloride		0.00	0.40	0.40
Soybean Oil		462.57	154.19	154.19
Water		104.14	1.91	1.91
TOTAL (kg/h)		598.36	3737.83	3737.83

Stream Name	BIODIESEL	S-149
Source	P9	Vacumn Sys
Destination	OUTPUT	OUTPUT
Stream Properties		
Activity (U/ml)	0.00	0.00
Temperature (°C)	25.10	120.00
Pressure (bar)	4.46	0.00
Density (g/L)	875.14	0.01
Component Flowrates (kg/h averaged)		
Biodiesel	3579.65	0.00
Glycerin	1.11	0.01
Methanol	0.15	31.64
NaOCH ₃	0.43	0.00
Sodium Chloride	0.40	0.00
Soybean Oil	154.19	462.57
Water	1.91	104.14
TOTAL (kg/h)	3737.83	598.36



Appendix B

Below are the results of the simulation for biodiesel production, using two continuous stirred tank reactors (case III), and obtaining glycerin of 80% purity.

Input Material	(kg/hr)
HCl	10.60
Water	185.76
Methanol	453.44
NaOCH ₃	13.27
Soybean Oil	4,250.16
Sodium Hydroxide	1.80
TOTAL	4,915.03

Heat Transfer Agent	Total Heat Transfer Agent Demand (kg/h)
MP-Steam	2,716.35
HP-Steam	2,150.53
CT Water	57,227.31
CT Water2	13,728.04
CT Water3	69.01
Cooling Adjust	72,634.02

Total Power Demand (kWh/hr)
109.39

Stream Name	Soybean Oil	S-130	S-106	S-103
Source	INPUT	P1	Storage Tank 3	P4
Destination	P1	Storage Tank 3	P4	HX1
Stream Properties				
Temperature (°C)	25.00	25.08	25.08	25.16
Pressure (bar)	1.01	4.46	1.01	4.46
Density (g/L)	898.80	898.80	898.80	898.80
Component Flowrates (kg/h averaged)				
Soybean Oil	4250.16	4250.16	4250.16	4250.16
TOTAL (kg/h)	4250.16	4250.16	4250.16	4250.16

Stream Name	S-131	Catalyst	S-128	S-110
Source	HX1	INPUT	P2	Storage Tank 2
Destination	REACTOR1	P2	Storage Tank 2	P5
Stream Properties				
Temperature (°C)	60.00	25.00	25.07	25.07
Pressure (bar)	4.46	1.01	4.46	1.01
Density (g/L)	898.80	925.50	925.43	925.43
Component Flowrates (kg/h averaged)				
Methanol	0.00	39.80	39.80	39.80
NaOCH ₃	0.00	13.27	13.27	13.27
Soybean Oil	4250.16	0.00	0.00	0.00
TOTAL (kg/h)	4250.16	53.07	53.07	53.07

Stream Name	S-127	Methanol	S-125	NAOH
Source	P5	INPUT	P3	INPUT
Destination	Mixer1	P3	Storage Tank 1	P11
Stream Properties				
Temperature (°C)	25.14	25.00	25.07	25.00
Pressure (bar)	4.46	1.01	4.46	1.01
Density (g/L)	925.36	789.61	789.54	1913.35
Component Flowrates (kg/h averaged)				
Methanol	39.80	413.64	413.64	0.00
NaOCH ₃	13.27	0.00	0.00	0.00
Sodium Hydroxid	0.00	0.00	0.00	1.80
TOTAL (kg/h)	53.07	413.64	413.64	1.80

Stream Name	S-141	WATER	HCL	S-145
Source	P11	INPUT	INPUT	Mixer2
Destination	MIXING3	Mixer2	Mixer2	MIXING1
Stream Properties				
Temperature (°C)	25.04	25.00	25.00	25.00
Pressure (bar)	4.46	1.01	1.01	1.01
Density (g/L)	1913.33	994.70	4.25	94.57
Component Flowrates (kg/h averaged)				
HCl	0.00	0.00	2.47	2.47
Sodium Hydroxid	1.80	0.00	0.00	0.00
Water	0.00	166.08	4.59	170.67
TOTAL (kg/h)	1.80	166.08	7.07	173.15

Stream Name	S-122	REMEOH	S-118	S-132
Source	HX5	MEOH DISTILL	MEOH DISTILL	P15
Destination	MEOH DISTILL	P15	P18	Storage Tank 1
Stream Properties				
Temperature (°C)	80.56	64.44	102.44	64.52
Pressure (bar)	4.46	1.01	1.01	4.46
Density (g/L)	16.36	751.82	1029.30	751.74
Component Flowrates (kg/h averaged)				
Biodiesel	1.17	0.00	1.17	0.00
Glycerin	378.36	0.00	378.36	0.00
HCl	0.10	0.00	0.10	0.00
Methanol	568.19	568.00	0.06	568.00
Sodium Chloride	16.44	0.00	16.44	0.00
Soybean Oil	0.00	0.00	0.00	0.00
Water	970.36	0.10	970.26	0.10
TOTAL (kg/h)	1934.61	568.10	1366.39	568.10

Stream Name	S-101	S-126	S-123	S-120
Source	Storage Tank 1	P6	Mixer1	P-1
Destination	P6	Mixer1	P-1 REACTOR2	
Stream Properties				
Activity (U/ml)	0.00	0.00	0.00	0.00
Temperature (°C)	47.90	47.98	46.91	46.91
Pressure (bar)	1.01	4.46	4.46	4.46
Density (g/L)	767.67	767.60	774.54	774.54
Component Flowrates (kg/h averaged)				
Methanol	981.64	981.64	1021.44	102.14
NaOCH ₃	0.00	0.00	13.27	1.33
Water	0.10	0.10	0.10	0.01
TOTAL (kg/h)	981.73	981.73	1034.80	103.48

Stream Name	S-107	S-104	S-102	S-146
Source	P-1	REACTOR1	CFUGE1	CFUGE1
Destination	REACTOR1	CFUGE1	HX2	P17
Stream Properties				
Temperature (°C)	46.91	60.29	25.00	25.00
Pressure (bar)	4.46	4.46	1.01	1.01
Density (g/L)	774.54	882.53	873.06	1030.68
Component Flowrates (kg/h averaged)				
Biodiesel	0.00	3580.37	3580.01	0.36
Glycerin	0.00	370.69	22.24	348.45
Methanol	919.30	532.43	319.46	212.97
NaOCH ₃	11.94	11.94	7.16	4.78
Soybean Oil	0.00	685.98	685.29	0.69
Water	0.09	0.09	0.05	0.04
TOTAL (kg/h)	931.32	5181.48	4614.21	567.27

Stream Name	S-124	S-134	S-138	S-135
Source	HX2	REACTOR2	CFUGE2	CFUGE2
Destination	REACTOR2	CFUGE2	MIXING1	Mixing 2
Stream Properties				
Temperature (°C)	60.00	59.60	59.60	59.60
Pressure (bar)	1.01	1.01	1.01	1.01
Density (g/L)	870.05	869.11	869.12	868.92
Component Flowrates (kg/h averaged)				
Biodiesel	3580.01	4061.89	4061.48	0.41
Glycerin	22.24	72.13	4.33	67.80
Methanol	319.46	369.53	221.72	147.81
NaOCH ₃	7.16	8.49	5.10	3.40
Soybean Oil	685.29	205.59	205.38	0.21
Water	0.05	0.06	0.04	0.03
TOTAL (kg/h)	4614.21	4717.69	4498.04	219.65

Stream Name	S-147	RWATER	S-137	S-111
Source	P18	H2O DISTILL	H2O DISTILL	HX9
Destination	H2O DISTILL	HX9	P13	MIXING1
Stream Properties				
Activity (U/ml)	0.00	0.00	0.00	0.00
Temperature (°C)	102.48	100.00	127.74	60.00
Pressure (bar)	4.46	1.01	1.01	1.01
Density (g/L)	3.62	913.52	1156.38	981.94
Component Flowrates (kg/h averaged)				
Biodiesel	1.17	0.00	1.17	0.00
Glycerin	378.36	0.04	378.32	0.04
HCl	0.10	0.00	0.10	0.00
Methanol	0.06	0.06	0.00	0.06
Sodium Chloride	16.44	0.00	16.44	0.00
Soybean Oil	0.00	0.00	0.00	0.00
Water	970.26	889.73	80.53	889.73
TOTAL (kg/h)	1366.39	889.83	476.56	889.83

Stream Name	S-119	S-112	S-105	S-114
Source	MIXING1	CFUGE3	CFUGE3	P17
Destination	CFUGE3	HX4	Mixing 2	Mixing 2
Stream Properties				
Temperature (°C)	57.71	25.00	25.00	25.06
Pressure (bar)	1.01	1.01	1.01	4.46
Density (g/L)	888.80	877.11	953.36	1030.63
Component Flowrates (kg/h averaged)				
Biodiesel	4061.48	4061.08	0.41	0.36
Glycerin	4.37	0.22	4.15	348.45
Methanol	223.95	22.15	201.80	212.97
NaOCH ₃	1.43	0.14	1.29	4.78
Sodium Chloride	3.96	0.40	3.57	0.00
Soybean Oil	205.38	184.84	20.54	0.69
Water	1060.44	106.04	954.40	0.04
TOTAL (kg/h)	5561.01	4374.87	1186.14	567.27

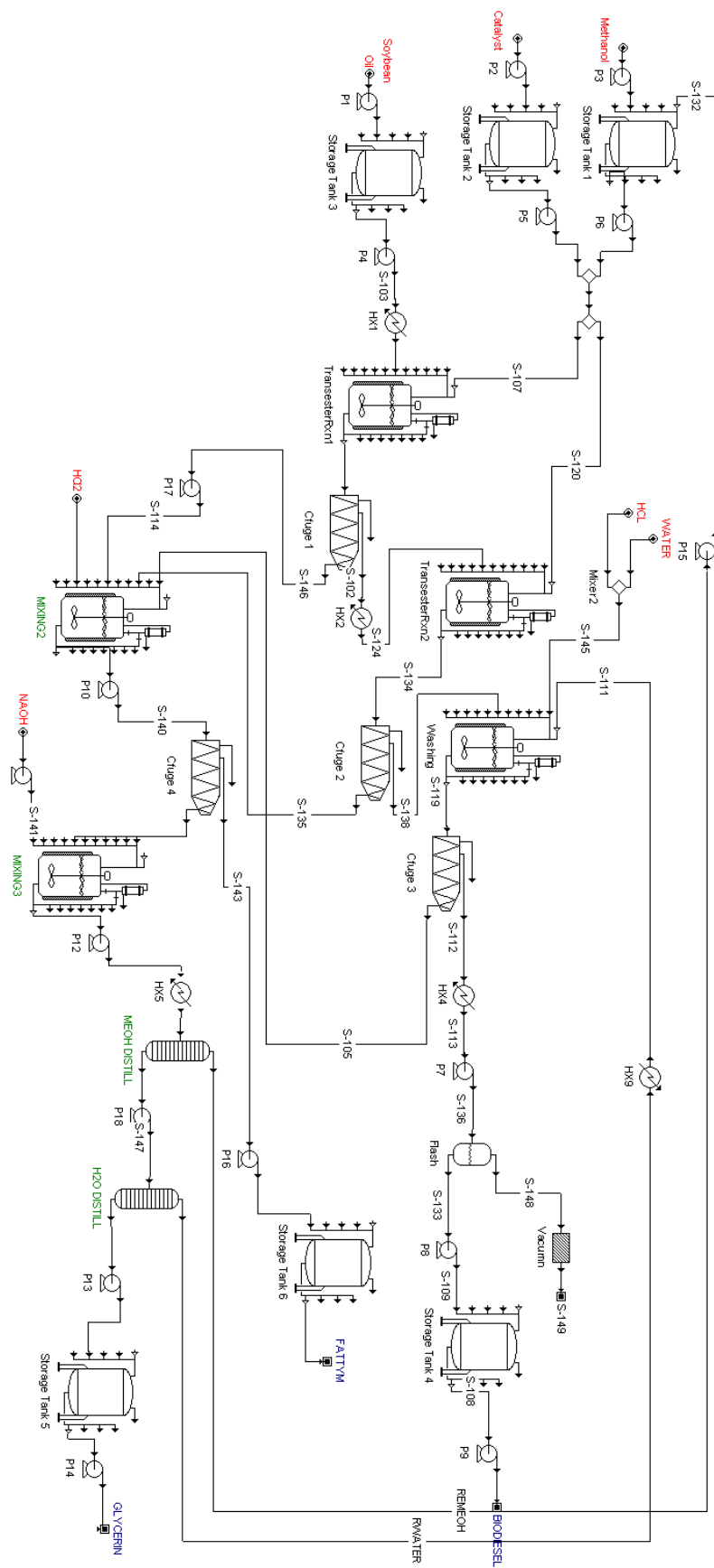
Stream Name	HCl2	S-115	S-140	S-143
Source	INPUT	Mixing 2	P10	CFUGE4
Destination	Mixing 2	P10	CFUGE4	P16
Stream Properties				
Temperature (°C)	25.00	27.89	27.94	25.00
Pressure (bar)	1.01	1.01	4.46	1.01
Density (g/L)	4.25	615.64	855.86	1108.48
Component Flowrates (kg/h averaged)				
Biodiesel	0.00	1.17	1.17	0.00
Glycerin	0.00	420.40	420.40	42.04
HCl	8.13	1.74	1.74	0.00
Methanol	0.00	568.19	568.19	0.00
Sodium Chloride	0.00	13.80	13.80	0.00
Soybean Oil	0.00	21.43	21.43	21.43
Water	15.09	969.55	969.55	0.00
TOTAL (kg/h)	23.22	1996.28	1996.28	63.47

Stream Name	S-117	S-116	S-142	S-129
Source	CFUGE4	MIXING3	P12	P13
Destination	MIXING3	P12	HX5	Storage Tank 5
Stream Properties				
Temperature (°C)	25.00	25.00	25.05	127.79
Pressure (bar)	1.01	1.01	4.46	4.46
Density (g/L)	609.73	934.60	957.56	14.12
Component Flowrates (kg/h averaged)				
Biodiesel	1.17	1.17	1.17	1.17
Glycerin	378.36	378.36	378.36	378.32
HCl	1.74	0.10	0.10	0.10
Methanol	568.19	568.19	568.19	0.00
Sodium Chloride	13.80	16.44	16.44	16.44
Soybean Oil	0.00	0.00	0.00	0.00
Water	969.55	970.36	970.36	80.53
TOTAL (kg/h)	1932.81	1934.61	1934.61	476.56

Stream Name	S-139	GLYCERIN	S-144	FATTYM
Source	Storage Tank 5	P14	P16	Storage Tank 6
Destination	P14	OUTPUT	Storage Tank 6	OUTPUT
Stream Properties				
Temperature (°C)	127.79	127.84	25.06	25.06
Pressure (bar)	1.01	4.46	4.46	1.01
Density (g/L)	3.23	14.12	1108.46	1108.46
Component Flowrates (kg/h averaged)				
Biodiesel	1.17	1.17	0.00	0.00
Glycerin	378.32	378.32	42.04	42.04
HCl	0.10	0.10	0.00	0.00
Methanol	0.00	0.00	0.00	0.00
Sodium Chloride	16.44	16.44	0.00	0.00
Soybean Oil	0.00	0.00	21.43	21.43
Water	80.53	80.53	0.00	0.00
TOTAL (kg/h)	476.56	476.56	63.47	63.47

Stream Name	S-113	S-136	S-148	S-133
Source	HX4	P7	FLASH	FLASH
Destination	P7	FLASH	Vacumn Sys	P8
Stream Properties				
Temperature (°C)	101.67	101.77	120.00	120.00
Pressure (bar)	1.01	4.46	0.00	0.00
Density (g/L)	21.12	86.07	0.00	874.28
Component Flowrates (kg/h averaged)				
Biodiesel	4061.08	4061.08	0.00	4061.08
Glycerin	0.22	0.22	0.00	0.22
Methanol	22.15	22.15	22.05	0.10
NaOCH ₃	0.14	0.14	0.00	0.14
Sodium Chloride	0.40	0.40	0.00	0.40
Soybean Oil	184.84	184.84	138.63	46.21
Water	106.04	106.04	104.14	1.91
TOTAL (kg/h)	4374.87	4374.87	264.82	4110.05

Stream Name	S-109	S-108	BIODIESEL	S-149
Source	P8	Storage Tank 4	P9	Vacumn Sys
Destination	Storage Tank 4	P9	OUTPUT	OUTPUT
Stream Properties				
Temperature (°C)	120.10	25.00	25.10	120.00
Pressure (bar)	3.45	1.01	4.46	0.00
Density (g/L)	713.81	874.30	874.30	0.00
Component Flowrates (kg/h averaged)				
Biodiesel	4061.08	4061.08	4061.08	0.00
Glycerin	0.22	0.22	0.22	0.00
Methanol	0.10	0.10	0.10	22.05
NaOCH ₃	0.14	0.14	0.14	0.00
Sodium Chloride	0.40	0.40	0.40	0.00
Soybean Oil	46.21	46.21	46.21	138.63
Water	1.91	1.91	1.91	104.14
TOTAL (kg/h)	4110.05	4110.05	4110.05	264.82



Appendix C

Below are the details of the base-case scenario for the production of bioethanol.

Input Materials	(MT/hr)
HP-Steam	30.00
Hydrolase	0.28
Water	392.78
Biomass	83.33
Air	1686.90
Amm. Sulfate	0.09
TOTAL	2193.38

Heat Transfer Agent	Total Heat Transfer Agent Demand (MT/h)
Steam	126.45
Cooling Water	13,328.58
Well Water	102.76

Total Power Demand (kWh/hr)
6,844.9

Stream Name	Feedstock	S-103	Air-In-1	S-132
Source	INPUT	P-1	INPUT	P-18b
Destination	P-1	P-2	P-18b	P-18
Stream Properties				
Temperature (°C)	25.00	25.00	25.00	40.00
Pressure (bar)	1.01	1.01	1.01	3.01
Density (g/L)	1172.34	1172.34	1.18	3.34
Component Flowrates (MT/h averaged)				
Ash	3.16	3.16	0.00	0.00
Cellulose	31.44	31.44	0.00	0.00
Hemicellulose	21.67	21.67	0.00	0.00
Lignin	16.03	16.03	0.00	0.00
Nitrogen	0.00	0.00	4.63	4.63
Other Solids	11.03	11.03	0.00	0.00
Oxygen	0.00	0.00	1.41	1.41
Water	83.33	83.33	0.00	0.00

TOTAL (MT/h)	166.66	166.66	6.04	6.04
Stream Name	RO Water	S-144	S-135	S-130
Source	INPUT	P-28	P-20	P-21a
Destination	P-28	P-27	P-21a	P-21b
Stream Properties				
Temperature (°C)	25.00	25.15	61.32	80.00
Pressure (bar)	1.01	16.01	1.01	1.01
Density (g/L)	994.70	994.65	1010.59	3.65
Component Flowrates (MT/h averaged)				
Amm. Sulfate	0.00	0.00	0.09	0.00
Ash	0.00	0.00	0.28	0.00
Cellulose	0.00	0.00	0.62	0.00
Ethyl Alcohol	0.00	0.00	20.62	20.42
Glucose	0.00	0.00	0.49	0.00
Hemicellulose	0.00	0.00	0.20	0.00
Hydrolase	0.00	0.00	0.24	0.00
Lignin	0.00	0.00	5.63	0.00
Other Solids	0.00	0.00	9.68	0.00
Water	224.99	224.99	176.64	26.49
Xylose	0.00	0.00	0.36	0.00
Yeast	0.00	0.00	2.49	0.00
TOTAL (MT/h)	224.99	224.99	217.34	46.91

Stream Name	S-116	S-102	S-133	S-134
Source	P-21a	P-21b	P-21b	INPUT
Destination	P-25a	P-20	P-19	P-25a
Stream Properties				
Temperature (°C)	100.00	80.00	100.00	25.00
Pressure (bar)	1.01	1.01	1.01	1.01
Density (g/L)	1043.57	1.74	959.33	994.70
Component Flowrates (MT/h averaged)				
Amm. Sulfate	0.09	0.00	0.00	0.00
Ash	0.28	0.00	0.00	0.00
Cellulose	0.62	0.00	0.00	0.00
Ethyl Alcohol	0.21	19.80	0.61	0.00
Glucose	0.49	0.00	0.00	0.00
Hemicellulose	0.20	0.00	0.00	0.00
Hydrolase	0.24	0.00	0.00	0.00
Lignin	5.63	0.00	0.00	0.00
Other Solids	9.68	0.00	0.00	0.00
Water	150.13	1.85	24.64	0.00
Xylose	0.36	0.00	0.00	0.00
Yeast	2.49	0.00	0.00	0.00

TOTAL (MT/h)	170.41	21.66	25.25	0.00
---------------------	---------------	--------------	--------------	-------------

Stream Name	S-137	VLP-Steam-1	S-139	S-139
Source	P-25a	P-25	P-25	P-25
Destination	P-25	OUTPUT	P-17	P-21
Stream Properties				
Temperature (°C)	100.00	40.00	81.15	40.00
Pressure (bar)	1.01	0.07	0.50	0.07
Density (g/L)	1043.57	0.05	11.24	1315.84
Component Flowrates (MT/h averaged)				
Amm. Sulfate	0.09	0.00	0.00	0.09
Ash	0.28	0.00	0.00	0.28
Cellulose	0.62	0.00	0.00	0.62
Ethyl Alcohol	0.21	0.06	0.10	0.04
Glucose	0.49	0.00	0.00	0.49
Hemicellulose	0.20	0.00	0.00	0.20
Hydrolase	0.24	0.00	0.00	0.24
Lignin	5.63	0.00	0.00	5.63
Other Solids	9.68	0.00	0.00	9.68
Water	150.13	44.84	75.11	30.17
Xylose	0.36	0.00	0.00	0.36
Yeast	2.49	0.00	0.00	2.49
TOTAL (MT/h)	170.41	44.90	75.22	50.29

Stream Name	S-141	S-138	Condensate-2	S-165
Source	P-17	P-25b	P-25b	P-2
Destination	P-25b	P-2	P-30	P-3
Stream Properties				
Temperature (°C)	81.16	81.16	81.23	28.09
Pressure (bar)	1.50	1.50	1.50	1.01
Density (g/L)	620.53	973.80	620.47	1170.74
Component Flowrates (MT/h averaged)				
Ash	0.00	0.00	0.00	3.16
Cellulose	0.00	0.00	0.00	31.44
Ethyl Alcohol	0.10	0.02	0.08	0.00
Hemicellulose	0.00	0.00	0.00	21.67
Lignin	0.00	0.00	0.00	16.03
Other Solids	0.00	0.00	0.00	11.03
Water	75.11	16.21	58.91	83.33
TOTAL (MT/h)	75.22	16.23	58.99	166.66

Stream Name	Waste Water 1	S-104	Fine Particles	S-105
Source	P-2	P-3	P-4	P-4
Destination	OUTPUT	P-4	OUTPUT	P-5
Stream Properties				
Temperature (°C)	56.17	28.09	28.09	28.09
Pressure (bar)	1.01	1.01	1.01	1.01
Density (g/L)	982.94	1170.74	1170.74	1170.74
Component Flowrates (MT/h averaged)				
Ash	0.00	3.16	0.16	3.00
Cellulose	0.00	31.44	1.57	29.87
Ethyl Alcohol	0.02	0.00	0.00	0.00
Hemicellulose	0.00	21.67	1.08	20.58
Lignin	0.00	16.03	0.80	15.23
Other Solids	0.00	11.03	0.55	10.48
Water	16.21	83.33	4.17	79.16
TOTAL (MT/h)	16.23	166.66	8.33	158.33

Stream Name	S-121	S-120	S-101	S-122
Source	P-5	P-14b	P-14c	P-6
Destination	P-14c	P-14c	P-6	P-7
Stream Properties				
Temperature (°C)	28.09	40.09	31.02	31.12
Pressure (bar)	1.01	1.01	1.01	10.01
Density (g/L)	1170.74	1347.30	1211.50	1211.45
Component Flowrates (MT/h averaged)				
Ash	3.00	4.07	7.07	7.07
Cellulose	29.87	1.63	31.50	31.50
Glucose	0.00	6.13	6.13	6.13
Hemicellulose	20.58	1.95	22.53	22.53
Hydrolase	0.00	0.06	0.06	0.06
Lignin	15.23	14.40	29.63	29.63
Other Solids	10.48	1.21	11.69	11.69
Water	79.16	22.84	102.00	102.00
Xylose	0.00	2.84	2.84	2.84
TOTAL (MT/h)	158.33	55.14	213.45	213.45

Stream Name	S-129	HP Steam	S-107	S-114
Source	P-7	INPUT	P-8	P-9
Destination	P-8	P-8	P-9	OUTPUT
Stream Properties				
Temperature (°C)	90.00	200.00	179.14	103.29
Pressure (bar)	10.01	10.00	10.00	1.01
Density (g/L)	1180.90	4.58	607.63	0.58
Component Flowrates (MT/h averaged)				
Ash	7.07	0.00	7.07	0.00
Cellulose	31.50	0.00	28.35	0.00
Glucose	6.13	0.00	9.63	0.00
Hemicellulose	22.53	0.00	6.76	0.00
Hydrolase	0.06	0.00	0.06	0.00
Lignin	29.63	0.00	29.63	0.00
Other Solids	11.69	0.00	11.69	0.00
Water	102.00	30.00	129.50	23.65
Xylose	2.84	0.00	20.76	0.00
TOTAL (MT/h)	213.45	30.00	243.45	23.65

Stream Name	S-136	S-108	Wash-Water-1	S-111
Source	P-9	P-10	INPUT	P-11
Destination	P-10	P-11	P-11	P-12
Stream Properties				
Temperature (°C)	103.29	50.00	25.00	45.76
Pressure (bar)	1.01	1.01	1.01	1.01
Density (g/L)	1186.70	1214.56	994.70	1201.53
Component Flowrates (MT/h averaged)				
Ash	7.07	7.07	0.00	6.93
Cellulose	28.35	28.35	0.00	27.79
Glucose	9.63	9.63	0.00	5.38
Hemicellulose	6.76	6.76	0.00	6.62
Hydrolase	0.06	0.06	0.00	0.03
Lignin	29.63	29.63	0.00	26.67
Other Solids	11.69	11.69	0.00	6.53
Water	105.85	105.85	34.51	78.45
Xylose	20.76	20.76	0.00	11.61
TOTAL (MT/h)	219.80	219.80	34.51	170.01

Stream Name	S-110	Hydrolase-1	S-109	S-106
Source	P-11	INPUT	P-12	P-13
Destination	P-14d	P-12	P-13	P-14
Stream Properties				
Temperature (°C)	45.76	25.00	43.73	43.83
Pressure (bar)	1.01	1.01	1.01	1.01
Density (g/L)	1137.55	994.70	1183.08	1378.46
Component Flowrates (MT/h averaged)				
Ash	0.14	0.00	6.93	6.93
Cellulose	0.57	0.00	27.79	2.78
Glucose	4.25	0.00	5.38	33.17
Hemicellulose	0.14	0.00	6.62	3.31
Hydrolase	0.03	0.28	0.31	0.31
Lignin	2.96	0.00	26.67	26.67
Other Solids	5.16	0.00	6.53	6.53
Water	61.91	13.66	92.11	88.88
Xylose	9.16	0.00	11.61	15.37
TOTAL (MT/h)	84.30	13.94	183.95	183.95

Stream Name	Wash-Water-2	S-117	S-118	S-115
Source	INPUT	P-14	P-14	P-14b
Destination	P-14	P-14b	P-14d	P-26
Stream Properties				
Temperature (°C)	25.00	40.09	40.09	40.09
Pressure (bar)	1.01	1.01	1.01	1.01
Density (g/L)	994.70	1347.30	1266.22	1347.30
Component Flowrates (MT/h averaged)				
Ash	0.00	6.79	0.14	2.72
Cellulose	0.00	2.72	0.06	1.09
Glucose	0.00	10.22	22.95	4.09
Hemicellulose	0.00	3.25	0.07	1.30
Hydrolase	0.00	0.10	0.22	0.04
Lignin	0.00	24.00	2.67	9.60
Other Solids	0.00	2.01	4.52	0.81
Water	34.63	38.07	85.44	15.23
Xylose	0.00	4.74	10.63	1.90
TOTAL (MT/h)	34.63	91.89	126.68	36.76

Stream Name	S-123	S-131	Amm. Sulfate	S-142
Source	P-14d	P-15	INPUT	P-16
Destination	P-15	P-16	P-16	P-16a
Stream Properties				
Temperature (°C)	42.42	42.42	25.00	42.25
Pressure (bar)	1.01	1.01	1.01	1.01
Density (g/L)	1211.51	1211.51	1016.96	1209.60
Component Flowrates (MT/h averaged)				
Amm. Sulfate	0.00	0.00	0.09	0.09
Ash	0.28	0.28	0.00	0.28
Cellulose	0.62	0.62	0.00	0.62
Glucose	27.20	27.20	0.00	27.20
Hemicellulose	0.20	0.20	0.00	0.20
Hydrolase	0.24	0.24	0.00	0.24
Lignin	5.63	5.63	0.00	5.63
Other Solids	9.68	9.68	0.00	9.68
Water	147.35	147.35	1.67	149.02
Xylose	19.79	19.79	0.00	19.79
TOTAL (MT/h)	210.98	210.98	1.76	212.74

Stream Name	S-169	S-175	S-160	S-147
Source	P-16a	P-16a	P-16b	P-16b
Destination	P-16b	P-16c	P-17a	P-17b
Stream Properties				
Temperature (°C)	42.25	42.25	42.25	42.25
Pressure (bar)	1.01	1.01	1.01	1.01
Density (g/L)	1209.60	1209.60	1209.60	1209.60
Component Flowrates (MT/h averaged)				
Amm. Sulfate	0.01	0.08	0.00	0.01
Ash	0.03	0.25	0.01	0.02
Cellulose	0.06	0.56	0.01	0.05
Glucose	2.72	24.48	0.54	2.18
Hemicellulose	0.02	0.18	0.00	0.02
Hydrolase	0.02	0.22	0.01	0.02
Lignin	0.56	5.07	0.11	0.45
Other Solids	0.97	8.71	0.19	0.77
Water	14.90	134.12	2.98	11.92
Xylose	1.98	17.81	0.40	1.58
TOTAL (MT/h)	21.27	191.46	4.26	17.02

Stream Name	S-127	S-128	S-176	S-124
Source	INPUT	P-17a	P-17a	INPUT
Destination	P-17a	OUTPUT	P-17b	P-17b
Stream Properties				
Temperature (°C)	25.00	37.00	37.00	25.00
Pressure (bar)	1.01	1.01	1.01	1.01
Density (g/L)	1.18	1.18	1083.68	1.18
Component Flowrates (MT/h averaged)				
Amm. Sulfate	0.00	0.00	0.00	0.00
Ash	0.00	0.00	0.01	0.00
Carb. Dioxide	0.00	1.37	0.00	0.00
Cellulose	0.00	0.00	0.01	0.00
Glucose	0.00	0.00	0.02	0.00
Hemicellulose	0.00	0.00	0.00	0.00
Hydrolase	0.00	0.00	0.01	0.00
Lignin	0.00	0.00	0.11	0.00
Nitrogen	6.87	6.87	0.00	35.13
Other Solids	0.00	0.00	0.19	0.00
Oxygen	2.09	0.73	0.00	10.66
Water	0.00	0.00	3.52	0.00
Xylose	0.00	0.00	0.02	0.00
Yeast	0.00	0.00	0.34	0.00
TOTAL (MT/h)	8.96	8.98	4.24	45.79

Stream Name	S-126	S-168	S-170	S-172
Source	P-17b	P-17b	P-16c	P-18
Destination	OUTPUT	P-16c	P-18	OUTPUT
Stream Properties				
Temperature (°C)	37.00	37.00	41.71	37.00
Pressure (bar)	1.01	1.01	1.01	1.01
Density (g/L)	1.17	1082.98	1195.69	1.55
Component Flowrates (MT/h averaged)				
Amm. Sulfate	0.00	0.01	0.09	0.00
Ash	0.00	0.03	0.28	0.00
Carb. Dioxide	5.55	0.00	0.00	20.56
Cellulose	0.00	0.06	0.62	0.00
Glucose	0.00	0.07	24.54	0.00
Hemicellulose	0.00	0.02	0.20	0.00
Hydrolase	0.00	0.02	0.24	0.00
Lignin	0.00	0.56	5.63	0.00
Nitrogen	35.13	0.00	0.00	4.63
Other Solids	0.00	0.97	9.68	0.00
Oxygen	5.19	0.00	0.00	1.41
Water	0.00	17.63	151.75	0.00
Xylose	0.00	0.08	17.89	0.00
Yeast	0.00	1.73	1.73	0.00
TOTAL (MT/h)	45.87	21.18	212.64	26.60

Stream Name	S-112	S-125	S-140	S-145
Source	P-18	P-19	P-20	P-21
Destination	P-19	P-20	P-22	P-26
Stream Properties				
Temperature (°C)	37.00	44.88	78.34	40.01
Pressure (bar)	1.01	1.01	1.01	1.07
Density (g/L)	1027.45	1018.43	754.00	1315.83
Component Flowrates (MT/h averaged)				
Amm. Sulfate	0.09	0.09	0.00	0.09
Ash	0.28	0.28	0.00	0.28
Cellulose	0.62	0.62	0.00	0.62
Ethyl Alcohol	20.01	20.62	19.80	0.04
Glucose	0.49	0.49	0.00	0.49
Hemicellulose	0.20	0.20	0.00	0.20
Hydrolase	0.24	0.24	0.00	0.24
Lignin	5.63	5.63	0.00	5.63
Other Solids	9.68	9.68	0.00	9.68
Water	152.00	176.64	1.85	30.17
Xylose	0.36	0.36	0.00	0.36
Yeast	2.49	2.49	0.00	2.49
TOTAL (MT/h)	192.09	217.34	21.66	50.29

Stream Name	S-113	BB-Air-In	Flue Gas	S-155
Source	P-26	INPUT	P-27	P-27
Destination	P-27	P-27	OUTPUT	P-29
Stream Properties				
Temperature (°C)	40.04	25.00	200.00	201.42
Pressure (bar)	1.01	1.01	1.01	16.01
Density (g/L)	1328.94	1.18	0.71	7.31
Component Flowrates (MT/h averaged)				
Amm. Sulfate	0.09	0.00	0.00	0.00
Ash	3.00	0.00	0.00	0.00
Carb. Dioxide	0.00	0.00	78.90	0.00
Cellulose	1.71	0.00	0.00	0.00
Ethyl Alcohol	0.04	0.00	0.00	0.00
Glucose	4.58	0.00	0.00	0.00
Hemicellulose	1.50	0.00	0.00	0.00
Hydrolase	0.28	0.00	0.00	0.00
Lignin	15.23	0.00	0.00	0.00
Nitrogen	0.00	208.00	208.00	0.00
Other Solids	10.48	0.00	0.00	0.00
Oxygen	0.00	63.15	3.01	0.00
Water	45.40	0.00	65.21	224.99
Xylose	2.25	0.00	0.00	0.00
Yeast	2.49	0.00	0.00	0.00
TOTAL (MT/h)	87.05	271.15	355.12	224.99

Stream Name	Ash	HP-Steam	LP-Steam	S-159
Source	P-27	P-29	P-29	P-29
Destination	OUTPUT	OUTPUT	OUTPUT	P-30
Stream Properties				
Temperature (°C)	250.00	179.89	152.58	99.97
Pressure (bar)	1.01	10.00	5.10	1.01
Density (g/L)	1992.58	4.78	2.60	967.38
Component Flowrates (MT/h averaged)				
Amm. Sulfate	0.09	0.00	0.00	0.00
Ash	3.00	0.00	0.00	0.00
Water	0.00	36.00	112.49	76.50
TOTAL (MT/h)	3.08	36.00	112.49	76.50

Stream Name	wat-in	S-149	S-150	wat-out
Source	P-30	INPUT	P-31	P-31
Destination	P-31	P-31	OUTPUT	OUTPUT
Stream Properties				
Temperature (°C)	91.82	25.00	25.00	25.00
Pressure (bar)	1.01	1.01	1.01	1.01
Density (g/L)	705.13	1.18	1.19	994.53
Component Flowrates (MT/h averaged)				
Ethyl Alcohol	0.08	0.00	0.00	0.08
Nitrogen	0.00	1039.30	1039.30	0.00
Oxygen	0.00	315.51	315.51	0.00
Water	135.40	0.00	14.75	120.65
TOTAL (MT/h)	135.48	1354.82	1369.56	120.73

Stream Name	S-119	S-163	S-164	S-143
Source	P-22	INPUT	P-23	P-23
Destination	P-23	P-23	OUTPUT	P-24
Stream Properties				
Temperature (°C)	25.00	85.00	26.14	25.00
Pressure (bar)	1.01	1.01	1.01	1.01
Density (g/L)	800.28	0.98	15.73	786.04
Component Flowrates (MT/h averaged)				
Ethyl Alcohol	19.80	0.00	0.00	19.80
Nitrogen	0.00	0.11	0.11	0.00
Oxygen	0.00	0.03	0.03	0.00
Water	1.85	0.00	1.84	0.02
TOTAL (MT/h)	21.66	0.15	1.98	19.82

Stream Name	Product
Source	P-24
Destination	OUTPUT
Stream Properties	
Temperature (°C)	25.00
Pressure (bar)	1.01
Density (g/L)	786.04
Component Flowrates (MT/h averaged)	
Ethyl Alcohol	19.80
Water	0.02
TOTAL (MT/h)	19.82

